CELLULAR MECHANISMS UNDERLYING GLUTAMATERGIC CALCIUM RESPONSES IN DEVELOPING AUDITORY BRAINSTEM NEURONS

by

Florenta Aura Negoita

BS, Bucharest University, Romania, 1995

MS, Bucharest University, Romania, 1996

Submitted to the Graduate School of

Medicine, Department of Neurobiology in partial fulfillment

of the requirements for the degree of

Doctor of Philosophy

University of Pittsburgh

2003

UNIVERSITY OF PITTSBURGH

SCHOOL OF MEDICINE

This dissertation was presented

by

Florenta Aura Negoita

It was defended on

November 18 2003

and approved by

Stephen D. Meriney, PhD, Associate Professor, Department of Neurobiology

Elias Aizenman, PhD, Professor, Department of Neurobiology

Guo-Qiang Bi, PhD, Assistant Professor, Department of Neurobiology

Major advisor: Karl Kandler, PhD, Assistant Professor, Department of Neurobiology

Committee chairperson: Peter W. Land, PhD, Associate Professor, Department of Neurobiology
Dissertation Director

CELLULAR MECHANISMS UNDERLYING GLUTAMATERGIC CALCIUM RESPONSES IN DEVELOPING AUDITORY BRAINSTEM NEURONS

Florenta Aura Negoita, PhD

University of Pittsburgh, 2003

Spontaneous and sound-driven activity, glutamatergic synaptic transmission and Ca^{2+} signaling are critical for formation, maturation, refinement and survival of neuronal circuits including the auditory system. The present study investigated the mechanisms by which glutamatergic inputs from the cochlear nucleus regulate intracellular calcium concentration ($[Ca^{2+}]_i$) in developing lateral superior olive (LSO) neurons, using Ca^{2+} imaging in fura-2AM labeled brainstem slices.

AMPA/kainate receptors primarily mediated Ca^{2+} responses elicited by single stimuli and contributed to Ca^{2+} responses elicited by low and high frequency bursts by approximately 75% and 50% respectively. Both AMPAR and kainate receptors were Ca^{2+} impermeable and increased $[Ca^{2+}]_i$ via membrane depolarization and activation of voltage gated calcium channels (VGCCs). NMDARs contributed approximately 50% to Ca^{2+} responses independent of the stimulus frequency. Their high contribution to Ca^{2+} responses was consistent with their contribution (30-60%) to EPSPs triggered by stimulation of AVCN-LSO synapses. mGluRs contributed to Ca^{2+} responses only under high frequency stimulation (>20Hz). Group I mGluR-

mediated Ca^{2+} responses had two components: release from internal stores and influx from the extracellular milieu. The influx was mediated by a channel sensitive to Ni^{2+}, La^{3+} and 2-APB, consistent with it being a member of the TRP family. During development, the contribution of this channel decreased and it was lost after hearing onset, suggesting that it might be downregulated by auditory experience.

In summary, distinct temporal patterns of synaptic activity in the LSO activate distinct GluR types and each receptor type employs a distinct Ca^{2+} entry pathway. This could possibly lead to activation of distinct intracellular cascades and distinct gene expression programs (West et al., 2001) that may be involved in distinct developmental aspects.

TABLE OF CONTENTS

LIST OF TABLES

LIST OF FIGURES

PREFACE

I would like to thank people who have contributed to the accomplishment of this dissertation. I am very grateful to my advisor, Dr. Karl Kandler, for guidance and help during these years. I learned from him to always push for an extra mile, to believe in my results and to present them in a very clear, concise and exciting way.

I thank my committee members for discussion and ideas about the project; to Dr. Paul Kullmann for teaching me Ca^{2+} imaging and for helpful discussions; and to lab members for providing a fun and interesting working environment.

I thank CNUP staff for great help in handling all the graduate program requirements, course paper work, administrative and computer problems.

Lately but not lastly, my gratitude goes to my family and siblings for love and support during this time. A special thank you goes to my beloved friend Viorel, who believed in me and encouraged and supported me along these years. Also I thank my friend Paul who helped and encouraged me during the last years.

1. INTRODUCTION

Glutamatergic neurotransmission is the basic mechanism for encoding, transmission and processing of sensory information in the auditory system, including the auditory brainstem of mammals (Rhode and Greenberg, 1992; Sanes and Walsh, 1998).

In the developing auditory system, glutamatergic synaptic transmission is elicited by spontaneous activity and by sensory-evoked activity after hearing onset (review: Rubel et al., 1990; Sanes and Friauf, 2000). Spontaneous and sensory driven neuronal activity play an important role in the correct formation, maturation, refinement and survival of neuronal circuits including those in the auditory system (review auditory: Rubel et al., 1990, Sanes and Friauf, 2000; other systems: Hubel and Wiesel, 1970; Van der Loos and Woolsey, 1973; Constantine-Paton et al., 1990; Shatz 1990; Brunjes, 1994; Katz and Shatz, 1996; Corriveau 1999; but for a different view see also Crowley and Katz, 2002). In the auditory system, altering the afferent input by cochlea removal or blockade of spontaneous activity of the auditory nerve, induces changes in the morphology and physiology of anteroventral cochlear nucleus (AVCN) neurons and their targets (Rubel et al., 1990; Moore, 1993; Moore et al., 1993; Parks, 1997), including the lateral superior olive (LSO) in which cochlea removal alters glutamatergic neurotransmission (Kotak and Sanes, 1996; 1997).

One way by which glutamatergic neurotransmission accomplishes its functions is via elevation of the postsynaptic intracellular calcium concentration ($[Ca^{2+}]_i$). Ca^{2+} is a ubiquitous second messenger that is critically involved in development and plasticity in the CNS (reviews: Ghosh and Greenberg, 1995; Gallin and Greenberg, 1995; Berridge, 1998). How can specific pathways be triggered using a ubiquitous ion? Neurons use an extensive repertoire of Ca^{2+} entry pathways and intracellular signaling components that can be assembled in different combinations to maintain the individuality of each incoming signal and at the same time to decipher the meaning of each signal. Maturational changes in glutamatergic neurotransmission, which involve

changes in the expression of glutamate receptors (GluRs) (Hunter et al., 1993; Caicedo and Eybalin, 1999) or changes in glutamate (Glu) transmitter levels (Sanes and Walsh, 1998), are therefore likely to affect Ca^{2+} signaling in auditory brainstem nuclei. Specific Ca^{2+} signaling cascades may affect specific aspects of the LSO maturation. Thus, a clear understanding of Ca^{2+} entry routes during development is critical.

The aim of this study is to determine the Ca^{2+} entry routes and of the mechanisms that affect $[Ca^{2+}]_i$ during development by investigating GluR-mediated Ca^{2+} responses in developing LSO neurons.

1.1. LSO CIRCUITRY AND FUNCTION

The lateral superior olive, LSO, is a binaural nucleus in the auditory brainstem involved in sound localization (Irvine, 1992). The LSO receives anatomically separated *excitatory* input from the *ipsilateral* ear and *inhibitory* input from the *contralateral* ear (Figure 1) (Boudreau and Tsuchitani, 1968). The excitatory input arises from the spherical bushy cells in the anteroventral cochlear nucleus (AVCN) via ventral acoustic stria (VAS) and is mediated by Glu (Irvine, 1992; review: Thompson and Schofield, 2000). The inhibitory input arises from principal cells in the medial nucleus of the trapezoid body (MNTB) and is mediated by glycine (Gly; Kandler and Friauf, 1995a) in adulthood and by GABA and Gly during development (Kotak et al., 1998, Kullmann et al., 2002; review: Thompson and Schofield, 2000). The primary target of LSO neurons is the inferior colliculus (IC). The projections to the ipsilateral IC are excitatory and mediated by Glu; the projections to the contralateral IC are mainly inhibitory and mediated by Gly, with a smaller proportion presumably excitatory (review: Thompson and Schofield, 2000). Inputs to the LSO are tonotopically organized and match perfectly along the LSO tonotopic axis in adults (i.e. neurons in the medial limb of the LSO are tuned to high frequencies while neurons in the lateral limb are tuned to low frequencies; Boudreau and Tsuchitani, 1968; Irvine, 1992).

This arrangement allows LSO neurons to detect interaural sound level differences, reflecting azimuthal position of the sound source, by comparing the amount of excitation and inhibition from each ear (Irvine, 1992).

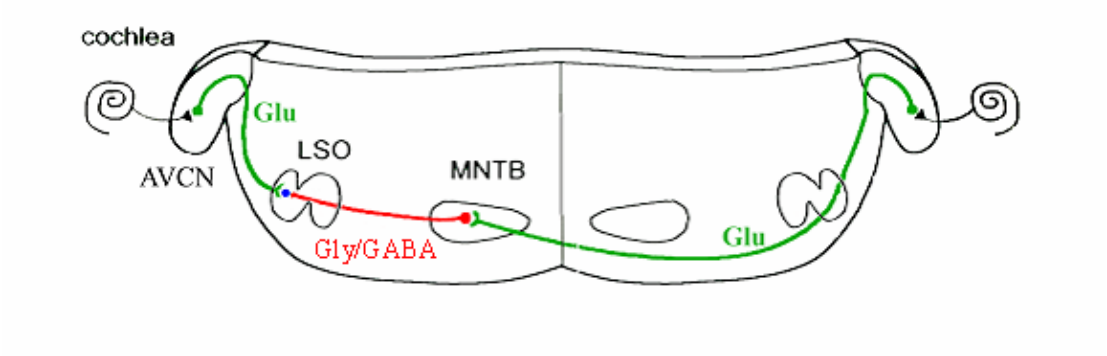

Figure 1. LSO circuitry.

Green - excitatory glutamatergic input from the ipsilateral ear via AVCN.
Red - inhibitory glycinergic/GABAergic input from the contralateral ear via MNTB.
Adapted from Friauf and Lohmann, 1999.

1.2. CELL TYPES IN THE LSO

The adult LSO contains several cell types (5-7 types; mouse: Ollo and Schwartz, 1979; gerbil: Helfert and Schwartz, 1987; rat: Rietzel and Friauf, 1998). Because they have been described in different species and the nomenclature is slightly different, I summarize here findings from several species. The principal cells comprise approximately 75% of LSO neurons (mouse: Ollo and Schwartz, 1979; gerbil: Helfert and Schwartz, 1987; rat: Rietzel and Friauf,

1998). These cells are fusiform, described as multipolar (gerbil: Helfert and Schwartz, 1987) or bipolar and multipolar (rat: Rietzel and Friauf, 1998), with the dendritic arbor oriented dorsoventrally (rat: Rietzel and Friauf, 1998). The other classes of LSO neurons include small multipolar cells (~11%), marginal cells (~6%), bushy cells, unipolar cells and banana-like cells (mouse: Ollo and Schwartz, 1979; gerbil: Helfert and Schwartz, 1987; rat: Rietzel and Friauf 1998). In this study recordings are most likely from principal cells of the LSO as they represent the predominant population of this nucleus. Small multipolar cells and marginal cells identified based soma size and on their location, most likely made no considerable contribution to the data as they represent a very small percentage of the entire LSO population.

1.3. DEVELOPMNENT OF LSO NEURONS AND CIRCUITRY

The development of the LSO circuitry, including anatomy and physiology, has been largely investigated in rodents (reviews: Cant, 1998; Sanes and Friauf, 2000). Figure 2 presents a summary of major events taking place during development of the LSO circuitry. Data presented here are from both mice and rats since development follows similar time lines in both species.

Many steps in the development of LSO circuitry take place before hearing onset (P12 in mice: Ehret, 1976). Cell number in the LSO does not change significantly during postnatal development but the packing density decreases to about 50% from the first postnatal week to adult (mouse: Ollo and Schwartz, 1979). Synaptic connections are established and become functional during fetal life (E18 rat: Kandler and Friauf, 1993; 1995a). The establishment of crude tonotopy, i.e. neurons located in high frequency areas of the cochlear nucleus (CN) project to neurons located in the high frequency areas of LSO, occurs before birth (rat: Kandler and Friauf, 1993; chick: Jhaveri and Morest, 1982; reviews: Friauf and Lohmann, 1999; Sanes and Friauf, 2000). Dendritic and axonal growth takes place also during postnatal development, peaking before hearing onset (quantified by dendritic length and branching points: Sanes et al.,

1992). Drastic remodeling of synaptic connections also takes place during the first three to four postnatal weeks. Axonal projections from the MNTB to the LSO and the dendritic tree of LSO neurons undergo an activity-dependent refinement (gerbil: Sanes and Takacs, 1993; Sanes and Siverls, 1991; Sanes et al., 1992; review: Sanes and Friauf, 2000). This refinement is accompanied by massive elimination of functional inhibitory synapses such that LSO neurons lose ~ 75 % of their inputs from the MNTB (rat: Kim and Kandler, 2003), and results in sharpening of functional tonotopic organization of auditory connections. Excitatory and inhibitory synapses to LSO are depolarizing and can increase $[Ca^{2+}]_i$ early in development (Kandler and Friauf 1995a; Ehrlich et al., 1999; Kullmann et al., 2002; Ene et al., 2003). The glycinergic/GABAergic input becomes hyperpolarizing around P3/4 in mice (Kullmann and Kandler, 2001) and around P7/8 in rats (Kandler and Friauf, 1995a). The depolarizing phase of glycinergic/GABAergic inputs may allow these inputs to use Ca^{2+}-dependent signal transduction pathways similar to those used by the excitatory inputs for their refinement (Kandler et al., 2003).

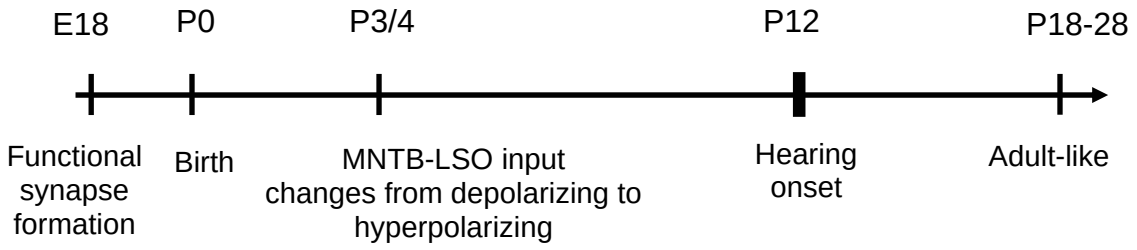

Figure 2. Major events in the development of LSO.

Morphologically, the most dramatic change occurs in the dendritic tree of the LSO neurons, where the number of dendritic endpoints is drastically reduced (by about 80% from P4 toP36) by selective pruning of the distal dendrites (rat: Rietzel and Friauf, 1998). The number of dendritic branches and endpoints decreases mostly because of the elimination of small thin dendrites. As a result, the complexity of the dendritic tree decreases and the arbors become visibly bipolar shaped. Despite this loss of dendrites, the dendritic field increases (from P4-36 with most of the increase taking place after P22). However, the relative size of the dendritic field decreases due to a large increase in the LSO area (rat: Rietzel and Friauf, 1998).

It is not known whether the axonal projections of the excitatory inputs from AVCN to LSO undergo a functional and morphological refinement process similar to that of the inhibitory input. Since in other developing sensory systems the excitatory inputs are remodeled in order to achieve precise synaptic connectivity (Goodman and Shatz, 1993; Shatz, 1996) it is very likely that the input from the AVCN to the LSO undergo refinement. Supposing that there is refinement, it will be interesting to know the time course in relationship to the refinement of the inhibitory synapses.

Maturation of LSO neurons includes the expression of different transmitter receptors and receptor subunits (Caicedo and Eybalin, 1999; Korada and Schwartz, 1999). In the following, I will summarize data from several species including mouse, rat and gerbils, concerning the expression of glutamate receptors (GluRs: AMPARs, kainate receptors, NMDARs, mGluRs).

AMPARs are assembled from a variety of subunits (GluR1 to GluR4), splice variants and mRNA editing combinations that confer diverse functional properties (Borges and Dingledine, 1998; Parks, 2000). The expression of AMPAR subunits in developing rat LSO was investigated using immunohistochemistry (Figure 3A adapted from Caicedo and Eybalin, 1999). According to this study, the expression of the GluR1 subunit decreases to the adult level during the first 3 postnatal weeks. The GluR2 subunit, which confers Ca^{2+} impermeability to AMPARs (Hollmann et al., 1991; Verdoorn et al., 1991), is expressed early in development and its expression level decreases after hearing onset. The GluR4 subunit, whose incorporation results in a receptor with faster kinetics (review: Trussell, 1999) is expressed mostly after hearing onset. Other studies found that GluR1-GluR4 mRNA and/or protein are expressed in adult rat LSO (Sato et al., 2000; Schmid et al., 2001) and gerbil LSO (Schwartz and Eager, 1999). The cellular localization of GluRs was studied in adult gerbils and found along dendrites of principal cells of LSO and on

their somata. Functionally, AMPARs were investigated using electrophysiology. These studies indicate that synaptic transmission between AVCN and LSO is mostly mediated by AMPARs (Caspary and Faingold, 1989; Kotak and Sanes, 1996; Wu and Kelly, 1992).

Kainate receptors are homomeric or heteromeric receptors composed of several subunits: GluR5-7, KA1, and KA2 (review: Chittajallu et al., 1999). In the auditory brainstem, kainate receptor subunits are expressed in several nuclei including nucleus magnocellularis (NM) of chick (Lachica et al., 1998), MNTB of developing to adult rat (P2-59; Lohrke and Friauf, 2002), CN of adult rat (Petralia et al., 1994; 1996; review: Petralia et al., 2000). To date no anatomical study investigated the expression of kainate receptors in the LSO, although their presence was suggested by electrophysiological experiments. These experiments show a kainate-evoked current, resistant to the AMPAR antagonist GYKI 52466, thus most likely mediated by kainate receptors (Vitten et al., 1999). Also Ca^{2+} imaging experiments (this study) indicate the presence of kainate receptors in the developing LSO.

NMDARs are composed of different combinations of subunits NR1, NR2A-D and NR3. Functional channels are produced when the NR1 subunit is assembled together with one of the four NR2 subunits (reviews: Mori and Mishina, 1995; Dingledine et al., 1999). Their expression has been investigated in the developing LSO of rat (P4-30; Caicedo and Eybalin, 1999). According to this study, all subunits are detected and the expression of the NR1 subunit decreases after hearing onset (Figure 3B adapted from Caicedo and Eybalin, 1999). In other brainstem nuclei, NMDARs are involved in synaptic transmission (developing rat IC: Ma et al., 2002). In developing LSO neurons, previous electrophysiological studies suggested that NMDARs do not participate in synaptic transmission under normal circumstances (Caspary and Faingold, 1989; Wu and Kelly, 1992; Kotak and Sanes, 1996; Kandler and Friauf, 1995). However, in experiments in which neuronal activity was blocked by cochlea ablation, the ipsilateral evoked EPSP had an NMDAR component, suggesting that NMDARs participate to synaptic transmission under these circumstances (Kotak and Sanes, 1995).

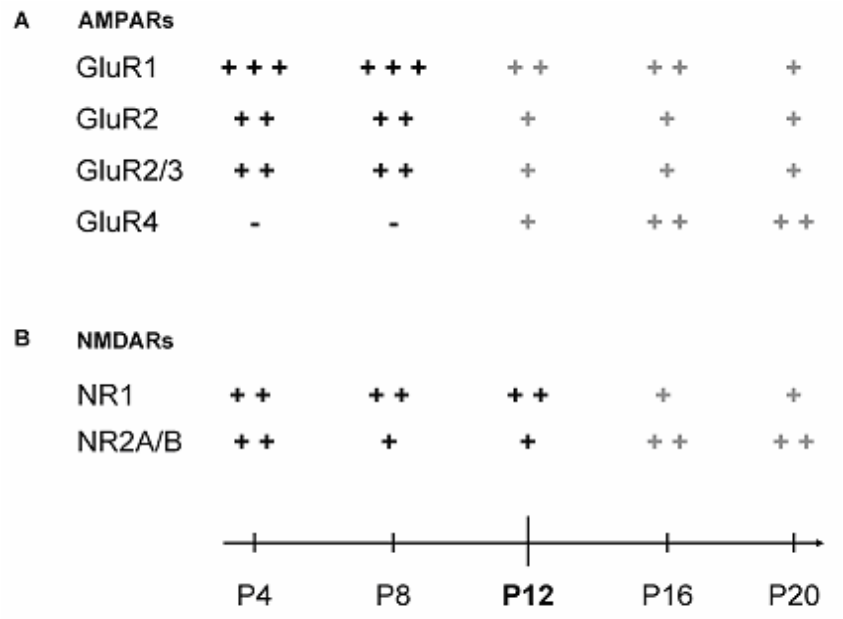

Figure 3. Developmental changes in the expression of GluRs.

Expression of GluRs subunits in developing rat LSO, assessed using antibody.
- = no detection; + = low levels; ++ = moderate levels; +++ = high levels of expression.
Data points before hearing onset (P12) are in black while data points after hearing onset are in gray. **A**. AMPARs. **B.** NMDARs. Adapted from Caicedo and Eybalin, 1999.

Metabotropic glutamate receptors (mGluRs) are a family of proteins that have seven transmembrane segments and are coupled to G proteins. They differ from ionotropic glutamate receptors in that they do not form ion channels but instead activate intracellular signal-transduction cascades (reviews: Pin and Duvoisin, 1995; Conn and Pin, 1997; De Blasi et al., 2001). To date, eight genes coding for different subtypes of mGluRs have been identified, mGluR1 to 8 (reviews: Pin and Duvoisin, 1995; Conn and Pin, 1997; De Blasi et al., 2001). Based on primary amino acid sequence homology, pharmacology, and second-messenger coupling the family of mGluRs has been subdivided in three main groups: group I (mGluR1, 5), group II (mGluR2, 3) group III (mGlu R4, 6, 7, 8). Intracellular signaling pathways through

mGluRs are very complex and thus mGluRs are implicated in a variety of functions including synaptic plasticity (review: Holscher et al., 1999), modulation of ion channels (review: Anwyl, 1999), and neurodegeneration (reviews: Bruno et al., 1998; Holscher et al., 1999).

The expression of mGluRs has been poorly investigated in the LSO. Immunohistochemistry studies indicate the expression of mGluR2/3 in a small population of LSO neurons and their processes (adult rat: Petralia et al., 1996). Electrophysiological studies indicate the presence of group II and/or group III mGluRs on presynaptic glutamatergic terminals (mouse: Wu and Fu, 1998) and group I mGluR on postsynaptic LSO neurons (gerbil: Kotak and Sanes, 1995).

GABARs and GlyRs also undergo developmental changes. For example, in developing rat LSO GABARs expression markedly decreases with age, especially in the neuropil (Korada and Schwartz, 1999). GlyRs undergo a change in the subunit composition from the neonatal $\alpha 2$ to the adult $\alpha 1$, resulting in a receptor with faster kinetics (Rajendra et al., 1997), ensuring fast neurotransmission. In addition, an increasing expression of the glycine transporter GLYT2, which is involved in the re-uptake of Gly from the synaptic cleft, contribute to fast glycinergic neurotransmission (Friauf et al., 1999; review: Sanes and Friauf, 2000). Other maturational processes of LSO neurons include changes in membrane properties (Kandler and Friauf, 1995b) and changes in the expression of Ca^{2+} binding proteins (Friauf, 1993; 1994; Lohmann and Friauf, 1996).

Most of the developmental changes described above occur before hearing onset. After hearing onset, the functional properties of LSO neurons refine further until the adult-like connectivity and functionality is achieved in the third to fourth postnatal week (reviews: Sanes and Walsh, 1998; Cant, 1998; Sanes and Friauf, 2000). The ability of LSO neurons to encode the intensity of the sound improves. This has been characterized by the dynamic range (dB), maximum possible output (discharge rate) and the resolution of the response (discharges/dB) (Sanes and Rubel, 1988). Also, binaural properties improve. For example, topographical alignment characterized by the degree of matching of the characteristic frequencies of excitatory and inhibitory inputs which is present at birth it refines (Sanes and Rubel, 1988).

In summary, the developing LSO circuitry undergoes an array of maturational processes. At the level of circuitry, there is an activity dependent pruning of MNTB inputs to LSO and of the dendritic tree of LSO, taking place over the first three postnatal weeks. At the functional

level there is synapse elimination such that the LSO lose approximately 75% of their MNTB inputs which takes place mostly before hearing onset. At the level of receptors, AMPARs and GlyRs expression undergo developmental changes that result in faster synaptic transmission.

1.4. ROLE OF NEURONAL ACTIVITY IN DEVELOPMENT OF LSO

Numerous studies in different sensory systems have established that neuronal activity plays an important role in the correct formation, maturation and refinement of neuronal circuits (reviews: Constantine-Paton et al., 1990; Shatz, 1990; Katz and Shatz, 1996; Corriveau, 1999; but for a different view see also Crowley and Katz, 2002). The integrity of presynaptic inputs is crucial for maintaining and shaping the organization and function of target neurons (Hubel and Wiesel, 1970; Van der Loos and Woolsey, 1973; Brunjes, 1994). Early experiments in different sensory systems have shown that removal of the presynaptic input or altering the activity of the presynaptic input during a certain "critical period" of development induces profound changes in the physiology, morphology, and function of the target neurons (Hubel and Wiesel, 1970; Van der Loos and Woolsey, 1973; Brunjes, 1994).

In the auditory brainstem, evidence from both chick and mammals suggests that neuronal activity plays a critical role in development. It influences cell survival, it affects dendritic and axonal growth, and it influences fine-tuning of circuits (reviews: Rubel et al., 1990; Friauf and Lohmann, 1999; Sanes and Friauf, 2000). Because many developmental steps take place before hearing onset, it is important to distinguish between the role of neuronal activity before and after hearing onset.

Spontaneous activity before hearing onset has been found to originate in the cochlea since removal of the cochlea results in cessation of spontaneous activity in CN neurons (Born and Rubel, 1985; Pasic and Rubel, 1989). *In vivo* recordings from different auditory brainstem nuclei have shown that the average activity level is low (below 1 Hz), but spontaneous spike

activity is sustained and rhythmic, consisting of brief bursts interrupted by periods of quiescence (Romand and Ehret, 1990; Lippe, 1994; Gummer and Mark, 1994; Kotak and Sanes, 1995; Kros et al., 1998; Glowatzki and Fuchs, 2000). The meaning of these bursts is not understood. There is some evidence that interfering with patterned activity affects the development of the auditory circuitry (Sanes and Constantine-Patton, 1985, Ehrlich et al., 1998). For example, in organotypic cultures of brainstem slices containing LSO and MNTB, where the level and the pattern of spontaneous activity is completely different from *in vivo*, glycinergic synaptic transmission remains in an immature state (Ehrlich et al., 1998). Most likely, the change in the subunit composition of GlyRs (neonatal $\alpha 2$ to adult $\alpha 1$) is impaired, while the development of other membrane properties of LSO or MNTB neurons appears not to be affected (Ehrlich et al., 1999).

Manipulations intended to decrease or eliminate spontaneous activity, i.e. cochlea ablation or inhibition of the auditory nerve activity by TTX, revealed a critical role of spontaneous activity for the correct formation of auditory circuitry (review: Sanes and Friauf, 2000) and for survival (review: Rubel et al., 1990). For the LSO circuitry, unilateral cochlea ablation before hearing onset prevents synaptic refinement of MNTB to LSO input. As a consequence, the dendritic length of LSO neurons and the number of branch points do not decrease and an immature-like connectivity pattern is retained in adults (Sanes and Takacs, 1993; Sanes and Siverls, 1991; Sanes et al., 1992; review: Sanes and Friauf, 2000). For the development of the AVCN to LSO input, experimental evidence suggests that glutamatergic transmission weakens, such that fewer neurons respond to ipsilateral stimulation and their EPSP amplitude decreases (Kotak and Sanes, 1997). There are also morphological effects including atrophy of LSO soma and dendrites (Sanes et al., 1992), suggesting that spontaneous activity and the integrity of presynaptic input are critical for correct development of the LSO circuitry and thus for the correct functioning of these neurons.

A large number of studies demonstrate the necessity of neuronal activity for the survival of CN and NM neurons. Cochlear removal or inhibition of auditory nerve activity results in massive death of CN and NM neurons in the ablated side, significant reduction in soma size of the surviving neurons (in chick: Born and Rubel, 1985; review: Rubel et al., 1990; in gerbil: Tierney et al., 1997; in mouse: Trune, 1982a, b, 1983; Mostafapour et al., 2000; in rat: Moore, 1998; in ferret: Moore, 1990), decreased protein synthesis (Durham and Rubel, 1985; Steward and Rubel, 1985; Garden et al., 1994; review: Rubel et al., 1990), upregulation of mitochondrial

metabolism (Hyde and Durham, 1990; 1994 a, b), and increases in intracellular calcium (Zirpel et al., 1995a). An interesting observation is the existence of a "*sensitive period*" in which these effects are more pronounced. In both avian and mammalian auditory brainstem this period is related to the hearing onset (P12 in rodents and E12-14 in chick; Rubel and Parks, 1988; Tierney et al., 1997; Mostafapour et al., 2000). For example, cell death in the AVCN of mice is approximately 40 % when the cochlea is removed at P7, it decreases to 5-10 % when the cochlea is removed is at P11 and to less than 1 % when the cochlea is removed at P14 (Mostafapour et al., 2000). Effects of cochlea ablation are also seen trans-synaptically in nuclei receiving input from the deprived CN. These effects include ectopic projections from the intact CN to the deinnervated nuclei LSO, MSO, MNTB and IC (Rubel et al., 1981; Nordeen et al., 1983; Moore and Kitzes, 1985; Russell and Moore, 1995; Kitzes et al., 1995; Moore and Kowalchuk, 1988), dendritic changes (atrophy and/or hypertrophy; LSO: Sanes et al., 1992; Russell and Moore, 1999), changes in the receptors and membrane properties of neurons (LSO: Kotak and Sanes, 1996; 1997; review: Sanes and Friauf, 2000) and changes in soma size (LSO: Sanes et al., 1992; MNTB: Pasic et al., 1994). Although there was no assay for cell death in the LSO following cochlea ablation, the size of the nucleus was smaller and a general atrophic condition was observed (i.e. the entire area of LSO was reduced), suggesting that there might be cell loss (Sanes et al., 1992).

Taken together these studies indicate that afferent activity is not only important for correct circuitry formation but also has a trophic role during development. In addition, there is a "*sensitive period*" when spontaneous activity and the integrity of presynaptic input are much more critical for normal development and maturation of target neurons than it is for maintenance after neurons have matured.

Sensory-driven activity after hearing onset also has been shown to play a critical role in development and plasticity of the auditory brainstem (review: Friauf and Lohmann, 1999). It has been suggested that acoustically driven activity is involved in dendritic and somatic growth and refinement (Feng and Rogowski, 1980; Conlee and Parks, 1981; 1983). For example, in rats, monaural occlusion, which drastically reduces the level of auditory input (noise attenuation by approximately 40dB) impairs the MSO dendritic remodeling corresponding to the deprived side (Feng and Rogowski, 1980). In chickens, monaural occlusion retards of the continuous growth of soma of NM neurons corresponding to the deprived side (Conlee and Parks, 1981) and changes

the dendritic length of neurons from nucleus laminaris corresponding to the plugged ear (Gray et al., 1982; Smith et al., 1983). Other studies have shown that sensory driven activity, especially the pattern of activity, is involved in the sharpening of frequency tuning curves in IC neurons (Sanes and Constantine-Paton, 1983; 1985).

In summary, neuronal activity before and after hearing onset plays an important role in the development of auditory brainstem nuclei. In the LSO, the role of spontaneous activity before hearing onset has been investigated in studies concerning the development of the inhibitory glycinergic/GABAergic input and has shown that the refinement of these inputs is prevented. The role of activity for the development of glutamatergic input to LSO has been much less examined.

1.5. ROLE OF CALCIUM AND CALCIUM ENTRY ROUTES FOR THE DEVELOPMENT OF LSO NEURONS

Glutamatergic neurotransmission can induce morphological changes and many of these changes involve intracellular calcium signaling. Numerous studies have shown that increases in the $[Ca^{2+}]_i$ in neurons affect processes that are central to the development and plasticity of the nervous system, including activity-dependent cell survival, modulation of synaptic strength, and calcium-mediated cell death (reviews: Ghosh and Greenberg, 1995; Gallin and Greenberg, 1995, Berridge, 1998; West et al., 2001).

For the auditory brainstem nuclei, several lines of evidence from both chick and rodents indicate that calcium plays a critical role for survival and development. First, removal of cochlea in embryonic chicken results in an increase in $[Ca^{2+}]_i$ in nucleus magnocellularis (NM; the avian equivalent of the mammalian cochlear nucleus), a nucleus receiving direct input from the auditory nerve (Zirpel et al., 1995a). This increase in Ca^{2+} is toxic and contributes to the massive cell death occurring after deafferentiation. It can be prevented if neurons are stimulated

orthodromically or if mGluRs are activated (Zirpel et al., 1995a, b; Zirpel and Rubel, 1996; Zirpel et al., 1998). These experiments suggest that glutamatergic transmission via mGluRs plays protective role for auditory neurons. Second, cultured organotypic rat brainstem slices containing the LSO develop normally only when an optimal level of calcium is provided via activation of L-type voltage gated Ca^{2+} channels (Lohmann et al., 1998).

Not only is the amount of calcium critical but also the route of entry. Many studies suggest that distinct Ca^{2+} entry routes affect distinct intracellular pathways which in turn affect distinct cellular processes and distinct gene expression important for survival, development or synaptic plasticity (reviews: Ghosh and Greenberg, 1995; Gallin and Greenberg, 1995, Berridge, 1998; West et al., 2001). Sources of $[Ca^{2+}]_i$ increases consist of: a) influx of calcium from the extracellular milieu through ligand-gated channels (i.e. NMDARs, AMPARs, kainate receptors), voltage-gated calcium channels (VGCCs) or store-operated channels (SOC), and b) release of calcium from internal stores. Immature LSO neurons express all major classes of GluRs (Kandler and Friauf, 1995a; Kotak and Sanes, 1996) but whether and under what stimulus conditions specific GluRs contribute to synaptic Ca^{2+} responses and moreover the mechanisms underlying Ca^{2+} responses during development are unknown.

1.6. TRP CHANNELS

The mechanisms of calcium signaling through GluRs have been investigated in different systems and it is well documented that calcium signaling through GluRs plays critical role in development, synaptic plasticity and cell death (reviews: Hardingham and Bading, 2003; Wong and Ghosh, 2002; West et al., 2001; Kullmann et al., 2000; Tanaka et al., 2000; Konig et al., 2001). Much less is known about the mechanisms of calcium signaling through internal stores and through calcium channels activated by internal stores. Moreover, the relevance of this signaling for cellular processes is largely unknown. In this section I will review some of the

literature concerning store-operated calcium channels and transient receptor potential (TRP) channels, as they might be expressed in the LSO neurons during development and perhaps in adulthood.

1.6.1. A short history of discovery of TRP channels

The concept of "store-operated calcium entry" (SOC) or “capacitive calcium entry” (CCE) was based on a series of experiments conducted in parotid acinar and smooth muscle cells (Putney, 1976a, b). Application of the muscarinic receptor agonist carbachol triggered a biphasic release of $^{86}Rb^{+}$, used to monitor Ca^{2+} efflux from these cells. The first efflux component was unaffected by the removal of the extracellular Ca^{2+} while the second, sustained phase, was abolished by either removal of the extracellular Ca^{2+} or by incubation with La^{3+} (Putney, 1976a, b). Independent experiments conducted by Casteels and Droogmans (1981) in vascular smooth muscle cells, showed that depletion of intracellular stores stimulated the rate of $^{45}Ca^{2+}$ uptake from the extracellular solution. This Ca^{2+} entry pathway differed pharmacologically from other Ca^{2+} entry pathways in that it was coupled to Ca^{2+} stores and blocked by manganese ions (Casteels and Droogmans, 1981). Similar mechanisms were later found in many cell types including pancreatic cells, lymphocytes, mast cells (review: Putney, 1997), cerebellar granule cells (Simpson et al., 1995), astrocytes (Lo et al., 2002), and recently in neurons in the neocortex (Prothero et al., 2000) and hippocampus (Baba et al., 2003).

Based on these experiments, Putney proposed a model of SOC activation: ligand binding to G-protein linked membrane receptors initiates a sequence of events resulting in generation of inositol-1,4,5-trisphosphate (IP_3), which, in turn, leads to an initial emptying of the intracellular Ca^{2+} stores followed by a rapid influx of Ca^{2+} from the extracellular milieu and refilling of the stores (reviews: Putney, 1986; 1990). The first electrical measurement of SOCs was achieved in mast cells, where depletion of intracellular Ca^{2+} stores induced a sustained Ca^{2+} inward current through a very low conductance channel (~0.02pS; ~ three orders of magnitude smaller than single channel conductance of most ionic channels; Zweifach and Lewis, 1993; Hoth and Penner, 1992). The current was highly selective for Ca^{2+} ions over Ba^{2+}, Sr^{2+} and Mn^{2+}, was not voltage-

activated (Hoth and Penner, 1992) and was blocked by Mg^{2+}, by micromolar concentrations of lanthanides and by micromolar concentrations of divalent ions including Zn^{2+}, Co^{2+}, Ni^{2+}, Cd^{2+} and Mn^{2+} (Hoth and Penner, 1992; Lepple-Wienhues and Cahalan, 1996; review: Parekh and Penner, 1997). This current was termed "calcium-release-activated calcium current" (CRAC) (Hoth and Penner, 1992). Since then I_{CRAC} has been characterized in many cell types (review: Parekh and Penner, 1997). It was found that I_{CRAC} could be activated by a variety of procedures that empty the intracellular IP_3 sensitive stores, such as application of thapsigargin or muscarinic agonists. However, store operated Ca^{2+} entry might not occur solely through I_{CRAC} channels.

Although the SOC currents were characterized physiologically and pharmacologically, the molecular nature of the store-operated channels and their activation mechanisms remained elusive. A considerable advance has come from investigations of a Drosophila mutant that exhibited defects in the visual signal transduction pathway (Hardie and Minke, 1995; Ranganathan et al., 1995). In the fly rhabdomeres (and other invertebrates), light activates rhodopsin which in turn activates a heterotrimeric G_q-type protein. Subsequent stimulation of phospholipase C (PLC) causes an increase in intracellular IP_3 followed by release of Ca^{2+} from intracellular stores and capacitive Ca^{2+} influx. This process is associated with activation of a Ca^{2+} conductance called the receptor potential. In the rhabdomeres of the mutant fly, light induces a transient rather than a sustained, plateau-like increase in intracellular Ca^{2+}. The mutant was therefore termed *trp,* for transient receptor potential (Cosens and Manning, 1969; review Hardie and Minke, 1993; Minke and Selinger, 1996; Hardie, 1996). The defect in Ca^{2+} entry in trp mutant flies suggested the trp gene products, TRP proteins, as candidates for the plasma membrane channel activated by Ca^{2+} store depletion. The Drosophila trp gene was cloned in 1989 (Montell and Rubin, 1989) and subsequently shown to code for a Ca^{2+} permeable cation channel (Hardie and Minke, 1992). Evidence that TRPs function as ion channels comes from studies of insect Sf9 cells where TRPs expression increases store-operated Ca^{2+} entry and membrane conductance (Vaca et al., 1994).

1.6.2. Structure of TRP channels

Homologues of TRPs have been found, cloned and characterized in flies, worms and mammals including humans (reviews: Harteneck et al., 2000; Clapham et al., 2001; Zitt et al., 2002). To date, the mammalian TRP family comprises at least 21 unique proteins. They are tetramers, assembled from subunits with 6 transmembranare domains (TM1–6), cytoplasmic N- and C-termini and a pore region between TM5 and TM6 (Clapham, et al., 2001). Based on sequence homology TRP channels have been divided into three subfamilies (Clapham et al., 2001): TRPC (C for Canonical), TRPV (V for Vanilloid) and TRPM (M for Melastatin). Each subfamily contains several members numbered in the order of their discovery: TRPC1-7, TRPV1-2, 4-6 and TRPM1-7 (reviews: Clapham et al., 2001; Zitt et al., 2002). Furthermore, based on the sequence homology and functional similarities, each subfamily is divided in subgroups. The TRPC subfamily was divided into four subgroups: TRPC1, TRPC4,-5, TRPC3,-6,-7 and TRPC2. Particular members of a family exhibit high sequence similarity between species (i.e. TRPC1 shows 95% sequence similarity between bovine, murine and human species). Functional channels tend to assemble from subunits from the same subgroup (review: Clapham et al., 2001).

1.6.3. Tissue expression of TRP channels

The expression of TRP channels seems to be ubiquitous among tissue type including brain, liver, muscle, heart, kidney, and many other (reviews: Hofmann et al., 2000; Clapham et al., 2001; Montell, 2001; Riccio et al., 2002). Members of the TRPC family have been found in a variety of tissues including brain (TRPC1-7), heart (TRPC1, 3, 4, 6, 7), testis (TRPC1-6), kidney (TRPC1, 3, 6), lung (TRPC1, 3, 4, 7), vomeronasal organ (TRPC2) and eye (TRPC7) (reviews: Montell, 2001 and Garcia and Schilling, 1997). In the CNS, mRNA of all TRPC1-7 is widely distributed with TRPC3 and 5 highly enhanced (Riccio et al., 2002). Detailed studies show that TRPC3 protein is predominantly expressed in neurons in brainstem (perhaps LSO) and cortex,

during a narrow period of development (from ~E18 to P20 in rat and mice; Li et al., 1999). TRPC1 is highly expressed in all layers of the hippocampus and amygdala and in the Purkinje cell layer of the cerebellum. Here, it seems to co-assemble with TRPC5 to form a distinct channel (Strubing et al., 2001). TRPC4 is found in the olfactory bulb in the internal granular layer, and in the hippocampus in CA1 pyramidal cells where it is co-expressed with TRPC5 (Philipp et al., 1998).

In summary, TRPC channels are widely expressed in the brain. To date, only TRPC3 expression was shown to be developmentally regulated such that the channel is expressed in a narrow window around birth (Li et al., 1999).

1.6.4. Signal transduction and activation of TRPs

The signal transduction pathways for the activation of TRPs have been investigated in numerous heterologous systems and in different cell types (review: Hoffmann et al., 2000). Two main questions are still largely unanswered. One of them is whether TRPs are the channels that mediate store-operated calcium entry (TRP=SOC)? Some studies suggest that a number of TRPs are activated as a result of internal stores depletion while other TRPs are activated independently of stores. For example, TRPC4 (Phillip et al., 1996) and TRPC1 (Zitt et al., 1996; Sinkins et al., 1998) have been implicated in store-operated calcium entry. However, for TRPC3 the evidence is contradictory. In COS M6 and HEK 239 cells TRPC3 was activated by agonist-promoted store depletion, suggesting TRPC3 as an SOC (Zhu et al., 1996; Kiselyov et al., 1998). In contrast, in CHO cells it was found that TRPC3 is a nonselective cation channel independent of store depletion (Zitt et al., 1997), which can be activated by diacylglycerol (DAG) (Hofmann et al., 1999). The disparate observations may reflect differences in the cell types used for the expression studies. Recently, it was suggested that TRPs are associated with other proteins forming signaling complexes (review: Harteneck, 2003). Thus, differences in the association of TRPs with these proteins in different heterologous systems may also account for the observed discrepancies.

Another open question is what exactly activates TRP channels? The most common pathway involves metabotropic receptors coupled to G_q proteins which stimulate PLC. This in turn hydrolyses phosphatidylinositol-4,5-bisphosphate (PIP_2), which is further cleaved into two second messengers, the membrane-bound diacylglycerol (DAG) and soluble IP_3. Signaling downstream of these initial steps involves mobilization of Ca^{2+} from IP_3 sensitive intracellular stores and Ca^{2+} influx through the plasma membrane (reviews: Montell 2001, Zitt et al., 2002). From here, how exactly the TRP channels are activated is unclear. Three dominant hypotheses have been proposed: (i) diffusible messengers (cGMP, IP3, DAG, a small G protein, arachidonic acid derivatives) or calcium influx factors (CIFs) generated by store depletion (Parekh et al., 1993; Randriamampita and Tsien, 1993); (ii) exocytotic insertion of vesicular channels into the plasma membrane (Kanzaki et al., 1999); and (iii) direct interaction ("conformational coupling") between proteins in organellar and plasma membranes (Berridge, 1995). To date, there is evidence to support all three hypotheses though none has yet been proven conclusively (reviews: Montell, 2001; Hoffmann et al., 2000; Zitt et al., 2002).

In summary TRPs comprise a diverse family of Ca^{2+} channels, some of which are receptor-operated other store-operated. The mechanism(s) of TRPs activation and TRPs properties in native cells and in vivo remain to be studied.

1.6.5. Function of TRP channels

TRPs have been involved in a variety of functions including vision, temperature detection, pheromone detection, touch, sound, taste and pain (review: Voets and Nilius, 2003).

Members of the TRPC subfamily have functions in signal transduction. TRPC2 was found to be a transduction channel for sensing pheromone in the vomeronasal organ (Liman et al., 1999). TRPC2-deficient mice do not show the normal aggressive behavior towards other males. Instead they display sexual behavior towards male intruders, indicating that the absence of TRPC2 resulted in loss of sexual discrimination (Leypold et al., 2002; Stowers et al., 2002).

TRPC3 may be involved in activity-dependent changes occurring early in CNS development (Li et al., 1999). Protein expression of TRPC3 was found in a narrow window

during development (rat E18-P20) and expression paralleled that of the transmembrane receptor protein tyrosine kinase TrkB (Li et al., 1999). Activation of TRPC3 involved TrkB activation by the neurotrophin BDNF (Li et al., 1999). Since BDNF is involved in a variety of processes during development, including neuronal differentiation, survival and synaptic plasticity (review: Huang and Reichardt, 2001), it is possible that some of its effects are mediated by BDNF-stimulated Ca^{2+} influx through TRPC3.

Members of the TRPV subfamily are mostly expressed in sensory neurons and have been identified as primary sensors of both physical (heat, cold, mechanical stress) and chemical (pH, pheromones, "hot pepper" compounds) external stimuli (review: Voets and Nilius, 2003). TRPV1, the best characterized member of the family, was found to be a Ca^{2+}-permeable channel activated by vanilloids such as capsaicin and other pungent pepper compounds, and also by temperatures above 43°C, and it is believed to be involved in pain pathways (Caterina et al., 1997).

The TRPM family seems to have a role in cell-cycle regulation, as it has been shown that the downregulation of TRPM1 gene expression is related to skin cancer (Duncan et al., 1998) and TRPM8 is upregulated in prostate cancer, breast, colon, lung and skin tumors (Tsavaler et al., 2001).

TRPs may also be involved in neurodegenerative diseases. Recent studies suggest that reductions in the activity of TRP channels might be an early event leading to Alzheimer's disease (Leissring et al., 2000; Yoo et al., 2000; review: Montell, 2001). Oxidative stress could result in constitutive activation of TRP proteins. Since TRPs function as Ca^{2+} channels, increase in Ca^{2+} influx may account for cell death (review: Montell, 2001). Support for these conclusions comes from studies of the Drosophila photoreceptor cells, where mutations that cause constitutive activation of TRP result in neurodegeneration (Yoon et al., 2000).

Taken together, mammalian TRP channels function as Ca^{2+} permeable channels activated by a multitude of factors that have in common activation of PLC. In CNS, TRPC channels are expressed in individual neurons and their subunit expression pattern is region and cell-type specific. In the brainstem area, the expression of TRPC3 has been found during development only (Li et al., 1999).

1.7. SUMMARY AND SIGNIFICANCE

In summary, evidence from the auditory system and other sensory systems suggests that afferent activity via glutamatergic synaptic transmission (triggered either spontaneously or by sensory input) induces changes in the intracellular calcium levels that affect survival, growth and refinement. Thus, a clear understanding of the Ca^{2+} entry routes and of the mechanisms that affect $[Ca^{2+}]_i$ during development is critical. These questions are addressed in this study. The first chapter investigates the Ca^{2+} entry pathways activated by synaptic stimulation of AVCN-LSO synapses in developing neurons. The second chapter investigates the mechanisms by which GluRs increase $[Ca^{2+}]_i$ in neonatal LSO neurons. The last chapter investigates developmental changes of mGluR-evoked Ca^{2+} responses and the possible involvement of a TRPC channel in mediating Ca^{2+} influx in LSO neurons. Together, this study provides a comprehensive understanding of Ca^{2+} entry routes and cellular mechanisms activated during development. These mechanisms may underlie morphological and physiological changes occurring in the LSO during that period.

2. METHODS

2.1. ANIMALS AND SLICE PREPARATION

Experiments were performed *in vitro* in acute brainstem slices of mice (C57Bl/6J from Jackson Laboratory, Bar Harbor, ME; Harlan, Indianapolis, IN; Charles River, Wilmington, MA), males or females aged between postnatal day 0 (P0 - the day of birth) and P19. Experimental procedures were in accordance with NIH guidelines and were approved by the IACUC at the University of Pittsburgh. Animals between P0 to P7 were anesthetized by hypothermia and older animals were anesthetized using isofluorane. Animals were quickly decapitated, the brains removed and placed into cold (4-8 °C) artificial cerebrospinal fluid with kynurenic acid (ACSF with KA, composition in mM: NaCl 124, $NaHCO_3$ 26, Glucose 10, KCl 5, KH_2PO_4 1.25, $MgSO_4$ 1.3, $CaCl_2$ 2, kynurenic acid 1, pH 7.4 when aerated with 95% O_2/5% CO_2). Transversal slices (200-300 μm thickness) were cut using a vibrotome (DTK-1500E, Ted Pella, Redding, CA). Slices in which the LSO could be identified were transferred into a holding chamber for labeling.

2.2. FURA-2AM BULK-LABELING

This method relies on the ability of the acetoxy-methyl-ester of Fura-2 (Fura-2AM) to passively diffuse across cell membranes into the cytosol, where it is cleaved by endogenous esterases to release the cell-impermeant fluorescent dye. The labeling protocol included two steps. First, slices were incubated in a concentrated Fura-2AM solution (100 μM; Molecular Probes, Eugene, OR; Tefflabs, TX) for 2-5 minutes. Slices were then immersed in aerated ACSF containing 10 μM Fura-2AM, for 2-5 hours at 30-32ºC (Peterlin et al., 2000). Stock solutions of 1mM Fura-2AM were prepared by dissolving Fura-2AM in DMSO with 20% (w/v) pluronic acid. This method ensured labeling of numerous neurons per LSO (20-80 cells in a camera view) in slices up to P8 (example in Figure 4). Older slices were poorly or not at all labeled most likely because of poor penetration of Fura-2AM through the dense extracellular matrix.

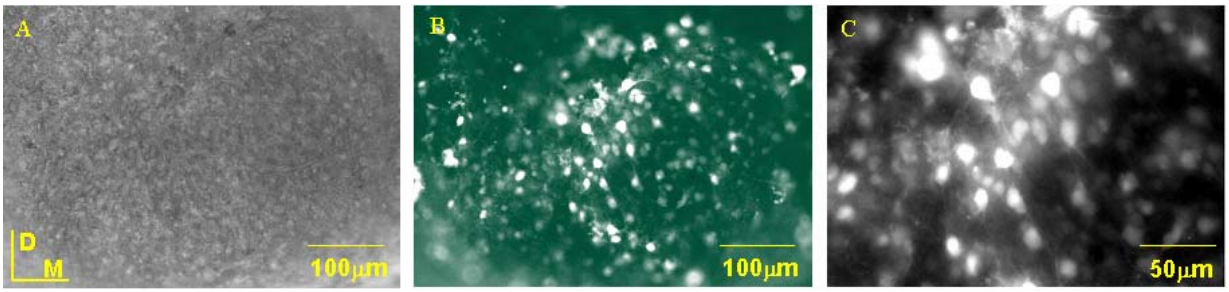

Figure 4. Fura-2 staining of LSO neurons in brainstem slices from neonatal mice.

A. Bright field image of the LSO from a P3 mouse. **B.** Fluorescence image with 380 nm excitation of the same LSO shown in A. Numerous cells along the extent of the LSO are labeled (10x objective). **C.** Higher magnification (20x objective) reveals that most labeled cells have a typical neuron-like appearance. D-dorsal, M-medial.

2.3. RETROGRADE LABELING OF LSO NEURONS

In order to establish that Fura-2AM-labeled cells were neurons as opposed to glia, rhodamine labeled beads (40 nl, Red Retrobeads, Lumafluor, Naples, FL) were injected bilaterally into the inferior colliculus (IC; the primary target of LSO neurons) of P1 rats, using a nanoliter injector (Nanoejector II, Drummond, Broomall, PA). During the procedure, pups were anesthetized by hypothermia. After injection, rats were sutured, kept under observation until they recovered and returned to their mothers. Brainstem slices (300 µm) were prepared at P3 and labeled with Fura-2AM as described above. Beads were visualized with 548 nm excitation (Monochromator Polychrome II, T.I.L.L. Photonics, Martinsried, Germany) and a 590 nm long pass emission filter (Chroma Technology, Brattleboro, VT). Double labeling was verified in n = 11 cells in N = 3 slices from 2 animals (Figure 5).

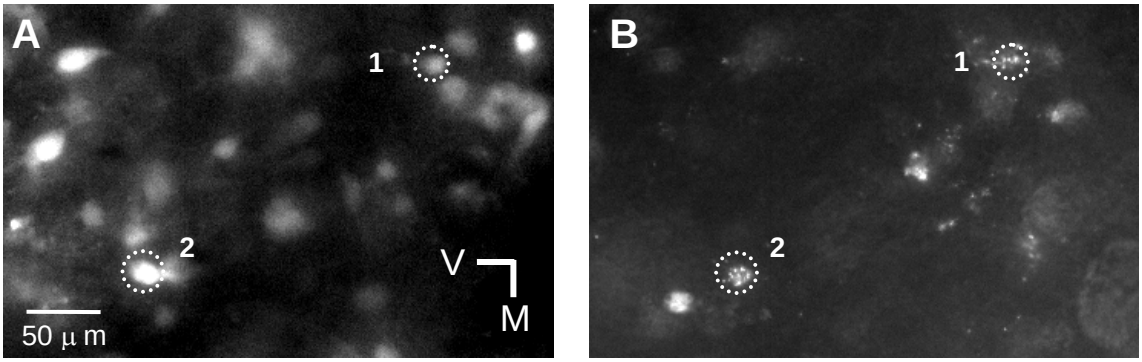

Figure 5. Fura-2 stains neurons in the LSO.

A. Fluorescence image with 380 nm excitation of Fura-2 labeled cells in a P3 rat. **B.** In the same slice some cells are retrogradelly labeled with rhodamine beads, identifying them as IC - projecting neurons. V-ventral, M-medial. Figure adapted from Kullmann et al., 2002.

2.4. FURA-2AM SPIN-LABELING: A NOVEL METHOD FOR JUVENILE MOUSE SLICES

For slices from older animals (>P10) a new method was developed: spin-labeling. This method uses centrifugation to force Fura-2AM to pass through the slice. For this, slices containing the LSO were cut in half and each hemisphere was placed on filter paper (12 μm pores; Corning Incorporated Life Sciences, Acton, MA) in an interface chamber to allow recovery for 15-30 minutes. Slices were then placed into a centrifugal filter device containing a 10 kDa cutoff molecular filter (molecular weight of Fura-2AM is 1001.86Da). The filter was inserted in a 1.5 ml microcentrifuge tube (Amicon, Milipore Corporation, Bedford, MA). Slices were covered with 75 μl Fura - 2AM (100 μM; dissolved in ACSF with KA) and aerated with 95% O_2/5% CO_2. The 1.5 ml microcentrifuge tube was placed into a 50ml plastic tube and then centrifuged for 15-20 min at 428g (IEC Clinical Centrifuge, International Equipment Company, USA) so that most of the Fura-2AM solution passed through the filter. Slices were returned to the interface chamber until they were used for calcium imaging. This method ensures labeling of several cells (>5) per slice while preserving the synaptic connections from the AVCN to the LSO.

To characterize the efficiency of the spin-labeling method versus the bulk-labeling method, two parameters were used: the number of labeled cells per area and the average fluorescence intensity of the cells at 360 nm. The reason for the first parameter is trivial: more labeled cells mean more data per slice, and therefore fewer animals are needed. The reason for the second parameter was to establish that by using this method cells are not too weakly labeled nor are they overloaded with calcium indicator. Although Fura-2 is a ratiometric dye and therefore the concentration of the dye in the cell should have no effect on $[Ca^{2+}]_i$ estimation, it was found that in high concentrations the dye can disturb the intracellular physiology of cells. It can also interfere with the endogenous buffering capacity of the cell leading to errors in estimation of Ca^{2+} concentrations (Neher and Augustine, 1992). The measurement at 360 nm was chosen since it is the isosbestic point of Fura-2 where the fluorescence is not affected by changes in Ca^{2+} concentration.

To determine the optimal conditions for spin-labeling several parameters were tested: Fura-2 concentration, ACSF osmolarity and the presence of TEA.

The effect of Fura-2AM concentration was tested in slices from P13-15 animals. Four concentrations were tested: 50μM (N=2 slices), 100μM (N=8 slices), 200μM (N=2 slices) and 500μM (N=2 slices). It was found that the number of labeled cells per area was independent of the Fura-2AM concentration above 100μM (ANOVA between groups, $p>0.05$; Figure 6). Given these results 100μM Fura-2AM was used as standard labeling protocol in subsequent experiments.

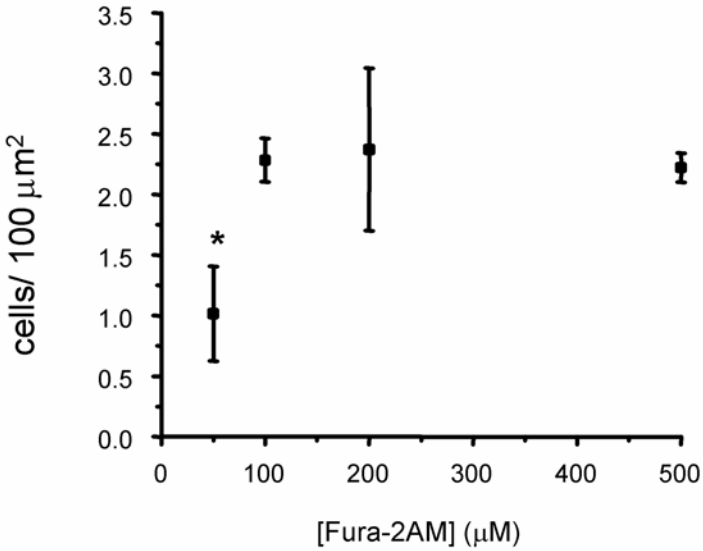

Figure 6. The effect of Fura-2AM concentration on the number of labeled cells.

For concentrations above 100μM the number of cells is not significantly different (ANOVA $p>0.05$). 50 μM is significantly different from 100μM (ANOVA $p<0.05$). Slices are from P13-15 animals, N= 2, 8, 2, 2 slices respectively.

The effect of osmolarity was also evaluated in slices from P13-15 animals. It was thought that a hyperosmotic shock produces shrinkage of cells and allows better Fura-2 penetration through the tissue, such that more Fura-2 gains access to the cell membrane. To test whether producing an osmolarity shock increases the quality of labeling, 100μM Fura-2 was suspended in 300 mOsm and 400 mOsm ACSF. At higher osmolarity, the number of cells per area decreased slightly but not significantly (from 2.2 ± 0.1 to 1.6 ± 0.1 cells/100 μm^2; t-test p= 0.0378, N=8 slices for 300 mOsm and N=4 slices for 400 mOsm). These results indicate that high osmolarity does not increase the quality of labeling. Subsequent experiments were performed with 300mOsm ACSF, the same osmolarity as used for bulk-labeling.

Finally, the effect of 10mM TEA was tested in two slices at P15 and P19. TEA has been shown to increase the labeling quality in cortical slices older than P10, though the mechanism is unknown (Peinado, 2001). In my hands, the labeling quality did not improve. In addition in the P19 slice, the few labeled cells failed to respond to 60mM KCl, suggesting that TEA might have deleterious effects on cell healthiness. Therefore subsequent experiments were performed without TEA.

After these tests, the standard protocol for labeling used 100μM Fura-2AM in 300mOsm ACSF + KA, without TEA. The following results (Figure 7; Figure 8) illustrate the efficiency of spin-labeling versus bulk-labeling. Data are from 3-11 slices per each age group. At younger ages (P0-5) both methods yield similar numbers of labeled cells. With age, the number of labeled cells decreases using both methods. However, the decrease is slower using spin-labeling (compare black trace with grey trace in Figure 7 A) and therefore enabled us to extend Ca^{2+} imaging up to P18-20. Slices older than P23 were poorly labeled (1-2 cells per slice). The fluorescence values measured at 360 nm were similar across ages (Figure 7 B). Examples from individual slices are shown in Figure 8 A-F.

Two additional controls were performed for Ca^{2+} profiles and resting Ca^{2+} concentrations. Figure 9 shows that Ca^{2+} responses after stimulation with the group I mGluR agonist DHPG (50μM, 90s) or with KCl (60mM, 30s) are similar (examples from P3 for spinning and P4 for incubation). Resting Ca^{2+} concentrations at the beginning of the experiment were not significantly different (spin-labeling: 109.2±57.6 nM, n=70 cells, N=3 slices, P3; bulk-labeling: 94.2 ± 47.6 nM, n=96 cells, N=4 slices, P2-4; t-test p>0.01).

Spin-labeling, similar to bulk-labeling, preserves the synaptic connections between AVCN and LSO. Figure 10 shows an example of Ca^{2+} response to electrical stimulation of the ventral acoustic stria (VAS) in a P11 slice. However due to the small number of labeled cells at older ages the number of cells responding to synaptic stimulation is very low (in average less than 1 cell/slice).

In summary, with limitations described above, this method can be used for labeling juvenile brainstem slices.

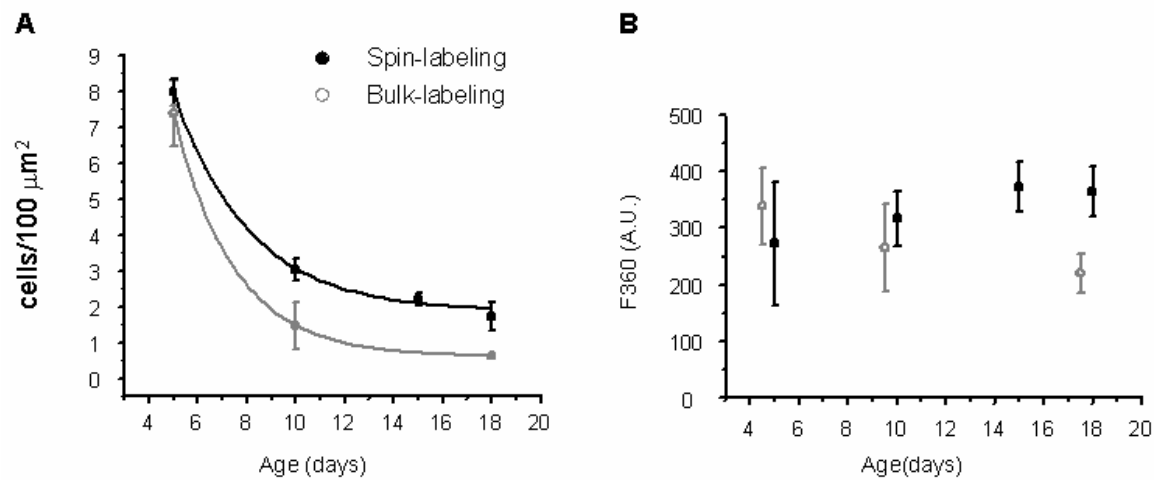

Figure 7. Bulk-labeling versus spin-labeling.

A. Number of labeled cells per area as a function of age. Grey data points are from bulk labeled slices; black data points are from spin-labeled slices. Data were fitted with a single exponential. Note the slower decrease in the case of the spin-labeling method. **B.** Fluorescence at 360 nm as a function of age (exposure time 20msec, 20x objective). Data are average ± SEM.

P0-5: N=7 slices for bulk-labeling; N=3 slices for spin-labeling,

P10: N=3 slices for bulk-labeling; N=8 slices for spin-labeling,

P15: N=11 slices for spin-labeling,

P18: N=3 slices for bulk-labeling; N=6 slices for spin-labeling.

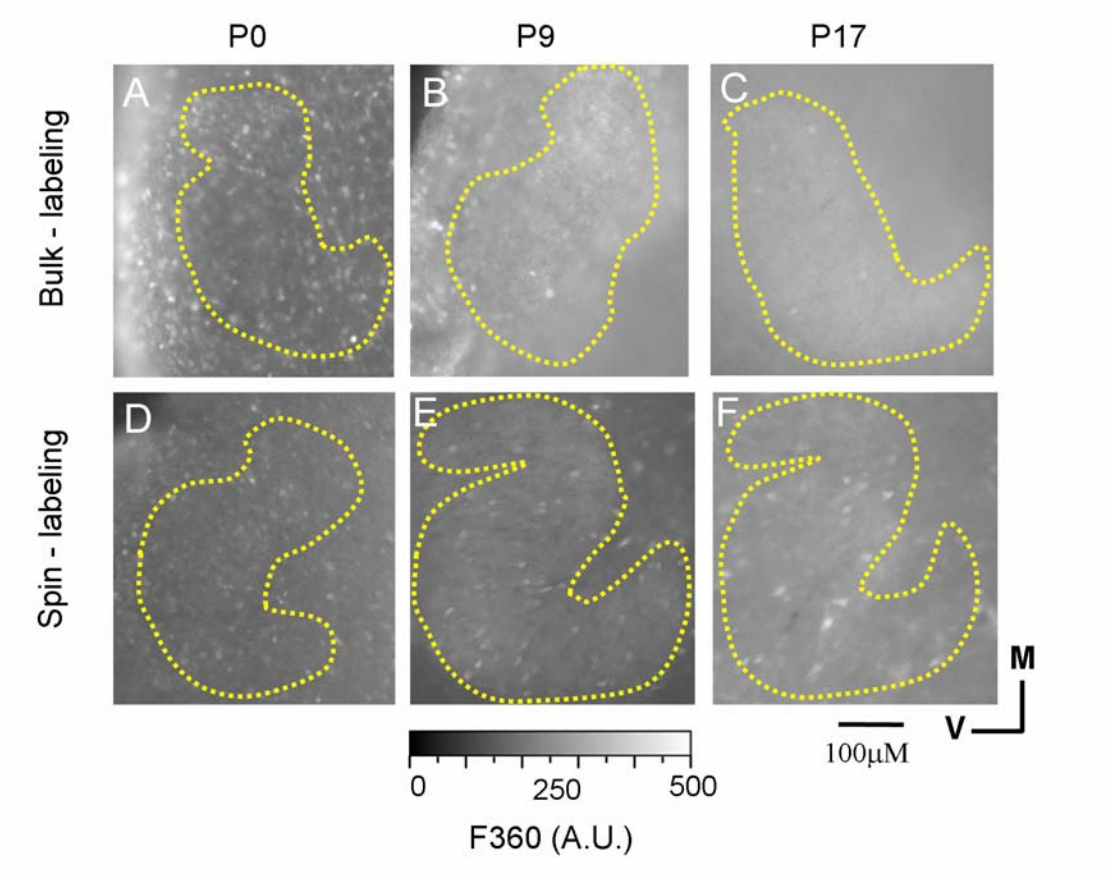

Figure 8. Examples of LSO slices labeled using bulk-(A-C) and spin-labeling (D-E).

Slices are at ages P0, P9, P17 respectively. The number of labeled cells in older slices is higher using the spin-labeling method (E, F). All images show fluorescence at 360 nm, exposure time 20msec, and 20 x objective. Yellow dotted lines outline the LSO. V-ventral, M-medial.

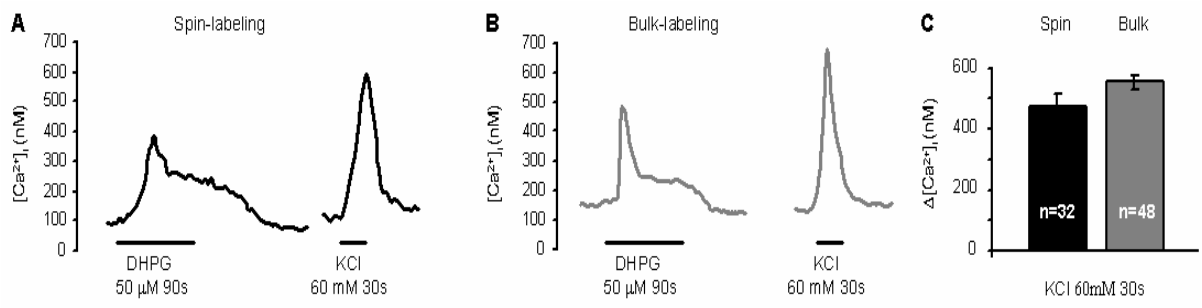

Figure 9. Ca^{2+} profiles in response to mGluR agonists and to KCl are similar using both labeling methods.

Ca^{2+} responses are elicited by bath application of DHPG (50µM, 90s) and KCl (60mM, 30s). **A.** Spin-labeling: example from a P3 slice. **B.** Bulk-labeling: example from a P4 slice. **C.** Average amplitude of Ca^{2+} responses to 60mM KCl; Summary from n=32 cells at P3 for spin-labeling and from n=48 cells at P2-4 for bulk-labeling.

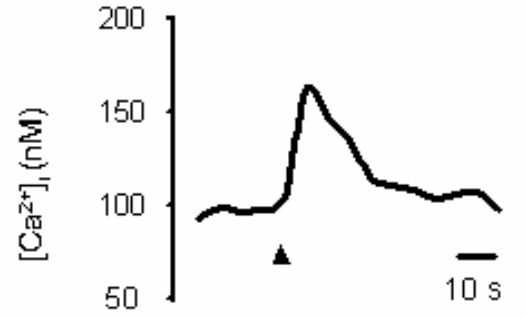

Figure 10. Spin-labeling preserves synaptic connections from AVCN to LSO.

Example of a P11 cell responding to electrical stimulation of the ipsilateral ventral acoustic stria. Arrowhead marks the beginning of stimulation. Stimulus consists of 10 pulses at 50Hz.

2.5. CALCIUM IMAGING

Individual slices were transferred into a recording chamber continuously perfused with oxygenated ACSF (30 - 32 ºC, perfusion rate 2-3 ml/min) for 15-20 minutes to wash out kynurenic acid and to remove excess Fura-2AM. To prevent photodamage of the cells the ACSF used during imaging contained a cell-permeant antioxidant, Trolox, (100μM prepared from 100mM stock solution in 0.1 N NaOH; Scheenen et al., 1996). Imaging was performed using either an upright epifluorescence microscope (BX50WI, Olympus America, Melville, NY) equipped with 10x and 20x water-immersion objectives (NA: 0.3 and 0.5 respectively; Olympus America, Melville, NY), or with an inverted epifluorescence microscope (Eclipse TE200 Nikon, Japan) equipped with 10x and 20x air objectives (NA: 0.5 and 0.75 respectively; Nikon, Japan). The LSO was identified using transmission images (Figure 4). Fura-2-loaded neurons (Figure 4 B, C) were alternately excited with UV light at 340 nm and 380 nm (bandwidth 15 nm) using a computer controlled monochromator (Polychrome II, T.I.L.L. Photonics, Martinsried, Germany). Image pairs were acquired every 1 to 20 s using an exposure time between 20 and 60 ms. Fluorescence emission was filtered (510/80 nm band pass filter, Chroma Technology Corp., Brattleboro, VT) and detected with a 12 bit, cooled, interline-transfer CCD camera (IMAGO, T.I.L.L. Photonics). Wavelength selection, timing of excitation, acquisition of images, and triggering of stimulating devices were controlled using the program Tillvision (T.I.L.L. Photonics) running on a Pentium based computer. Digital images were stored on hard disk for off-line analysis. The intensity of fluorescence was converted to $[Ca^{2+}]_i$ using the ratio (R) of the fluorescence recorded at 340 nm and 380 nm, in accordance to the Grynkiewicz equation (Grynkiewicz et al., 1985): $[Ca^{2+}]_i = K_d \beta (R-R_{min})/(R_{max}-R)$, where R_{min} is the fluorescence ratio of Ca^{2+}- free Fura-2, R_{max} is the ratio of Ca^{2+}- bound Fura-2, β is the ratio of the fluorescence intensity of Ca^{2+}- free Fura-2 at 380 nm to the fluorescence intensity of Ca^{2+}-bound Fura-2 at 380 nm. R_{min}, R_{max} and β were determined using a calibration procedure carried out in slices as described in Kao (1994). In short, slices were first incubated in Ca^{2+} - free ACSF (Ca^{2+} was replaced by Mg^{2+} and 2 mM EGTA was added) and 4 μM Ca^{2+} ionophore Br-A23187 to determine R_{min}. The Ca^{2+} - free ACSF was then replaced with ACSF containing 10 mM $CaCl_2$ to

determine R_{max}. Finally, 5 mM manganese was added to quench the fluorescence of Fura-2 in order to determine background values at 340 and 380 nm, which were than subtracted from all other measurements. Over the course of this study the system was calibrated repeatedly to correct for variations in the intensity of the light (i.e. aging of the fluorescence lamp). The values for R_{min} ranged from 0.25 - 0.31, for R_{max} from 1.22 - 1.8, and for β from 2.3 - 3.7.

2.6. ELECTRICAL STIMULATION

Excitatory afferents from the AVCN to the LSO were stimulated using bipolar electrodes (manufactured from two stainless steel microelectrodes, insulated except at the tip; tip distance 100–200 μm; FHC, Bowdoingham, ME). Stimulation electrodes were placed in the ipsilateral ventral acoustic stria (VAS; which carries the majority of excitatory afferents from the AVCN; review: Thompson and Schofield, 2000), lateral to the LSO (Figure 11). Current pulses were produced using a programmable pulse generator (Master-8; A.M.P.I., Israel) and an isolation unit (ISO-Flex; A.M.P.I., Israel). Ca^{2+} responses were evoked in LSO neurons using single pulses (S; pulse duration 100 μs) and trains of pulses at low frequencies (LF; 10 pulses at 5 Hz-10 Hz) and high frequencies (HF; 10 pulses at 20 Hz-100 Hz). The stimulus intensity ranged from 50 - 300 μA.

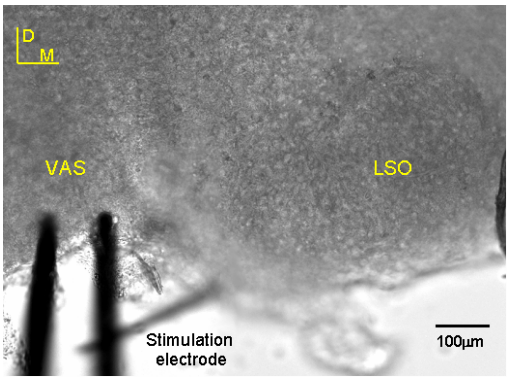

Figure 11. Electrical stimulation of the ipsilateral ventral acoustic stria.

Brightfield image of a brainstem slice from a P3 mouse, illustrating the position of the stimulation electrode relative to the LSO. D-dorsal, M-medial. Figure adapted from Ene et al., 2003.

2.7. ELECTROPHYSIOLOGY

These experiments were carried out in collaboration with Dr. Deda Gillespie.

a) For AMPA ionophoresis, visualized whole-cell patch clamp recordings were performed in voltage clamp mode (V_{hold}: –65mV) at room temperature. Recording electrodes had resistances of 2–3 MΩ and were filled with a solution containing (in mM): 110 d-gluconic acid, 110 CsOH-H_2O, 11 EGTA, 10 CsCl, 1 $MgCl_2$, 1 $CaCl_2$, 10 HEPES, 0.3 Na-GTP, and 2 Mg-ATP-3.5H_20. To isolate AMPAR-mediated currents, DL - APV (50µM), MCPG (1mM), bicuculline (10µM), strychnine (5µM), and TTX (1µM) were added to the ACSF. Desensitization of AMPARs was prevented with CTZ (50µM). AMPA (10mM in 0.15 M NaCl, pH 7.5) was ionophoretically applied close to the soma using pipettes with resistances ~ 70 MΩ. Retaining current was 20-50

nA (BVC-700, Dagan Corp., Minneapolis, MN) and ejection current was 30-50 nA for 2s. Membrane currents were filtered at 1 kHz (Axopatch 1D, Axon Instruments), digitized (National Instrument AD board), and stored for off-line analysis. Data acquisition and analysis was performed using custom-written software running under the LabVIEW environment (National Instruments, Austin, TX), Origin (OriginLab Corporation; Northampton, MA) and Excel (Microsoft product).

b) For recordings of excitatory postsynaptic potentials (EPSP), the internal solution contained (in mM): 110 K-gluconate, 11 EGTA, 10 KCl, 1 $MgCl_2$, 1 $CaCl_2$, 10 HEPES, 0.3 Na-GTP, and 2 Mg-ATP-3.5H_20 and QX-314 (5mM), which was added to prevent cell spiking. Recordings were performed in current clamp, adjusting current injection to yield a V_m of ~ -60mV. The ipsilateral pathway was stimulated as described in section 2.6, using low and high intensity single stimuli and low frequency stimulus trains. The minimal current that elicited reliable EPSPs (failure rate < 10%) was used for low intensity stimuli. An amplitude 3x threshold was used for high intensity stimulation. For low frequency stimulus trains, 10 stimuli were applied at 10 Hz with low stimulus intensities.

2.8. DRUG APPLICATION

Drugs were dissolved in ACSF from concentrated stock solutions and delivered via bath application or via pressure application using short pressure pulses (10 psi, 100 – 1000 ms duration; PV 820 picopump, WPI, Sarasota, FL).

Several categories of drugs were used in this study and they are listed in the following table (Table 1):

Table 1. Drugs used in this study.

Receptors/channels	Drug	Concentration	Effect	Source
NMDAR	NMDA	50 μM	agonist	Tocris, Ballwin, MO
NMDAR	D-L APV	50-100 μM	antagonist	Tocris, Ballwin, MO
AMPAR	AMPA	20 μM; 1mM	agonist	Sigma, St. Louis, MO
AMPAR	GYKI 52466	50 μM	antagonist	Gift from Dr. E. Aizenman
AMPAR	CTZ	50 μM	prevents receptor desensitization	RBI, Natick, MA
AMPAR, kainate receptor	CNQX	10-20 μM	antagonist	Tocris, Ballwin, MO
kainate receptor	kainic acid	25 μM	agonist	Sigma, St. Louis, MO
group I mGluR	DHPG	10-20 μM	agonist	Tocris, Ballwin, MO
group II mGluR	4C3HPG	200 μM	agonist	Tocris, Ballwin, MO
group III mGluR	L-AP4	200 μM	agonist	Tocris, Ballwin, MO
group I, II mGluR	ACPD	20-50 μM	agonist	Tocris, Ballwin, MO
group I, II mGluR	MCPG	1 mM	antagonist	Tocris, Ballwin, MO
$GABA_AR$	Bicuculline	10 μM	antagonist	Tocris, Ballwin, MO
GlyR	Strychnine	2-10 μM	antagonist	Sigma, St. Louis, MO
VGCCs and TRP channels	Ni^{2+}	2-5 mM	nonspecific blocker of all VGCCs and nonspecific blocker of TRP channels	Sigma, St. Louis, MO
L-type VGCC	nifedipine	10 μM	specific inhibitor	Tocris, Ballwin, MO

Table 1 (continued).

N - type VGCC	ω-Conotoxin GVIA	50-1000 nM	irreversible inhibitor	Alomone Labs, Jerusalem, Israel
P/Q - type VGCC	ω - Agatoxin TK	50 nM	irreversible inhibitor	Alomone Labs, Jerusalem, Israel
VGCCs	KCl	30- 60 mM	Activates VGCCs	Sigma, St. Louis, MO
TRP channels	La^{3+}	100-2000 μM	nonspecific blocker of TRP channels	Sigma, St. Louis, MO
TRP channels	2-APB	1-100 μM	nonspecific blocker of TRP channels; inhibitor of IP_3Rs	Calbiochem, San Diego, CA
PLC inhibitor	U73122	10μM	inhibitor	RBIChemicals,Natick,MA
Na^+-channel	tetrodotoxin (TTX)	1 μM	blocker	Alomone Labs, Jerusalem, Israel
endoplasmatic reticulum ATPases	thapsigargin	10 μM	inhibitor	Alomone Labs, Jerusalem, Israel

Experiments using electrical stimulation of the excitatory afferents were performed in the presence of bicuculline (10 μM) and strychnine (10 μM) to block possible ipsilateral glycinergic and GABAergic synaptic responses (Wu and Kelly, 1994). Bath applications of agonists of GluRs were performed in TTX (1 μM) to block spike-dependent neurotransmitter release. In experiments performed in the absence of external calcium, calcium was exchanged for magnesium and 2mM EGTA was added (ACSF composition in mM: NaCl 124, $NaHCO_3$ 26,

Glucose 10, KCl 5, KH_2PO_4 1.25, $MgSO_4$ 1.3, $MgCl_2$ 2, EGTA 2, pH 7.4 when aerated with 95% O_2/5% CO_2). In experiments performed in the absence of external magnesium, magnesium was removed from the ACSF.

2.9. HISTOLOGY

Histology using Nissl stain was performed to verify that recordings were from LSO neurons. At the end of each experiment slices were fixed in 4% PFA and stored at 4 ºC. Slices were placed in 30% sucrose overnight (until they sank completely; at 4 ºC), and sectioned to 50 – 60 μm using a freezing microtome (American Optical Company, Buffalo, NY). Sections were collected in 0.1M PBS and Nissl-stained following a routine lab protocol. Data from slices in which the LSO was not clearly identified were discarded.

2.10. DATA ANALYSIS

2.10.1. Imaging data analysis

Image analysis was performed using the program Tillvision (T.I.L.L. Photonics). Data to be analyzed constituted a series of image pairs acquired at 340 and 380 nm excitation, before, during, and after drug application. Digital images were smoothed with a low-pass, Gaussian 3x3

kernel filter and the background was subtracted. The background subtraction was aimed to eliminate the camera dark noise and the tissue autofluorescence. To perform similar background subtraction for all experiments an empirical method similar to Betz and Bewick (1993) was employed. From each 380 nm image in a series, the lowest pixel value was subtracted. From the 340 nm images in a series, histograms of all pixel values in that series were constructed. The peak of the histogram, the mode, was determined for each image. An average of the mode values of images constituting the baseline was determined and 80% of this value was subtracted from all 340 nm images in that series. Using this procedure most of the cell bodies were visible against the background. Measurements were obtained from the soma of LSO neurons. An area of interest was drawn around the soma and the average value of all pixels included in this area was taken as one measurement. The intensity of fluorescence was converted in absolute $[Ca^{2+}]_i$ using the Grynkiewicz equation (as described above). Cells which were out of focus, cells with high resting $[Ca^{2+}]_i$ (>250nM; indicating sick cells; Zirpel and Rubel, 1996), cells in which the amplitude of Ca^{2+} responses saturated the Fura-2 signal ($[Ca^{2+}]_i$ >1500 nM; Fura-2 does not reliably report $[Ca^{2+}]_i$ above 1.5-2 μM), and cells which did not return to resting $[Ca^{2+}]_i$ after stimulation were excluded from further analysis. Excel and Origin were used for data analysis.

2.10.2. Electrophysiological data analysis

Five to ten EPSP traces were averaged and peak amplitude and area of the response were measured. The latter was determined by fitting a monoexponential curve to the decaying phase of responses, using the intersection of the fit with the baseline V_m as the end point of the response. Excel and Origin were used for data analysis.

2.10.3. Pharmacology data analysis

a) Quantification of Ca^{2+} responses elicited by electrical stimulation of the VAS. Baseline Ca^{2+} concentration was determined from the average of at least three measurements obtained in a time window of 2 s before electrical stimulation. Amplitude of Ca^{2+} responses was computed as the difference between the peak value and the baseline value. Peak value was measured in a time window of 1-2 s after stimulation. In order to count as Ca^{2+} responses, changes in $[Ca^{2+}]_i$ had to occur immediately after stimulation, and their amplitudes had to exceed 2 standard deviations (SD) of the baseline.

b) Quantification of Ca^{2+} responses elicited by the group I mGluR agonist DHPG (50uM, 90) during development. Traces were aligned to the onset of the response (time 0) and the following parameters were measured: baseline, peak amplitude, plateau amplitude, duration, area and decay time constant. Baseline was measured as an average of at least 5 measurements before drug application, in the window -50s to 0s. Peak amplitude was measured as the maximum response in the window 0 to 40s. Plateau amplitude was measured as average of 5 data points in the window 80 to100s (Figure 12 A). Duration was measured from the onset of the response until the response returned to baseline. Area was calculated as area under the curve (Figure 12 B). For decay time constant, baseline was subtracted and traces were fitted a single exponential to the falling phase of the response from peak to baseline (Figure 12 C). Additional parameters including ratio between peak amplitude and plateau amplitude, ratio between peak amplitude and area were calculated to better categorize the responses. Cells were classified in three groups: peak and plateau (pp), peak small plateau (psp) and peak no plateau (pnp). The following criteria were imposed when assigning cells to a certain group:

1. the existence of a plateau phase, which was quantified by the amplitude of the plateau.
2. duration of the response
3. ratio peak/plateau
4. decay time constant.

Using these criteria, responses without plateau phase (pnp) were immediately sorted out. For distinguishing between pp and psp cells additional criteria were imposed. These criteria were established empirically based on parameters from pp cells at P0-5. The constraints imposed were

that traces have a clear peak and plateau phase and all parameters (peak, plateau amplitude, and area) are at least 25% smaller than those of pp cells at P0-5. All cells could be easily assigned to a group, with the exception of 11 cells from the P17-19 age group. Four of these cells had a clear peak and plateau, long duration, long decay time constant, though the amplitudes of peak and plateau were smaller than the established criteria. They were assigned to the pp group. The remaining 7 cells did not have a clear peak and plateau and the duration was shorter; they were assigned to the psp group.

c) Dose response curves were fitted with the sigmoid function (already built in Origin): $y= A_2 + (A_1-A_2) / (1 + (x/x_0)^p)$, where x_0 = center, p = power, A_1 = initial y value, A_2 = final y value. The y value at x_0 is half way between the two limiting values A_1, A_2:
$y(x)= (A_1+A_2)/2$.

d) $[Ca^{2+}]_i$ oscillations. To determine the frequency of oscillations the number of local peaks occurring after the agonist application was counted and divided by the time interval. The first peak considered being the response to the agonist was not counted. The time interval was taken from the first to the last spike in a recorded sweep.

2.10.4. Statistics

Statistical significance of the data was analyzed, using paired t-test, ANOVA followed by Student Newman-Keuls post-hoc test, Fisher's exact test and linear (Pearson) correlation test. If data were not normally distributed, the Mann-Whitney non-parametric statistical test was used. Results are expressed as arithmetic mean ± SEM. GraphPad InStat software was used for statistical tests.

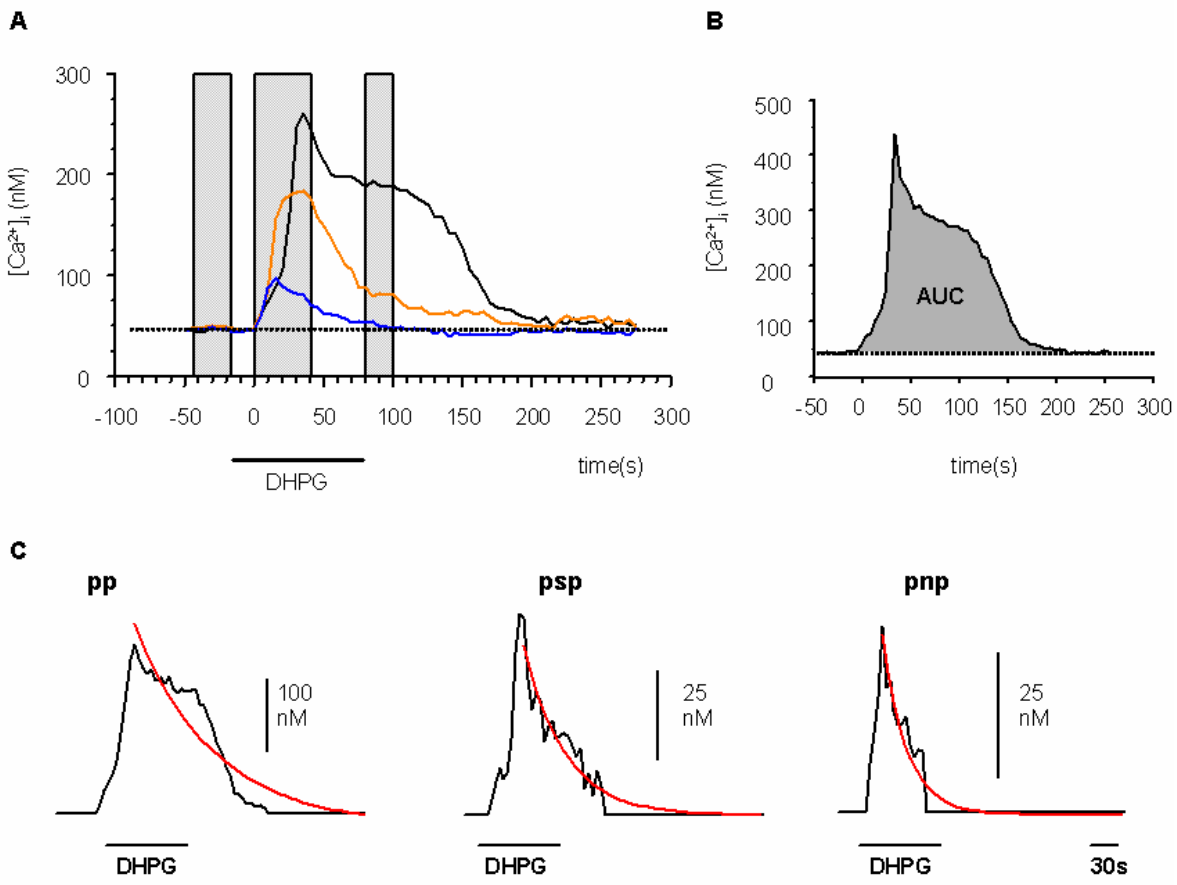

Figure 12. Measurements for response type classification.

A. Measurement of baseline, peak and plateau amplitude. Traces show pp, psp and pnp profiles aligned to the stimulus onset. Shadowed areas represent the windows in which baseline, peak and plateau amplitude were measured, respectively. **B.** Measurement of area under the curve (AUC). Dotted line represents baseline and grey area represents area of the response. **C**. Measurement of the decay time constants. Baseline was subtracted from each trace and the falling phase of the trace was fitted with a single exponential.

3. CHAPTER 3. CONTRIBUTION OF GLUTAMATE RECEPTORS TO SYNAPTICALLY ELICITED CALCIUM RESPONSES IN NEONATAL LSO NEURONS

3.1. INTRODUCTION

Spontaneous activity originating in the cochlea plays a critical role in the development of LSO circuitry prior to hearing onset (review: Sanes and Friauf, 2000). Manipulations intended to decrease or eliminate spontaneous activity, i.e. cochlea removal or inhibition of auditory nerve activity, results in profound alterations in the physiology and pathology of neurons and their circuitry (review: Sanes and Friauf, 2000). For example, unilateral cochlea ablation before hearing onset weakens glutamatergic transmission at synapses from AVCN to LSO (Kotak and Sanes, 1997). In the LSO ipsilateral to the ablated cochlea, maximum amplitude of the ipsilaterally elicited EPSP is significantly smaller in manipulated animals. Furthermore, the number of neurons responding with an EPSP decreases from over 90% in control animals to approximately 60% in ablated animals (Kotak and Sanes, 1997), most likely as a consequence of cell death in the AVCN (review: Rubel et al., 1990; Mostafapour et al., 2000). In the LSO contralateral to the ablated cochlea, the amplitude and duration of evoked EPSPs increases in manipulated neurons compared to age-matched controls. The duration of the EPSPs is reduced by hyperpolarizing the neurons and by the NMDAR antagonist APV, suggesting an increase in NMDAR expression (Kotak and Sanes, 1996). An interesting property of the spontaneous activity in the auditory system prior to hearing onset is its pattern which consists of bursts followed by periods of quiescence (Lippe 1994, Kotak and Sanes, 1995). Interfering with the pattern of activity has effects on development (see Introduction Section 1.4). In addition,

glutamate may also be a trophic factor early in ontogeny, regulating growth, differentiation and migration (review: Mattson, 1988; LoTurco et al., 1995; Gallo et al., 1996). Thus determining the nature of GluRs that mediate these effects is of great interest. Altogether, there is evidence that both spontaneous activity and glutamatergic transmission are crucial for the development and survival of auditory LSO neurons.

Neuronal activity is translated into morphological changes through intracellular calcium signaling. Several lines of evidence, from both chick and rodents, indicate that calcium plays a critical role for survival and development of auditory brainstem nuclei. For example, removal of cochlea in embryonic chicken results in an increase in $[Ca^{2+}]_i$ in nucleus magnocellularis, increase which is toxic and contributes to cell death occurring after deafferentiation (Zirpel et al., 1995a). Also, cultured organotypic brainstem slices containing the LSO develop normally only when an optimal level of calcium is provided via activation of L-type voltage gated Ca^{2+} channels (Lohmann et al., 1998).

In summary, spontaneous activity, glutamatergic transmission and intracellular calcium signaling play critical roles in development. However, the mechanisms by which glutamatergic synaptic activity affects $[Ca^{2+}]_i$ in the LSO are poorly understood. To address this question this study investigates the routes of Ca^{2+} entry into LSO neurons in response to stimulation of the excitatory synapses from the AVCN to the LSO.

Anatomical and electrophysiological data indicate that developing LSO neurons express all major classes of ionotropic and metabotropic glutamate receptors (Caspary and Faingold, 1989; Wu and Kelly, 1992; Kandler and Friauf, 1995a; Kotak and Sanes, 1995; Kotak and Sanes, 1996; Caicedo and Eybalin, 1999). Thus glutamatergic synapses could elicit calcium responses by activating ionotropic receptors (iGluRs: NMDARs, AMPARs, kainate receptors) and metabotropic glutamate receptors (mGluRs). In turn, activation of iGluRs can lead to membrane depolarizations and activation of VGCCs. Ca^{2+} responses were measured at the some of LSO neurons. However, in mature LSO neurons most glutamatergic inputs are located on dendrites (Cant and Casseday, 1986; Glendenning et al., 1985). Caution must be taken when interpreting these data. Using a combination of Ca^{2+} imaging, electrophysiology and pharmacology the following experiments were designed to assess the participation of each GluR type to changes in the $[Ca^{2+}]_i$.

3.2. RESULTS

Results presented here include data from 186 neurons from 16 slices from animals aged between P0-P7.

3.2.1. Synaptically elicited calcium responses

Electrical stimulation of the ipsilateral ventral acoustic stria (VAS) consistently evoked Ca^{2+} responses in neurons throughout the LSO (Figure 13 A). Consistent with previous electrophysiological studies (Caspary and Faingold, 1989; Wu and Kelly, 1992; Kandler and Friauf, 1995a; Kotak and Sanes, 1995), these responses were mediated by glutamate via activation of NMDA, AMPA and mGlu receptors. These responses were abolished by a mixture of the GluR antagonists, APV (50 - 100 μM), CNQX (20 μM), and MCPG (1 mM), and recovered after washout of all antagonists (n = 45 cells; Figure 13 B). The profile of these responses was dependent on the stimulation frequency (Figure 13 A, C). Ca^{2+} responses evoked by single stimuli were characterized by small amplitudes (51 ± 7 nM, n = 54 cells; Figure 13 A, C) and relative short durations, returning to the baseline within 2 - 5 s. Ca^{2+} responses evoked by low frequency stimulation (5, 10 Hz) were characterized by intermediate amplitudes (138 ± 13 nM, n = 66 cells; Figure 13 A, C) and longer durations, returning to the baseline within 5 - 15 s. Finally, Ca^{2+} responses evoked by high frequency stimulation (20-100 Hz) were characterized by large amplitudes (232 ± 19 nM, n = 66 cells; Figure 13 A, C) and long durations, returning slowly to the baseline (more than 15 s).

The effects of stimulus frequency on response amplitude and duration could be due to frequency-dependent recruitment of the number of GluRs and/or the type of ionotropic and metabotropic GluRs. To address these possibilities, the recruitment of different GluR types as a function of stimulation frequency was investigated next.

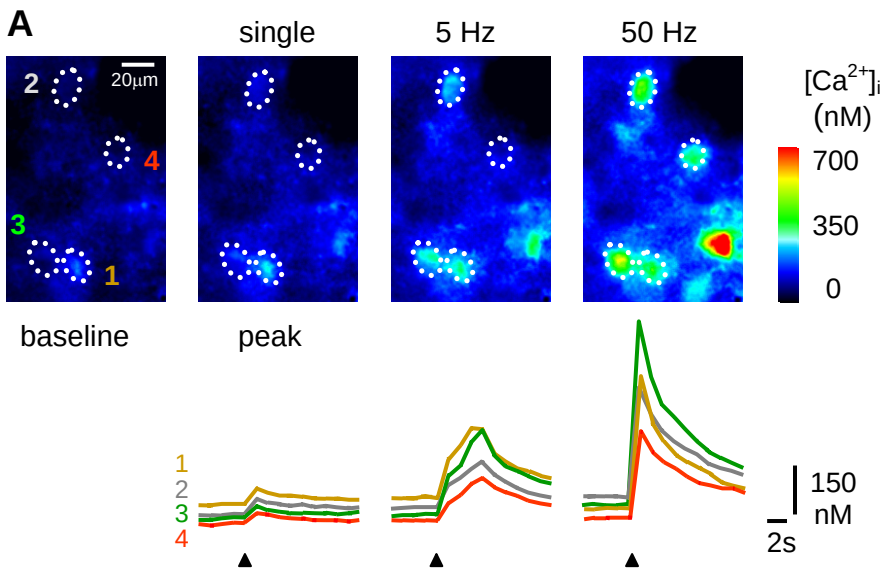
A
single
5 Hz
50 Hz
2
20μm
4
3
1
[Ca2+]i
(nM)
700
350
0
baseline
peak
1
2
3
4
150
nM
2s

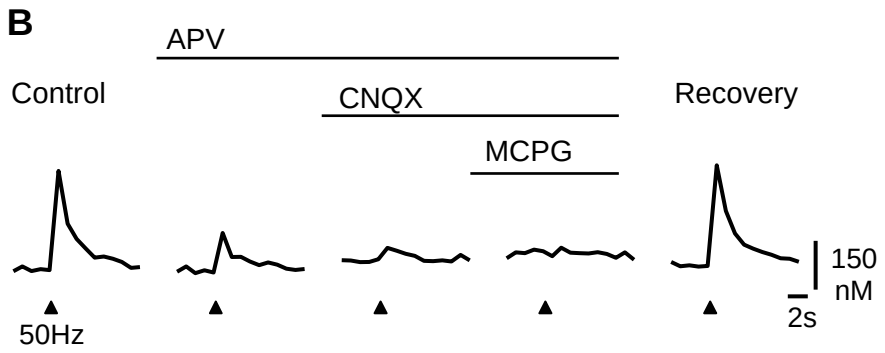
B
APV
Control
CNQX
Recovery
MCPG
50Hz
150
nM
2s

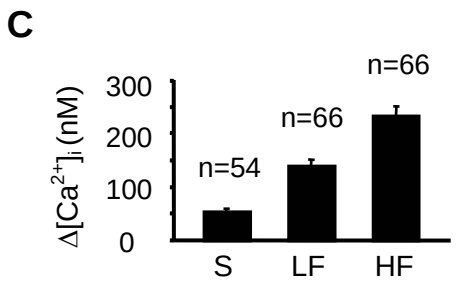
C
n=66
n=66
n=54
300
200
100
0
Δ[Ca2+]i (nM)
S
LF
HF

Figure 13. Synaptically elicited Ca^{2+} responses in LSO.

A. Examples of synaptically elicited Ca^{2+} responses. *Upper row*: Ca^{2+} concentrations before (baseline) and following electrical stimulation of the VAS with a single stimulus, low frequency (5 Hz), or high frequency (50 Hz) stimulus train. *Lower row*: Time course of Ca^{2+} responses from the cells delineated above. Arrowheads mark stimulation. **B.** Ca^{2+} responses are mediated by Glu via activation of NMDARs, AMPARs and mGluRs. Traces show examples from a single cell in response to 50Hz stimulation in control and in the presence of the GluR antagonists APV (50 μM), CNQX (20 μM), MCPG (1 mM). **C**. Average peak changes in $[Ca^{2+}]_i$ elicited by single pulses, low frequency and high frequency stimulation. S - single stimulus, LF - low frequency stimulation (10 pulses at 5 - 10 Hz), HF - high frequency stimulation (10 pulses at 20 - 100 Hz). Figure adapted from Ene et al., 2003.

3.2.2. Contribution of AMPA and kainate receptors

Previous electrophysiological studies have shown that VAS inputs to the LSO are mediated primarily by AMPARs (Caspary and Faingold, 1989; Wu and Kelly, 1992; Kandler and Friauf, 1995a). To determine the contribution of AMPARs to the observed Ca^{2+} signals, the VAS was stimulated in the presence of the AMPA/kainate receptor antagonist CNQX (20 μM). Under these conditions, responses elicited by a single stimulus were almost abolished (reduction 92 ± 2 %; peak amplitudes in control: 55 ± 8 nM, in CNQX: 4 ± 1 nM, n = 40 cells; paired t-test, $p < 0.01$; Figure 14). Responses to low frequency trains were reduced by 73 ± 3 % (control: 170 ± 17 nM, CNQX: 54 ± 11 nM, n = 43 cells; paired t-test, $p < 0.01$; Figure 14). Responses elicited by high frequency stimulation were the least affected by CNQX and were reduced by 48 ± 3 % (control: 277 ± 27 nM, CNQX: 148 ± 27 nM, n = 43 cells; paired t-test, $p < 0.01$; Figure 14). These data indicate that the relative contribution of AMPA/kainate receptors to Ca^{2+} responses decreases with increasing stimulus frequency (Figure 14 B). Ca^{2+} responses elicited by single stimuli were almost completely mediated by AMPA/kainate receptors, while Ca^{2+} responses elicited by bursts have an additional component which increases with stimulation frequency, suggesting that other receptor types might be recruited.

Electrophysiological data indicated that LSO neurons express kainate receptors (Vitten et al., 1999). Because the available AMPAR antagonists block also kainate receptors (i.e. CNQX) or do not completely block AMPARs (i.e. GYKI 52466), further dissection of AMPA and kainate receptors mediated Ca^{2+} responses contribution using electrical stimulation was not attempted. Instead, the presence of kainate receptors in the LSO and their involvement in mediating Ca^{2+} responses was tested using bath application of the specific agonist kainic acid (see chapter 4).

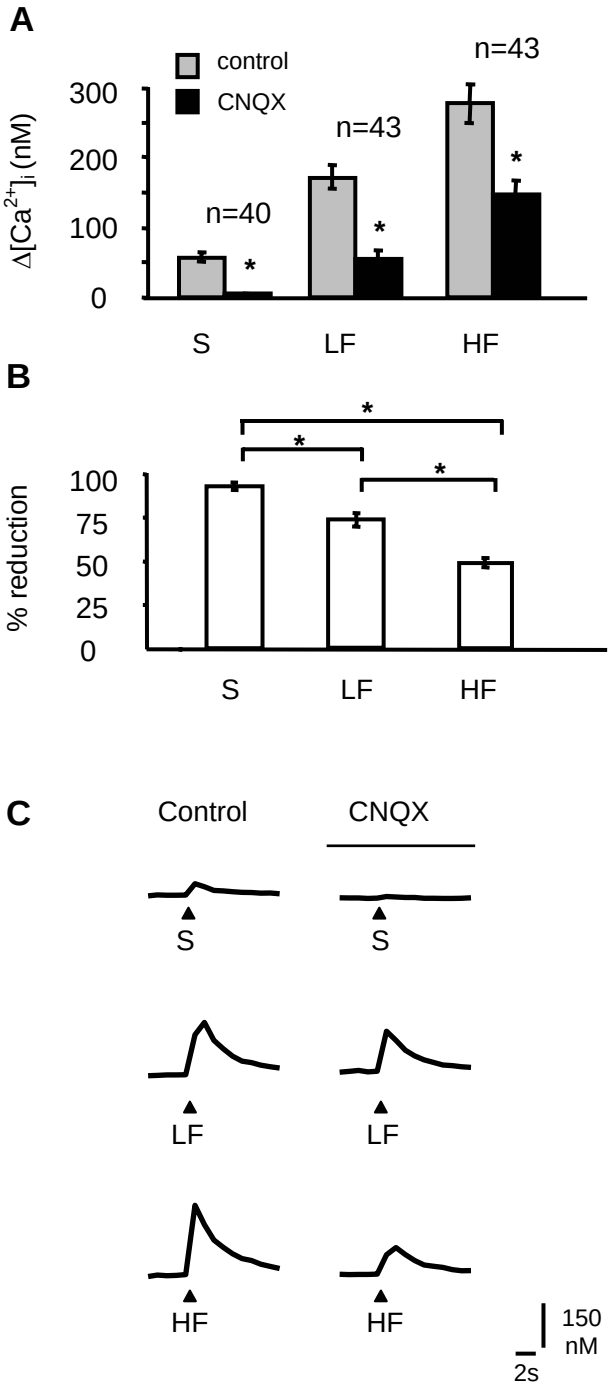
A
control
CNQX
n=43
n=43
n=40
300
200
100
0
Δ[Ca2+]i (nM)
*
*
*
S
LF
HF
B
*
*
*
100
75
50
25
0
% reduction
S
LF
HF
C
Control
CNQX
S
S
LF
LF
HF
HF
150
nM
2s

Figure 14. Contribution of AMPA/kainate receptors to synaptically elicited Ca^{2+} responses.

A. Average peak amplitude of changes in $[Ca^{2+}]_i$, elicited by single electrical stimuli (S), low frequency (LF) and high frequency stimulus trains (HF). Application of the AMPA/kainate receptor antagonist CNQX (20 μM) significantly reduces response amplitudes (black bars; Asterisks - $p < 0.01$; paired t-test). **B.** Reduction of Ca^{2+} responses by CNQX. Responses elicited by single stimuli are almost abolished by CNQX. Responses elicited by low frequency and high frequency stimulation are reduced approximately 70 % and 50 %, respectively. Asterisks – $p < 0.01$, ANOVA followed by Student-Newman-Keuls. **C.** Example from a single cell in response to S (upper panel), LF (middle panel) and HF (lower panel) stimulation under control conditions and in the presence of the AMPA/kainate receptor antagonist CNQX (20μM). Figure adapted from Ene et al., 2003.

3.2.3. Contribution of NMDARs

To examine the contribution of NMDARs to Ca^{2+} signals, the VAS was stimulated in the presence of the NMDAR antagonist APV (50 -100 μM; Figure 15 A, B). Ca^{2+} responses evoked by single stimuli were differentially affected by APV (Figure 15). In 42% of the cells (6 out of 14) APV did not have a significant effect on the Ca^{2+} responses, while in the remaining 58% of cells it considerably reduced the responses. A close analysis revealed that in the unaffected cells the initial Ca^{2+} responses were characterized by small amplitudes. The average amplitude in these cells varied from 8 ± 2 nM in control conditions to 10 ± 4 nM in the presence of APV (n = 6 cells; paired t-test, $p > 0.01$). In contrast, in cells in which APV had an effect, the initial Ca^{2+} responses were characterized by larger amplitudes. On average these responses decreased from 66 ± 13 nM to 28 ± 5 nM in the presence of APV (n = 8 cells; paired t-test, $p < 0.01$; Figure 15), a reduction of 55.1 ± 3.1 %. Responses evoked by stimulus trains at both low and high frequencies were always significantly affected by APV. The amplitudes of responses elicited by low frequency stimuli were reduced from 131 ± 20 nM to 48 ± 9 nM (n = 32 cells; paired t-test, $p< 0.01$; Figure 15), an averaged reduction of 60 ± 4%. The amplitudes of responses elicited by high frequency stimuli were reduced from to 220 ± 27 nM to 99 ± 16 nM (n = 32 cells; paired t-test, $p< 0.01$), an averaged reduction of 56 ± 3 %. There was no statistical significance between the percentage reduction of Ca^{2+} responses elicited by strong single stimuli or low and high frequency bursts of stimuli (Figure 15 B) indicating that recruitment of NMDARs occurs independent of the stimulus parameters as long as it elicits a strong response in LSO neurons.

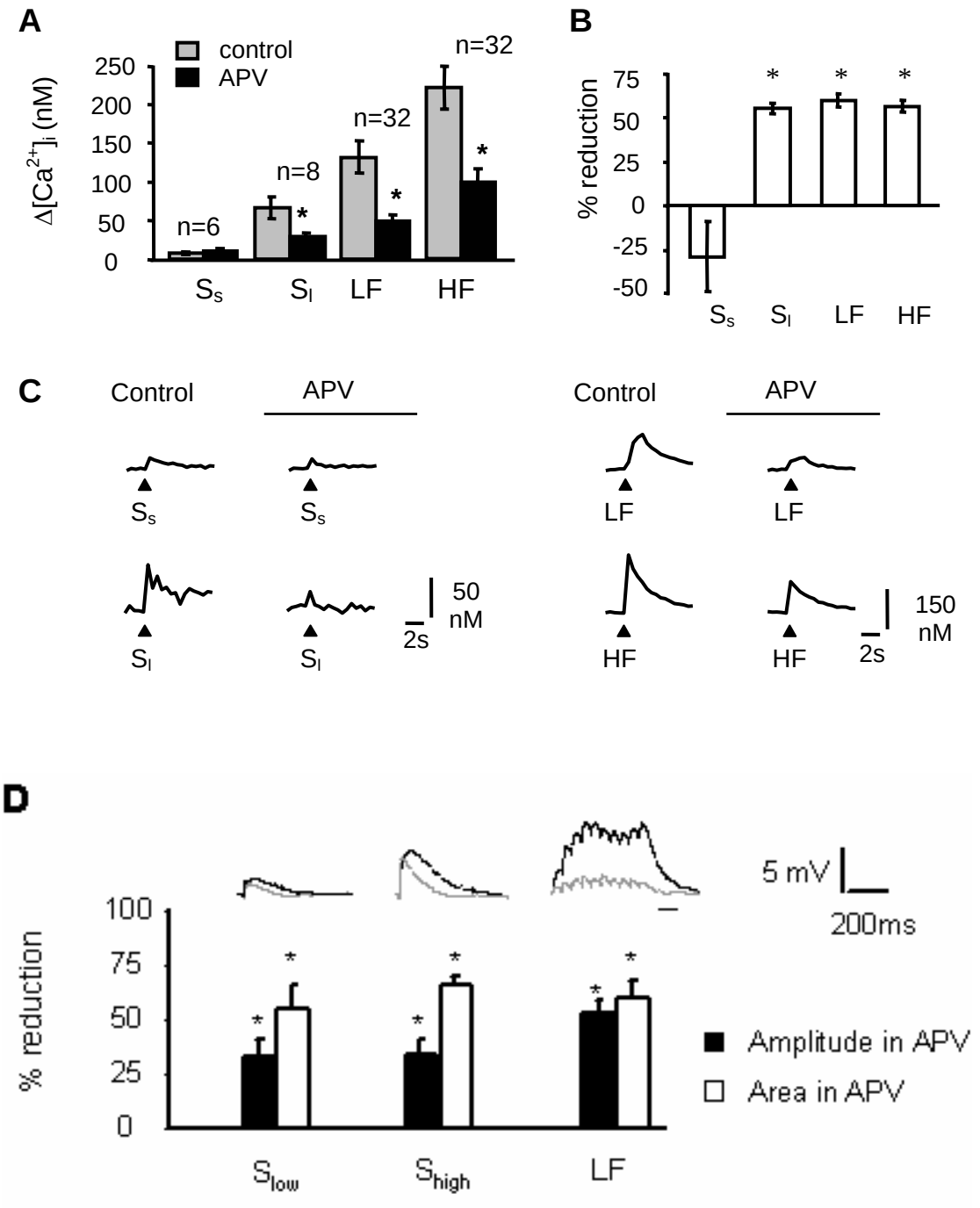
A
control
APV
Δ[Ca2+]i (nM)
250
200
150
100
50
0
n=6
n=8
n=32
n=32
*
*
*
Ss
Sl
LF
HF
B
% reduction
75
50
25
0
-25
-50
*
*
*
Ss
Sl
LF
HF
C
Control
APV
Control
APV
Ss
Ss
LF
LF
Sl
Sl
HF
HF
50
nM
2s
150
nM
2s
D
% reduction
100
75
50
25
0
*
*
*
*
*
*
Slow
Shigh
LF
5 mV
200ms
Amplitude in APV
Area in APV

Figure 15. Contribution of NMDARs to synaptically elicited Ca^{2+} responses.

A. Average peak amplitudes elicited by single, low frequency and high frequency stimuli, before (gray) and after (black) application of the NMDAR antagonist APV (50 -100 μM). Small responses elicited by single stimuli (S_s) are not affected by APV. Larger responses to single stimuli (S_l) and responses to low frequency and high frequency stimulus trains are reduced approximately 50 %. Asterisks – $p < 0.01$, paired t-test. **B.** Percent reduction of Ca^{2+} responses by APV. Asterisks indicate significant difference from S_s (ANOVA followed by Student-Newman-Keuls, $p < 0.01$). **C.** Example from individual cells in response to S_s, S_l (left side traces), LF and HF (right side traces) stimulation under control conditions and in the presence of the NMDAR antagonist APV (100 μM). **D.** Contribution of NMDARs to postsynaptic potentials. *Upper panel:* Traces of postsynaptic responses to a single stimulus at low intensity (S_{low}) and at high intensity (S_{high}) and to a train of low frequency stimuli (LF) before (black) and after (gray) APV. *Lower panel:* Mean reduction of EPSP amplitude and area by APV (100 μM). Asterisks indicate significant difference from control (paired t-test, $p<0.05$, n=5 cells). Recordings are from P 3-5 mice. Figure adapted from Ene et al., 2003.

The ~50% contribution of NMDARs to calcium responses was higher than expected, as previous electrophysiological studies indicated that ipsilateral excitation to LSO neurons is mediated primarily or exclusively by non-NMDARs (Caspary and Faingold, 1989; Wu and Kelly, 1992; Kandler and Friauf, 1995a). Therefore, the contribution of NMDARs to ipsilaterally elicited EPSPs in this preparation was investigated using electrophysiological methods (whole cell patch clamp). These experiments revealed that in neonatal mice (P3-P5), NMDARs contribute to EPSP amplitudes between 35% and 64%, and to response areas between 56% and 67%, depending on stimulus conditions (Table 2, Figure 15 D). Taken together, these results demonstrate that in neonatal mice, NMDARs contribute considerably to ipsilaterally elicited calcium and voltage responses.

Table 2. Contribution of NMDA receptors to ipsilateral elicited EPSPs.

Asterisks: $p<0.05$, Paired t-test, compared to control. N=5 cells from 4 animals.

	EPSP Amplitude (mV)			EPSP Area (mV∗ms)		
Stim	control	APV	% reduction	control	APV	% reduction
S_{low}	2.9 ± 1.6	1.9 ± 0.4	34.0 ± 6.5 *	343.5 ± 43.9	141.6 ± 34.7	55.9 ± 10.9 *
S_{high}	11.3 ± 2.7	7.4 ± 1.7	34.9 ± 6.3 *	1523.6 ± 321.3	559.6 ± 181.8	66.7 ± 5.2 *
LF	6.1 ± 1.0	2.7 ± 1.3	53.8 ± 6.5 *	4730.6 ± 884.1	1720.8 ± 280.2	60.1 ± 7.5 *

3.2.4. Contribution of mGluRs

To examine whether and to what extent mGluRs contribute to synaptic Ca^{2+} responses, the VAS was stimulated while blocking ionotropic GluRs with APV (50 - 100 μM) and CNQX (20 μM). These antagonists abolished Ca^{2+} responses elicited by single stimuli in all cells and abolished responses to low-frequency trains in about half of the cells (51 %, 23 out of 45 cells). Responses to high-frequency trains were abolished in significantly less cells, 13 % (6 cells out of the same 45 cells; Fisher's exact test, $p = 0.0002$). Consistent with this, application of the mGluR antagonist MCPG (1 mM) significantly reduced responses elicited by high frequency bursts that were still present in APV/CNQX by approximately 57 % (from 31 ± 3 nM to 13 ± 2 nM, n = 39 cells; paired t-test, $p < 0.01$; Figure 16). MCPG slightly but not significantly reduced Ca^{2+} responses elicited by low frequency bursts, by approximately 29 % (from 16 ± 3 nM to 11 ± 2 nM, n = 22 cells; paired t-test, $p > 0.01$; Figure 16). The relative contribution of mGluRs to total changes in $[Ca^{2+}]_i$ was 1.3 % ± 2.1 % at low frequency bursts and 6.3 ± 1.4 % at high frequency stimuli (t-test, $p = 0.0489$). These results indicate that mGluRs in LSO neurons are recruited by high-frequency stimulus trains. For individual cells, there was no correlation between the response amplitude and the contribution of mGluRs (Pearson correlation coefficient $r = 0.18$), suggesting that stimulation frequency determines mGluR activation and that response amplitude is not indicative for mGluR activation.

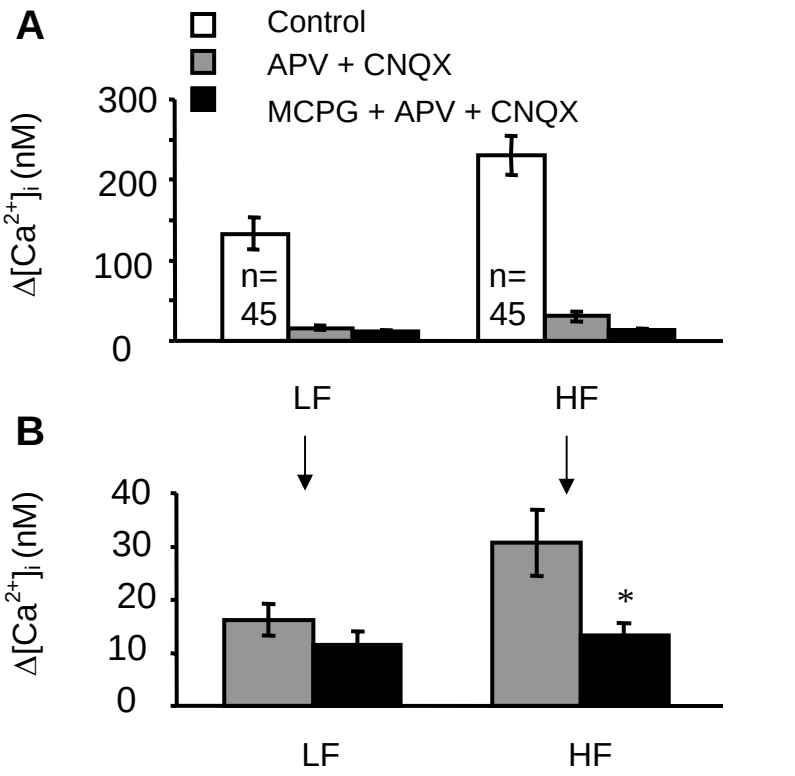
A
Control
APV + CNQX
MCPG + APV + CNQX
300
200
100
0
Δ[Ca2+]i (nM)
n=
45
n=
45
LF
HF
B
40
30
20
10
0
Δ[Ca2+]i (nM)
*
LF
HF

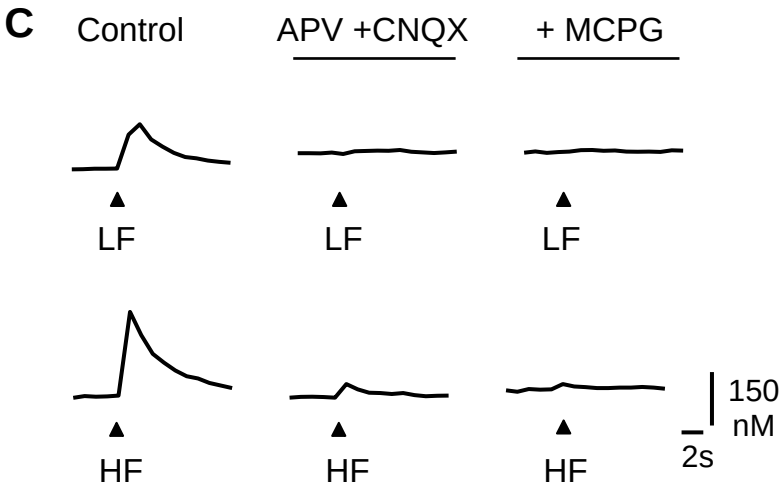
C
Control
APV +CNQX
+ MCPG
LF
LF
LF
HF
HF
HF
150
nM
2s

Figure 16. Contribution of mGluRs to synaptic Ca^{2+} responses.

A. Average peak amplitude of Ca^{2+} responses elicited by low frequency and high frequency stimulus trains in control conditions (white), in the presence of APV (50 - 100 μM) and CNQX (20 μM) (gray), and in the presence of MCPG (1 mM; black). **B.** Comparison of Ca^{2+} responses in the presence of APV/CNQX before and after application of MCPG. Responses to low frequency stimulus trains are slightly, but not significantly, reduced by MCPG, while Ca^{2+} responses to high frequency stimulus trains are significantly reduced. Asterisks - $p < 0.01$, paired t-test. **C.** Example from a single cell in response to LF (upper panel) and HF (lower panel) stimulation in control, in the presence of iGluR antagonists APV (100 μM) and CNQX (20μM) and in the presence of the mGluR antagonist MCPG (1mM). Figure adapted from Ene et al., 2003.

3.3. SUMMARY AND DISCUSSION

In summary, in neonatal LSO neurons, both ionotropic and metabotropic glutamate receptors mediate Ca^{2+} responses elicited by electrical stimulation of AVCN to LSO synapses. The recruitment of different types of GluRs was dependent on the stimulus frequency. AMPA/kainate receptors primarily mediate Ca^{2+} responses elicited by single stimuli (S) and contribute to Ca^{2+} responses elicited by low (LF) and high frequency (HF) bursts by approximately 75% and 50% respectively. NMDARs mediate large amplitude Ca^{2+} responses (defined as Ca^{2+} responses with amplitudes higher than 50nM) triggered by single stimuli (S_l) and bursts of stimuli (~ 50% contribution) but have no contribution to small amplitude Ca^{2+} responses (defined as Ca^{2+} responses with amplitudes smaller than 50nM) elicited by single stimuli (S_s). Finally, mGluRs contribute to Ca^{2+} responses triggered only by high frequency stimulation (20-100 Hz). Thus, a specific pattern of activity stimulates a specific set of GluRs, suggesting that the associated Ca^{2+} responses might represent a way by which the temporal pattern of spontaneous activity is detected by neonatal LSO neurons.

3.3.1. Ca^{2+} responses mediated by iGluRs

The participation of AMPA/kainate receptors to synaptically elicited Ca^{2+} responses is in accordance with previous electrophysiological studies that indicate that synaptic transmission is mediated by non-NMDARs (Caspary and Faingold, 1989; Wu and Kelly, 1992; Kandler and Friauf, 1995a). Their contribution was detected for any stimulus frequency (Figure 14 and summary above), suggesting synaptic transmission greatly relies on AMPA/kainate receptors. The Ca^{2+} entry pathways triggered by these receptors are dissected in chapter 4 and they most likely involve VGCCs. This study did not distinguished between AMPARs and kainate receptors but evidence that kainate receptors mediate Ca^{2+} responses in the LSO are presented in the next chapter, in which the mechanisms of AMPA and kainate receptors mediated $[Ca^{2+}]_i$ increases are investigated.

In neonatal LSO, NMDARs mediate ~ 50% of Ca^{2+} influx resulting from synaptic activation of GluRs at the AVCN-LSO synapses. They also contribute by ~50% to the EPSPs evoked by electrical stimulation of AVCN-LSO synapses. This is in contrast to previous studies which suggested that synaptic transmission is mediated almost exclusively by AMPA/kainate receptors (Caspary and Faingold, 1989; Wu and Kelly, 1992; Kandler and Friauf, 1995a). The differences could due to the fact that these studies were performed in different species and/or at different ages (mice >P21: Wu and Kelly 1992; rat E18-P17: Kandler and Friauf, 1995a). During development there is an age dependent increase in the Gly transporter GLYT2 in LSO (rat: Friauf et al., 1999), that could explain why in older preparation the NMDARs were not detected. A similar high contribution of NMDARs to Ca^{2+} responses triggered by synaptic stimulation has also been found in developing MNTB (rat P8-10: Bollmann et al., 1998) and in developing neocortex (~ 75% in rat P1-7: Yuste and Katz, 1991).

In this study, the contribution of NMDARs to both Ca^{2+} and EPSPs was similar for high intensity single stimuli and stimulus trains. In these conditions, the participation of NMDARs to Ca^{2+} responses was independent of the stimulus intensity and frequency, as long as the stimulus was able to relieve the Mg^{2+} block. For single small stimuli, no Ca^{2+} responses were detected at the soma although in electrophysiological experiments NMDARs participated by about 30% to EPSPs (Figure 15). In these conditions, Ca^{2+} responses were probably elicited locally in the dendrites, where NMDARs may be located, and remained undetected in the soma. Such local Ca^{2+} signals could be important for the stabilization of dendritic branches (review: Wong and Ghosh, 2002) or synaptic plasticity involving local mRNA synthesis (review: Steward and Schuman, 2001). The presumably undetected NMDAR-mediated Ca^{2+} responses reveal one of the limitations of the Ca^{2+} imaging method used here. Confocal imaging of dendrites, where most likely the glutamatergic synapses are located (Cant and Casseday, 1986; Glendenning et al., 1985), will provide detailed information on local Ca^{2+} entry. Low and high frequency stimuli triggered Ca^{2+} responses that spread throughout the neuron, resulting in global Ca^{2+} signals. Such global signals might be useful for processes where signals have to reach the nucleus, i.e. transcription factors that translocate to nucleus to alter gene expression (reviews: Bootman et al., 2001; Bradley and Finkbeiner 2002; Verkhratsky, 2002).

NMDARs have been implicated in multiple forms of synaptic plasticity during development and in the adult (reviews: Goodman and Shatz, 1993; Malenka and Nicoll, 1993;

Constantine-Paton and Cline, 1998). Morphological changes mediated via Ca^{2+} entry through NMDARs include dendritic growth in Xenopus tectum (Rajan and Cline, 1998) and in supraoptic nucleus (rat: Chevaleyre et al., 2002) and synapse elimination (rat cerebellum: Rabacchi et al., 1992). Since in the first postnatal week LSO neurons undergo major dendritic remodeling, it is possible that synaptic activation of NMDARs and Ca^{2+} influx via these receptors contribute to some of these developmental processes.

Glutamatergic inputs are mainly located in the dendrites in adult LSO neurons (Cant and Casseday, 1986; Glendenning et al., 1985), and most likely they are also located in the dendrites in developing LSO neurons. Developing principal LSO neurons have 2-6 primary dendrites and many small thin dendrites and appendages (rat: Rietzel and Friauf, 1998). The length of primary dendrites ranges from 100-400 μM and they are oriented dorsoventrally. During development the thin dendrites are eliminated and the dendritic tree increases mostly by increasing the length of the primary dendrites. In experiments presented here Ca^{2+} responses are measured at the soma while the inputs may be as far as 400 μM away from the soma. Thus, these Ca^{2+} responses are global responses that propagate through the entire cell. They involve Ca^{2+} entry via VGCCs activated by membrane depolarization. In support for this, as it will be shown in Chapter 4, AMPARs are not Ca^{2+} permeable and they increase $[Ca^{2+}]_i$ via VGCCs activation. Whether these depolarizations elicited an action potential it is not demonstrated here, as the membrane potential is not known in these types of Ca^{2+} imaging experiments. However, LSO neurons receive inhibitory input from the MNTB and during the first postnatal week this input is depolarizing and can induce $[Ca^{2+}]_i$ increases (Kullmann et al., 2002). Stimulation of these inputs with supra-threshold stimuli that elicit action potentials in LSO neurons results in Ca^{2+} responses that spread throughout the dendritic arbor. These global Ca^{2+} responses are due to the back-propagation of the action potential into the dendrites. Stimulation with sub-threshold stimuli induces restricted Ca^{2+} responses in dendrites (Kullmann and Kandler, 2002). Thus, at the MNTB-LSO synapses sub-threshold inputs are encoded by local Ca^{2+} responses while supra-threshold inputs are encoded by global Ca^{2+} responses. Similar encoding may take place at the AVCN to LSO inputs; future studies are necessary to perform simultaneous electrophysiological recordings and Ca^{2+} imaging to elucidate the involvement of action potentials and VGCCs in Ca^{2+} responses elicited by stimulation of the AVCN to LSO synapses.

3.3.2. Ca^{2+} responses mediated by mGluRs

In neonatal LSO neurons, mGluRs contributed to Ca^{2+} responses that spread at the soma when synapses were stimulated with high frequency stimuli (Figure 16). The equivalent of such stimuli in vivo might by the bursts of spontaneous activity encountered in electrophysiological recordings (Lippe 1994, Kotak and Sanes, 1995). The discharge rate in a burst varies around a mean of 37 spikes/s and it can increase to 180 spikes/s (gerbil IC P9-13: Kotak and Sanes, 1995). The functional significance of bursts is poorly understood. However they seem to play a special role in synaptic plasticity and information processing in other systems (review: Lisman, 1997). For example, single bursts are sufficient to produce LTP and LTD in hippocampus during cholinergic modulation (Huerta and Lisman, 1995; review Lisman, 1997). Thus, it makes sense to have specialized detection mechanisms for bursts, such as mGluRs.

The activation of mGluRs only with high frequency stimulation is also in accordance with the known perisynaptic location of these receptors (Takumi et al., 1999) and activation by glutamate spillover (reviews: Huang, 1998; Isaacson, 2000). Selective activation of mGluRs by high frequency stimuli was found in cerebellum of adult rat, where is likely to be involved in LTD at the parallel fiber-Purkinje cells synapses (Batchelor and Garthwaite, 1997). In other systems, mGluRs plays important role during development in dendritic growth (Catania et al., 2001) differentiation, maturation and survival of neurons (Flint et al., 1999; Catania et al., 2001), thus it is possible they play similar roles in developing LSO neurons.

In conclusion, each stimulation pattern activates different sets of GluRs. As Ca^{2+} entry through these receptors activates different intracellular pathways (reviews: Gallin and Greenberg, 1995, Berridge, 1998, West et al., 2001), this could represent a way by which the temporal pattern of synaptic activity is detected and interpreted by neonatal LSO neurons.

4. CHAPTER 4. MECHANISMS OF IONOTROPIC AND METABOTROPIC GLUTAMATE RECEPTOR-MEDIATED CACLIUM RESPONSES IN NEONATAL LSO NEURONS

4.1. INTRODUCTION

Ca^{2+} entry pathways are of critical importance for a variety of cellular processes including survival, development and homeostasis (reviews: Gallin and Greenberg, 1995; Berridge et al., 1998; 2000; 2003; West et al., 2001). The exact entry route determines what processes are triggered, what genes are expressed, and ultimately, survival or death of a neuron. For example, the neurotrophin BDNF plays a significant role in development, survival and synaptic plasticity (review: Huang and Reichardt, 2001). Its transcription is preferentially driven by calcium entry through L-type voltage gated calcium channel (VGCC) whereas it is poorly induced by calcium entry through NMDARs (Ghosh et al., 1994; review: West et al., 2001).

There are two main sources of Ca^{2+} in neurons: influx from the extracellular milieu, and release from internal stores. Influx takes place through ligand-gated channels and voltage-gated channels, VGCCs. Ligand-gated channels include the ionotropic glutamate receptor (iGluR) NMDARs, AMPARs and kainate receptors, which are activated by Glu released during synaptic transmission. VGCCs are activated by membrane depolarizations resulting from Glu action on iGluRs, among other processes. Release from intracellular stores, usually from the endoplasmatic reticulum (ER) can be activated as a result of group I and group II mGluR stimulation. In addition to Ca^{2+} release from internal stores, emptying of internal stores results in capacitive calcium entry. This is taking place through store-operated channels. It is now believed that many store-operated channels are members of the newly discovered TRP family (reviews: Montell,

2001; 2003; Clapham et al., 2001; Zitt et al., 2002; Nilius, 2003; and INTRODUCTION section 1.6).

The permeability of iGluRs to calcium depends on the subunit composition of each receptor type. AMPAR subunits, GluR1 to – 4 are expressed differentially at different postnatal ages in developing LSO (see INTRODUCTION section 1.3 and Figure 3 A). GluR2 subunit, which confers Ca^{2+} impermeability to AMPARs (Hollmann et al., 1991; Verdoorn et al., 1991) is expressed early in development and its expression level decreases after hearing onset. GluR4 subunit, which affects the receptor kinetics (review: Trussell, 1999), is expressed mostly after hearing onset. These anatomical studies suggest that the mechanism by which AMPARs increase $[Ca^{2+}]_i$ may be age dependent such that early in development AMPARs are Ca^{2+} impermeable and they become Ca^{2+} permeable after hearing onset. Their kinetics become also faster, suitable for the function they serve: fast synaptic transmission.

Kainate receptors may be present in the LSO (Vitten et al., 1999), though their expression pattern has been less studied. Structure-function relationships studies indicate that a glutamine (Q) or arginine (R) residue located in the membrane domain II of kainate receptors determines ion selectivity. Post-transcriptional editing replaces glutamine by arginine in GluR5 and GluR6 pre-RNA (process called Q/R-editing), and the unedited and edited versions of these receptors confer distinct Ca^{2+} permeability to kainate receptors. Receptors incorporating the Q/R-unedited form of GluR5 and GluR6 subunits are Ca^{2+} permeable (Bernard and Khrestchatisky, 1994; Burnashev et al., 1995; Paschen et al., 1995; Lee et al., 2001). Q/R- editing begins during embryonic development throughout the nervous system, and the adult CNS expresses different levels of edited and unedited receptors (Bernard and Khrestchatisky, 1994; Paschen et al., 1995; Bernard et al., 1999), suggesting the permeability of kainate receptors to Ca^{2+} changes during development. Indeed, in DRG neurons the permeability of kainate receptors to Ca^{2+} decreases dramatically between E18 and P6 (rat: Lee et al., 2001).

The NMDARs are highly permeable to calcium (Ascher and Nowak, 1986; MacDermott et al., 1986; reviews: Mori and Mishina, 1995; Dingledine et al., 1999) and sensitive to Mg^{2+} (reviews: Dingledine et al., 1999, Mori and Mishina, 1995). They also can depolarize the membrane and activate VGCCs. All subunits are expressed in neonatal LSO neurons (developing rat: Caicedo and Eybalin, 1999) and the expression of the NR1 subunit decreases after hearing onset (see INTRODUCTION section 1.3. and Figure 3 B).

Activation of all iGluRs can results in membrane depolarization and consequent activation of postsynaptic VGCCs followed by Ca^{2+} influx. The VGCCs activated by depolarizations include L-type N-type and P/Q type (review: Catterall 2000). L-type channel is mostly expressed postsynaptically while N-type and P/Q type are mostly expressed presynaptically (Soong et al., 1993; Yokoyama et al., 1995; Westenbroek et al., 1995, 1998). In developing LSO neurons L-type VGCCs mediate GABAergic/Glycinergic Ca^{2+} responses (Kullmann et al., 2003).

Metabotropic GluRs have been less studied in the developing LSO. Group I and group II mGluRs are expressed in postsynaptic LSO neurons and their activation induces long-lasting membrane depolarizations (gerbil P8-14: Kotak and Sanes, 1995). Group I mGluRs are coupled preferentially to $G_{q/11}$ proteins (review: Hermans and Challiss, 2001). They activate phospholipase Cβ (PLCβ) resulting in phosphoinositide (PI) hydrolysis, IP_3 production and consequent release of calcium from the internal stores (review: Conn and Pin, 1997). In turn, Ca^{2+} release activates Ca^{2+} permeable channels located in the cell membrane, possibly members of TRP channels (reviews: Montell, 2001; 2003; Clapham et al., 2001; Zitt et al., 2002; Nilius, 2003; and INTRODUCTION section 1.6.). In addition, PIP_2 hydrolysis results in production of DAG which further activates PKC and PKC dependent signaling pathways (Abe et al., 1992; review: De Blasi et al., 2001). PKC pathways are involved in receptor desensitization and in mGluR elicited Ca^{2+} oscillations (review: Alagarsamy et al., 2001). For example, translocation of PKCγ from the cytosol to the plasma membrane mediates group I mGluR-stimulated Ca^{2+} oscillations, suggesting that PKC works as a “decoding machine” (Oancea et al., 1998, Oancea and Meyer, 1998; Dale et al., 2001; review: Alagarsamy et al., 2001). Anatomically, group I mGluRs are largely located on the postsynaptic site, usually peri and/or extra-synaptic (Martin et al., 1992; review: Takumi et al., 1998). They are activated by spillover of glutamate which mostly occurs during high frequency stimulation (Huang, 1998; Isaacson, 2000).

Group II and III mGluRs are negatively coupled to adenylate cyclase (AC; Nakajima et al., 1993; Okamoto et al., 1994; reviews: Conn and Pin, 1997; De Blasi et al., 2001) and it is thought that they do not increase $[Ca^{2+}]_i$. However, recently, it has been shown that group II mGluRs can increase $[Ca^{2+}]_i$ via PLC activation and this mechanism is involved in long term depression (LTD) in prefrontal cortical neurons of rat (Otani et. al., 2002). Group II mGluRs are preferentially located outside the synapses in both pre and postsynaptic sites while group III

mGluRs are largely located on the presynaptic site (review: Takumi et al., 1998). They are mostly involved in modulating synaptic transmission (review: Anwyl, 1999).

In summary, numerous studies established that Ca^{2+} entry routes are critical for neuronal development, maturation, survival and synaptic plasticity. Previous studies attest the presence of iGluRs and mGluRs in developing LSO. Despite the importance of Ca^{2+} signaling through GluRs in development, no systematic study investigated the Ca^{2+} sources in neonatal LSO neurons. The following experiments use Ca^{2+} imaging combined with pharmacology to analyze the mechanisms of glutamatergic Ca^{2+} responses in developing LSO neurons.

4.2. RESULTS

Results presented here include data from 1361 neurons from 73 slices from animals aged between P0-P7.

4.2.1. Control experiments

To determine the specific doses for slices and to test the specificity of drugs used in this study, several control experiments were performed.

a) Dose response curves for KA were constructed in slices. Concentrations above 25 μM KA evoked Ca^{2+} responses that saturated Fura-2 (>2μM; n=18 cells) and therefore concentrations up to 25 μM were used in this study. These values were in the range of IC_{50} values reported in other neurons (EC_{50}: 6-23 μM; review Lerma, 2003).

b) To separate the kainate receptor component from the AMPAR component, GYKI 52466, a selective non-competitive antagonist of AMPARs was used (Tarnawa et al., 1989;

review: Bleakman and Lodge, 1998). AMPA (25 μM, 30s) mediated Ca^{2+} responses were reduced to 9.6 ± 1.9 % (paired t-test $p<0.01$, n=53 cells, P0-7) by GYKI 52466 (25 μM). In contrast, KA (25 μM, 30s) mediated Ca^{2+} responses were not affected by GYKI (25-50 μM) (103.4 ± 3.3 %, paired t-test $p>0.01$, n=51 cells, P0-3), suggesting that at this concentration KA activates mostly kainate receptor and not AMPARs.

c) Dose response relations were also determined for the mGluR agonists ACPD and DHPG in order to find the appropriate concentration in this preparation. 50-100 μM ACPD produced maximal responses (n= 47 cells, P2). For DHPG, 20- 50 μM produced maximal responses (n=31 cells, P2).

d) The efficacy of antagonists was also tested. Responses elicited by ACPD (50 μM, 30s) were greatly reduced by 1mM MCPG (peak reduced by 86.3 ± 0.92 % and area reduced by 92.3 ± 1.2 % n=45 cells, P3). Responses elicited by DHPG (20 μM, 30s) were completely blocked in the presence of 1mM MCPG (peak reduced by 96.1 ± 2.6 % and area reduced by 98.5 ± 0.9 %, n=18 cells, P2).

e) Because DHPG was used extensively (see chapter 5) as an agonist for group I mGluRs, it was tested whether DHPG might activate other receptor types present in the LSO. Responses mediated by DHPG were neither affected by APV (50 μM, peak: 88.1 ± 11.8 %, area: 79.6 ± 14.8, n=27cells, P0-4, paired t-test $p> 0.01$), nor by CNQX (20 μM, peak: 93.4 ± 7.8 %, area: 94.0 ± 4.2, n=34cells, P2, paired t-test $p> 0.01$), suggesting that DHPG elicits Ca^{2+} responses via activation of mGluRs only. Also, Bic (10 μM; a $GABA_AR$ antagonist) and Stry (10 μM, a GlyR antagonist) applied together had no effect on DHPG-mediated responses (peak: 115.8 ± 11.9 %, area: 111.9 ± 9.9 %, n=20cells, P0, paired t-test $p> 0.01$), suggesting that DHPG does not activate $GABA_AR$ or GlyRs.

All other methods are as described in chapter 2 with the following specifications. AMPA (bath and pressure application) was applied in the presence of a cocktail of Stry (10μM), Bic (10μM) and TTX (1μM). For AMPA ionophoresis in electrophysiological recordings NMDARs and mGluRs were blocked with APV (50 μM) and MCPG (1mM), respectively. CTZ (50 μM) was also added to prevent AMPARs desensitization (Partin et al., 1993).

4.2.2. Pharmacological analysis of AMPA and kainate receptor mediated responses

AMPARs can increase $[Ca^{2+}]_i$ by two mechanisms: AMPARs can either depolarize the membrane and activate VGCCs, or depending on the subunit composition they mediate calcium influx themselves. To distinguish between these two possibilities, AMPAR-mediated Ca^{2+} responses were compared before and after blockade of VGCCs with Ni^{2+} (2-5 mM, Gu et al., 1994; Figure 17). Responses elicited by either pressure application of AMPA (1mM, 50 ms, n=16 cells; Figure 17 A) or by bath application of AMPA (20µM, 10s, n=15 cells) were completely abolished by Ni^{2+} (2-5 mM; reduced to 2.3 ± 0.6 % of control, n=31 cells; paired t-test $p<0.01$; Figure 17 A, B). After Ni^{2+} was washed out AMPA elicited responses recovered (Figure 17 A). These results indicate that AMPARs in neonatal LSO neurons are not Ca^{2+} permeable and thus increase $[Ca^{2+}]_i$ through VGCC activation. However, it has been reported that Ni^{2+} can block AMPARs in cultured astrocytes (Telgkamp et al., 1996). Therefore, electrophysiological recordings were performed to determine whether Ni^{2+} blocks AMPAR-mediated currents in LSO neurons. Ni^{2+} (2 mM) had no effect on AMPA-elicited whole-cell currents (control: 154.1 ± 38.1 pA, in Ni^{2+}: 127.5 ± 42.9 pA; n=4 cells; paired t-test $p = 0.39$; n=4 cells; Figure 17 C). In conclusion, AMPARs of LSO neurons are not calcium permeable during the first postnatal week.

Several nuclei in the mature and developing auditory brainstem express kainate receptors (Lachica et al., 1998; Lohrke and Friauf, 2002; Petralia et al., 1994; 1996; review: Petralia et al., 2000). In the LSO, the presence of kainate receptors has been suggested in a single report (abstract: Vitten et al., 1999). To address the possibility that kainate receptors are present and contribute to increases in intracellular calcium, kainic acid was applied in the presence of GYKI 52466 (25 - 50 µM), a selective AMPAR antagonist (Tarnawa et al., 1989; review: Bleakman and Lodge, 1998). Under these conditions, KA (5 - 25 µM, 30 s) increased $[Ca^{2+}]_i$ (157 ± 23 nM, n=37 cells) and the AMPA/kainate receptor antagonist CNQX (20 µM) reduced these responses to 28 ± 5 % of control (54 ± 14 nM, n = 37 cells, P0 - P3; paired t-test $p < 0.01$) (Figure 18). The incomplete inhibition of the KA elicited response by CNQX might be due to poor efficiency of CNQX on kainate receptors (Paternain et al., 1996). Similar to AMPARs, kainate receptors can increase $[Ca^{2+}]_i$ by activating VGCCs and/or they may be Ca^{2+} permeable. Kainate receptor-

mediated responses were tested before and after blockade of VGCCs with Ni^{2+} (2mM). Ni^{2+} completely blocked KA (10μM, 30s; in the presence of 50 μM GYKI 52466) evoked responses (reduced by 95.2 ± 1.3 %; n = 8 cells; paired t-test $p < 0.01$; Figure 18 C). In summary, these results indicate that kainate receptors are present in neonatal LSO, they are Ca^{2+} impermeable and increase $[Ca^{2+}]_i$ by activating VGCCs.

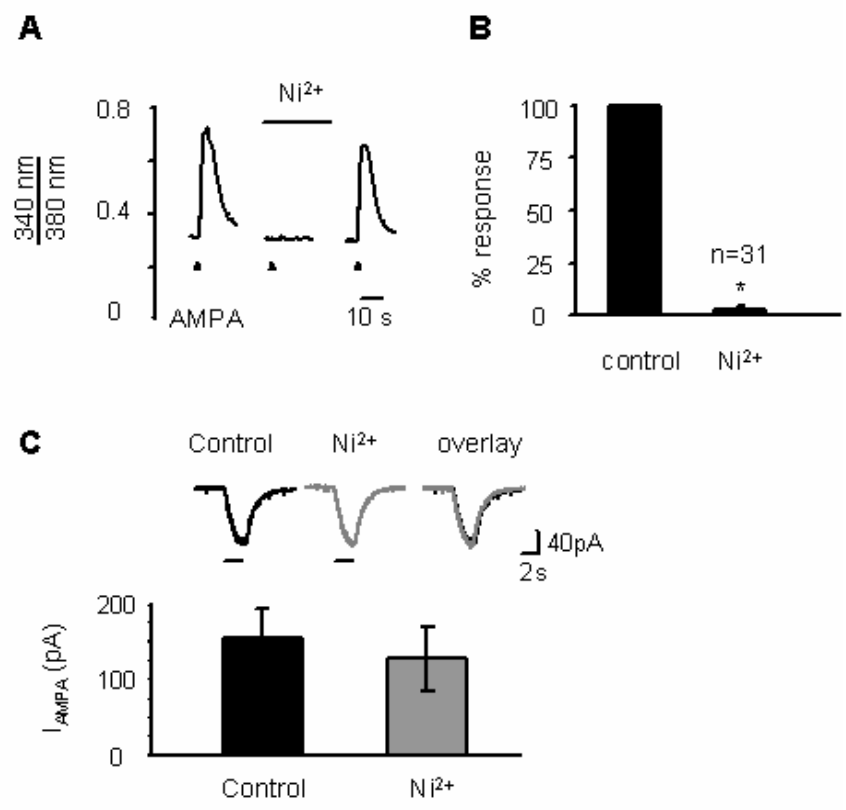

Figure 17. AMPARs in neonatal LSO neurons of mice are Ca^{2+} - impermeable.

A. Pressure application of AMPA (1 mM, 50 ms) induces a Ca^{2+} response reversibly abolished by blocking VGCCs with Ni^{2+} (5 mM). **B.** Summary of data from 31 neurons between P0 and P4. Asterisk- $p < 0.01$, paired t-test. **C.** Whole cell currents through AMPAR are not affected by 2 mM Ni^{2+}. Traces are single responses to AMPA iontophoresis. Bar indicates AMPA application. Graph shows average response from 4 cells. Figure adapted from Ene et al., 2003.

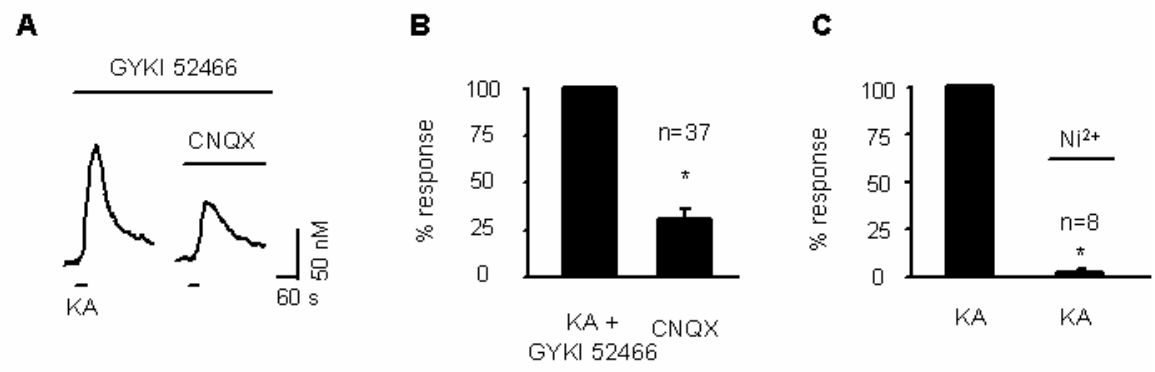

Figure 18. Kainate receptors are expressed in neonatal LSO neurons of mice.

Ca^{2+} response elicited by kainic acid (25 μM, 30s) in the presence of the selective AMPAR antagonist GYKI 52466 (50μM). Subsequent application of the AMPA/kainate receptor antagonist CNQX (20 μM) decreases the response. **B.** Summary from 37 cells (P0 - P3). **C.** kainate receptors neonatal LSO neurons of mice are Ca^{2+} impermeable. Ca^{2+} responses elicited by kainic acid (25 μM, 30s) in the presence of GYKI 52466 (50μM) are abolished by blocking VGCCs with Ni^{2+} (2 mM). Summary from 8 cells (P1). Asterisk - $p < 0.01$; paired t-test. Figure adapted from Ene et al., 2003.

4.2.3. Pharmacological analysis of NMDAR-mediated responses

As shown in chapter 3, NMDARs do not contribute to synaptically elicited Ca^{2+} responses evoked by single stimuli and associated with small response amplitudes. However, Ca^{2+} responses elicited by trains of stimuli always have a NMDAR-mediated component. This suggests that NMDARs in neonatal LSO neurons are blocked by magnesium (Mayer et al., 1984; Nowak et al., 1984). In support of this, application of NMDA (50 μM, 60 s) fails to elicit Ca^{2+} responses at physiological Mg^{2+} concentrations (1.3 mM) (n = 83 cells, P1 - P4; Figure 19) but elicits strong Ca^{2+} responses in Mg^{2+}-free ACSF (467 ± 87 nM, n=83 cells); these responses are

completely blocked by APV (50 µM). The NMDARs are Ca^{2+} permeable (Ascher and Nowak, 1996; MacDermott et al., 1986; reviews: Mori and Mishina, 1995; Dingledine et al., 1999) and they also can depolarize the membrane and activate VGCCs. The contribution of VGCCs to NMDAR-mediated Ca responses in neonatal LSO neurons was not tested in this study.

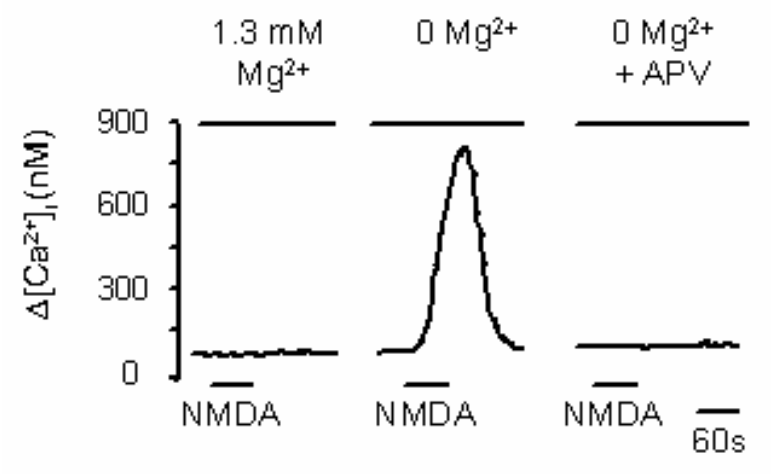

Figure 19. NMDARs are blocked by Mg^{2+}.

Bath application of NMDA (50 µM, 60 sec) in the presence of 1.3 mM Mg^{2+} fails to elicit a Ca^{2+}response. In the absence of Mg^{2+} (0 mM), NMDA evokes a large Ca^{2+} response, which is subsequently blocked by addition of APV (50 µM). Figure adapted from Ene et al., 2003.

4.2.4. Pharmacological analysis of mGluR-mediated responses

In the developing LSO, mGluRs have been poorly investigated. Electrophysiological evidence indicates that activation of mGluRs results in prolonged depolarizations in the LSO of gerbils (8-14 days old: Kotak and Sanes, 1995). However, no systematic study has been performed to identify what groups of mGluRs are present during development and, furthermore, how are they involved in Ca^{2+} signaling. Thus, in the following experiments it was determined

first which specific groups of mGluRs affect $[Ca^{2+}]_i$. The calcium entry routes and the mechanisms of Ca^{2+} responses were than dissected using pharmacological tools and calcium imaging.

4.2.4.1. Group I and II mGluRs but not group III mGluRs elicit Ca^{2+} responses

Group I mGluRs: Activation of group I mGluRs by the specific agonist DHPG (10-20 µM; Ito et al., 1992) consistently increased $[Ca^{2+}]_i$ (Figure 20 A). These responses had a distinctive profile consisting of a rapid, initial increase in $[Ca^{2+}]_i$ (peak response) followed by a long-lasting increase (plateau response). The amplitude of the plateau was approximately 35% of the amplitude of the peak response (average peak amplitude: 463 ± 26 nM, plateau amplitude: 162 ± 9 nM, n = 83 cells). The duration of the response was proportional to the duration of drug application (see inset Figure 20 A).

Group II mGluRs: Activation of group II mGluRs by LCCG-I (5-10 µM; Keele et al., 1999; Maiese et al., 1999) or by the group II agonist/group I antagonist 4C3HPG (200 µM; Hayashi et al., 1994; Keele et al., 1999), elicited Ca^{2+} responses with similar profiles as those elicited by group I mGluRs, i.e. a distinct peak and a plateau (Figure 20 B). Compared to group I responses, peak responses elicited by group II were significantly smaller (group II: 265 ± 28 nM, n = 45 cells; t-test $p< 0.01$) while plateau responses had similar amplitudes (group II: 183 ± 17 nM, n = 45 cells; t-test $p> 0.01$).

Group III mGluRs: The group III mGluR agonist L-AP4 (100 - 500 µM for 30 - 90s; Tanabe et al., 1993) never elicited Ca^{2+} responses (n = 42 cells; Figure 20 C). In the same slices, LSO neurons responded vigorously to KCl depolarizations (60 mM, 30 s) indicating that the absence of a response to L-AP4 was not due to decreased viability of these cells.

These results indicate that immature LSO neurons express group I and group II mGluRs, whose activation increases $[Ca^{2+}]_i$. Group III mGluRs, however, are either not expressed in LSO neurons or are not coupled to intracellular calcium mobilization.

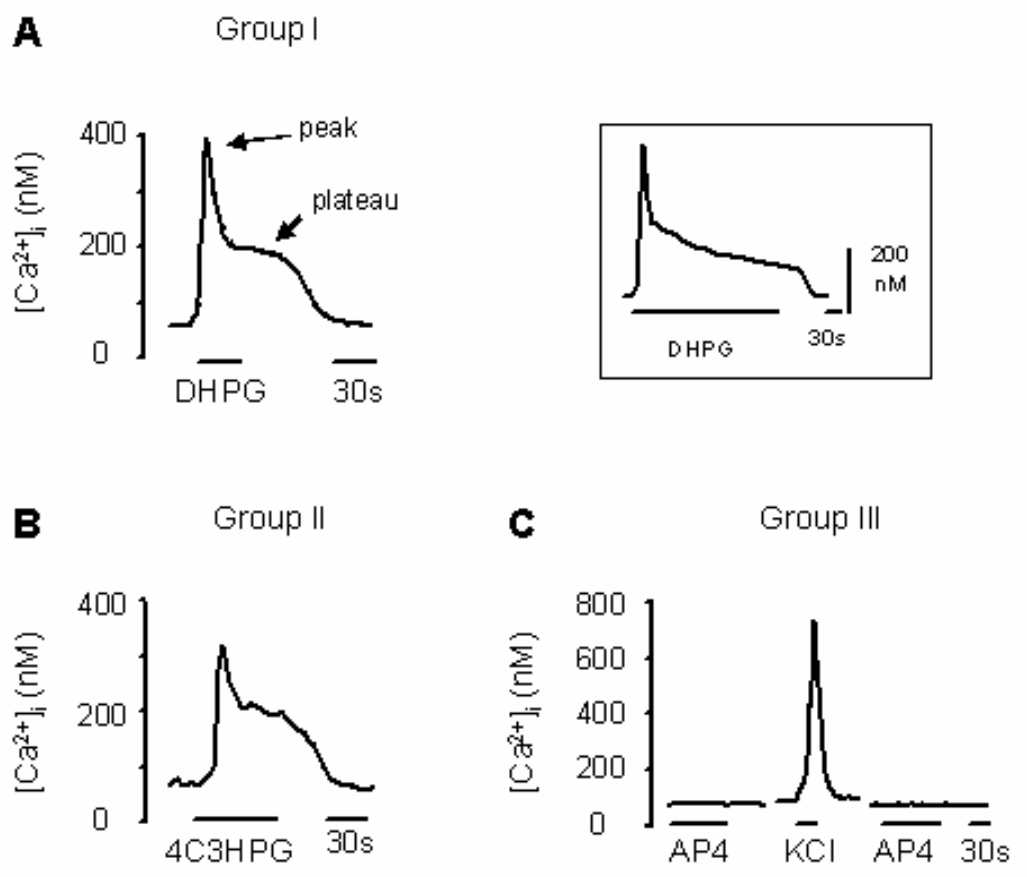

Figure 20. Ca^{2+} responses elicited by mGluRs.

A. Stimulation of group I mGluRs by the specific agonist DHPG (20 µM) induces Ca^{2+} responses consisting of a peak followed by a plateau phase. Inset shows that duration of plateau response is proportional to the duration of the agonist application (DHPG was applied for 300s). **B, C.** Stimulation of group II mGluRs by the agonist 4C3HPG (200 µM, 30 s) induces Ca^{2+} responses with a profile similar to those elicited by the group I mGluR agonist DHPG. **C.** Stimulation of group III mGluRs by the agonist L-AP4 (200 µM, 90 sec) fails to elicit Ca^{2+} responses. The same cells responded strongly to depolarization with KCl (60 mM, 30 s), indicating that their failure to respond to L-AP4 is not due to cell deterioration. Figure adapted from Ene et al., 2003.

4.2.4.2. Mechanisms of mGluR-mediated Ca^{2+} responses

The best characterized pathway by which mGluRs increase $[Ca^{2+}]_i$ is through activation of phospholipase C (PLC) and the production of IP_3, which, in turn, releases calcium from internal stores (Conn and Pin, 1997).

PLC involvement in mGluR-elicited Ca^{2+} responses

To test whether PLC is involved in mGluR-elicited Ca^{2+} responses in neonatal LSO neurons, a specific inhibitor of this enzyme, U73122 (Bleasdale et al., 1989), was used. In initial experiments, slices were first imaged for control responses and then incubated for 30 min to 1h in U73122 (10μM). In these conditions, U73122 had in most cases no effect on peak amplitude and duration of DHPG (10 μM, 30s) mediated responses (peak amplitude: 104 ± 19 %; control: 414 ± 46 nM, U73122: 426 ± 78 nM; duration: 89 ± 10 %, n= 32 cells, N=2 slices, paired t-test, $p>0.01$). The plateau response and area were slightly reduced to 76 ± 12 % (paired t-test $p<0.01$) and 73 ± 6 % (paired t-test $p=0.0169$), respectively (Figure 21 A). Given these results and because the drug incubation was performed in the recording chamber during continuous perfusion (2-3 ml/min), I thought that the incubation period might not have been long enough to allow diffusion of the drug through the membrane. Therefore, slices were placed in 10μM U73122 in the incubation chamber immediately after slicing for 2 to 5 hours. Because there were no control responses to DHPG prior to PLC inhibition, KCl was used as a control and as an indicator for cell healthiness. In 3 slices (P3) tested, a much smaller number of cells responding to DHPG than to KCl was observed. Only about 30% (28 out of 94) of cells that increased Ca^{2+} upon KCl application also responded to DHPG. In slices of similar age, this percentage was significantly higher, about 92 % (n= 240 cells, N=7 slices, P0-5; Fisher exact test $p<0.0001$). However, in the responding cells, Ca^{2+} profiles and amplitudes were not different from controls (Figure 21 C; peak amplitude: 401 ± 54 nM, plateau amplitude: 182 ± 22 nM; n = 28 cells). Although there was no good control, I believe that the U73122 drug might not have been effective in these cells (for presently unknown reasons: i.e. poor penetration, different cell types, and/or different coupling mechanisms). With these concerns and limitations, I interpret these results in the following way: in cells that did not respond to mGluR agonists the inhibition of

PLC was sufficient to abolish Ca^{2+} responses mediated by group I mGluRs. These results suggest that PLC represents a key step in group I mGluR-mediated Ca^{2+} responses in neonatal LSO neurons.

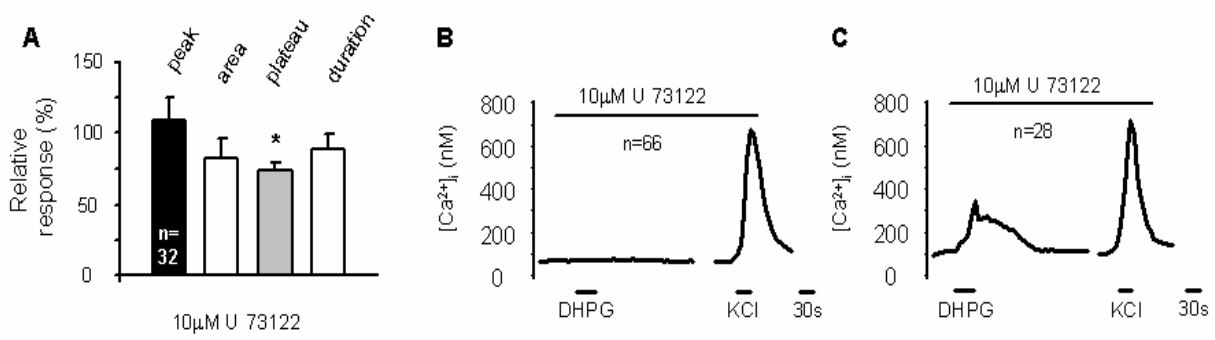

Figure 21. The effect of PLC inhibition on mGluR-mediated Ca^{2+} responses.

A. In slices incubated for 30-60 minutes with the PLC inhibitor U73122 (10μM) DHPG responses are only weakly affected. Bar graphs show peak amplitude, area, plateau and duration of responses relative to control. Summary from 32 cells. **B**. In slices incubated for 2-5h most cells (~70%) are unresponsive to DHPG. The same cells responded strongly to depolarization with KCl (60 mM, 30 s), indicating that their failure to respond to DHPG is not due to cell deterioration. **C.** In the same slices a small percentage (~30%) of cells still respond to DHPG and the response profile is not affected by U73122.

Dissection of Ca^{2+} sources: release from the internal stores and influx from the extracellular milieu

To test the contribution of internal calcium stores to mGluR-elicited Ca^{2+} responses in LSO neurons, calcium was depleted from the endoplasmatic reticulum with thapsigargin (10 μM, 1 - 2h incubation). This treatment completely blocked calcium responses following application of ACPD (100 μM). Upon application of KCl (60mM, 20s) cells were still able to increase $[Ca^{2+}]_i$

(n = 33 cells, N=2 slices; Figure 22). These results indicate that Ca^{2+} release from intracellular stores is necessary for mGluR-mediated Ca^{2+} responses. To test the possible contribution of extracellular calcium to mGluR-mediate Ca^{2+} responses, mGluRs were activated in Ca^{2+}- free ACSF. Under this condition, ACPD still increased $[Ca^{2+}]_i$, but the initial peak was greatly reduced and the plateau phase was almost completely abolished (peak reduced to 31 ± 8 %; area reduced to 18 ± 5 %, n = 9 cells, Figure 23). Similar results were also observed with the group I specific agonists DHPG (peak reduced to 32 ± 2 %, area reduced to 12 ± 1 %, n = 82 cells; paired t-test $p<0.01$) and the group II specific agonist 4C3HPG (peak reduced to 16 ± 2 %, area reduced to 23 ± 3 %, n = 19 cells; paired t-test $p<0.01$). These results indicate that Ca^{2+} release from internal stores contributes only ~ 30 % to the peak response whereas extracellular Ca^{2+} contributes ~ 70% to the peak response and is the sole source of the plateau phase.

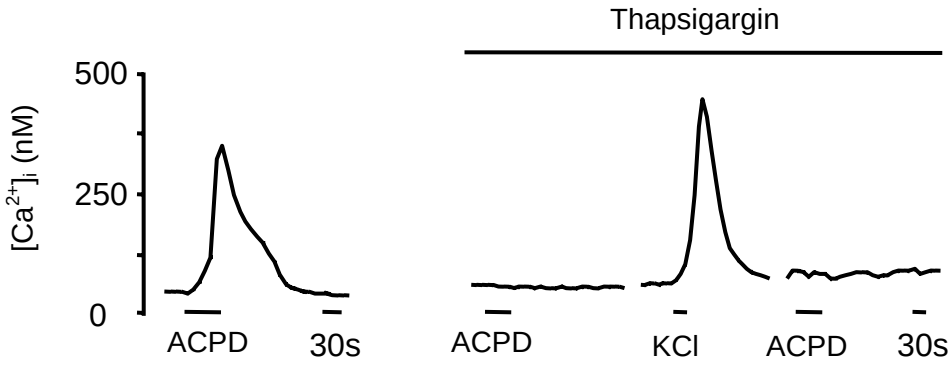

Figure 22. Internal stores are necessary for the mGluR-mediated Ca^{2+} responses.

Typical Ca^{2+} response elicited by the group I/II mGluR agonist ACPD (100 µM, for 60 s) in a control slice (left trace) and in a thapsigargin-treated slice (right traces; 10 µM). The neuron responds to KCl (60 mM, 30s), indicating that failure to respond to ACPD is not due to cell deterioration. Figure adapted from Ene et al., 2003.

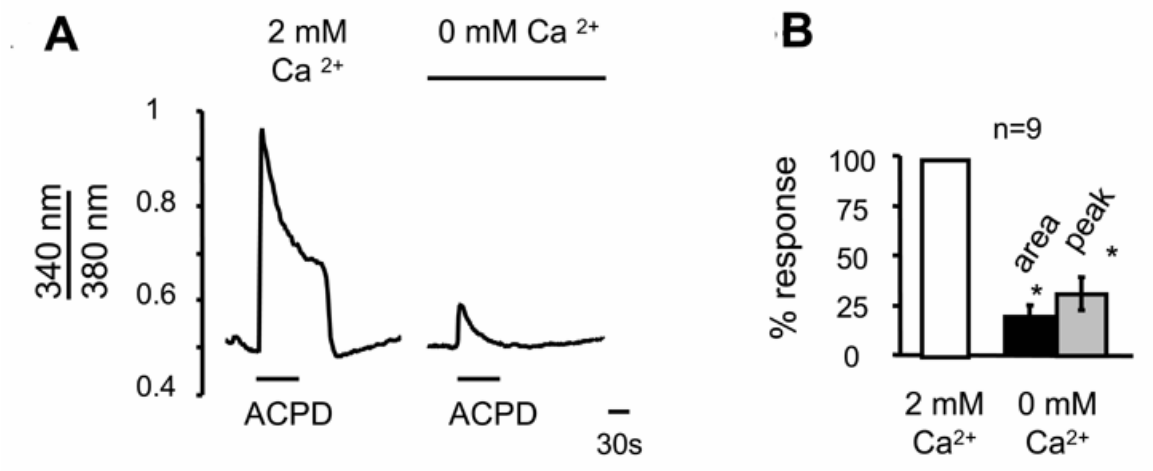

Figure 23. Influx from the extracellular milieu contributes to mGluR-mediated Ca^{2+} responses.

A. Example of ACPD-elicited responses (50 µM, for 60 s) in 2 mM and 0 mM external Ca^{2+}. In 0 mM Ca^{2+}, the peak response is greatly reduced and the plateau phase is completely abolished. **B.** Summary of ACPD responses from 9 cells. Figure adapted from Ene et al., 2003.

PKC involvement in group I mGluR-elicited Ca^{2+} responses

Activation of PLC results in hydrolysis of PIP_2 into DAG and IP_3. DAG activates PKC and thus the signaling cascades coupled to PKC (Conn and Pin, 1997). To test the involvement of the PKC pathway in group I mGluR-mediated Ca^{2+} responses, PKC was inhibited with chelerythrine (10µM). DHPG (10µM, 30s) elicited Ca^{2+} responses were compared in control and in the presence of the PKC inhibitor (Figure 24 A). In P4-5 slices, 10µM chelerythrine slightly increased the amplitude of Ca^{2+} responses (peak: 275 ± 12 nM to 365 ± 29 nM; n = 69cells, N=2 slices; paired t-test $p<0.01$; plateau: 133 ± 5 nM to 147 ± 6 nM; n = 69cells, paired t-test $p<0.01$). Baseline Ca^{2+} increased immediately after chelerythrine incubation (from 42 ± 1 nM to 117 ± 5 nM; n = 69cells, paired t-test $p<0.01$). Higher doses of chelerythrine (50µM) caused more drastic increases in the resting calcium levels and sustained Ca^{2+} elevations after DGPG stimulation

(Figure 24 B; n=18 cells, N=1 slice). Taken together, these experiments suggest that PKC is important for maintaining low resting Ca^{2+} levels and in the clearance process after an mGluR induced Ca^{2+} increase.

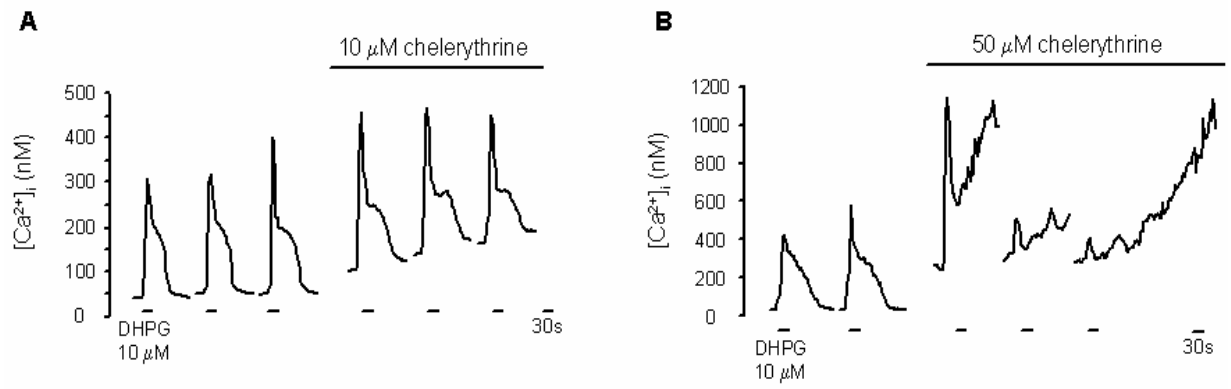

Figure 24. mGluR evoked Ca^{2+} responses are not mediated by PKC.

A. Responses elicited by DHPG (10 μM, 30s) are not significantly affected by inhibition of PKC with 10 μM chelerythrine. The main effect of PKC inhibition is an increase in resting $[Ca^{2+}]_i$. **B**. Cells treated with 50 μM chelerythrine are not able to maintain their low resting $[Ca^{2+}]_i$ and show sustained Ca^{2+} elevations after DHPG stimulation.

Voltage gated Ca^{2+} channels do not contribute to mGluR-mediated Ca^{2+} responses

Previous electrophysiological studies demonstrated that stimulation of mGluRs can induce long-lasting membrane depolarizations of neonatal LSO neurons (Kotak and Sanes, 1995). For this reason and because the plateau phase involves influx of extracellular calcium, the involvement of VGCCs in mGluR-mediated Ca^{2+} responses was examined next. ACPD (20 μM) was applied in the presence of specific antagonists for L - type (10 μM nifedipine), N - type (50 -1000 nM ω -

Conotoxin GVIA), and P/Q - type calcium channels (50 nM ω - Agatoxin TK; review conotoxins: Favreau et al., 1999). None of these VGCC blockers significantly decreased the amplitudes of the peak or the plateau (Figure 25) indicating that mGluR-activated influx of extracellular calcium does not involve VGCCs. Similar results were obtained using the group I specific agonist DHPG (20 µM, 30s) in the presence of the L-type Ca^{2+} channel inhibitor calcicludine (5-10nM: peak 103 ± 3 %, area 125 ± 10 % from control; n=89 cells, P1-3; t-test p>0.01) or nimodipine (20µM; peak 92 ± 6 %, area 131 ± 7 % from control, n=33 cells, P4; t-test p>0.01). These results indicate that mGluR activated influx of extracellular calcium does not involve VGCCs.

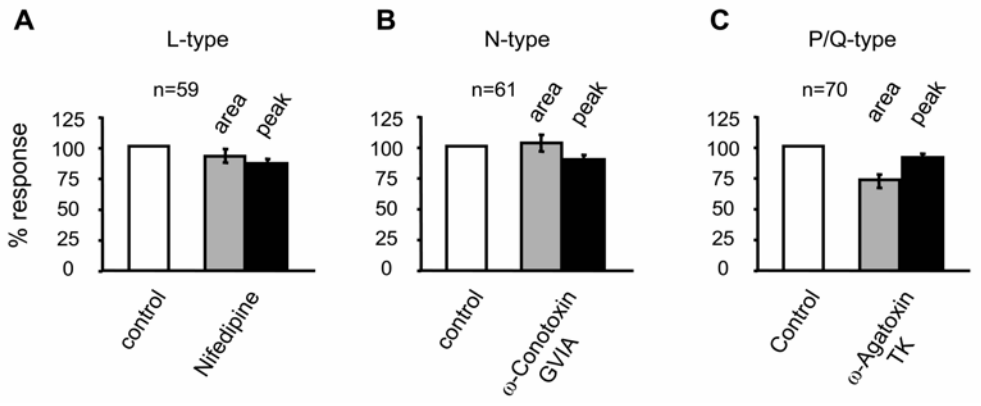

Figure 25. Voltage-gated calcium channels do not contribute to mGluR-elicited Ca^{2+} responses.

A-C. Effects of voltage-gated calcium channel antagonists on normalized areas and peak amplitudes of responses elicited by ACPD (20 µM, 90 s). **A.** Effects of the L-type Ca^{2+} channel antagonist nifedipine (10 µM). **B.** Additional application of the N-type Ca^{2+} channel antagonist ω-Conotoxin GVIA (0.05-1 µM) does not reduce responses in the presence of nifedipine (control). **C.** The P/Q-type Ca^{2+} channel antagonist ω -Agatoxin TK (50nM) slightly reduces ACPD-elicited responses elicited in the presence of nifedipine and ω-Conotoxin GVIA (control). Figure adapted from Ene et al., 2003.

4.3. SUMMARY AND DISCUSSION

This study investigated changes in the $[Ca^{2+}]_i$ following activation of ionotropic and metabotropic GluRs in developing LSO neurons. AMPA and kainate receptors are not calcium permeable and they mediate Ca^{2+} responses via membrane depolarization and activation of VGCCs. NMDARs are highly Ca^{2+} permeable and sensitive to Mg^{2+} block. Group I and group II mGluRs mediate Ca^{2+} responses that have two components: release from internal stores and influx from the extracellular milieu. Group III mGluRs never elicited Ca^{2+} responses in developing LSO neurons. The implications of these findings for the LSO development are discussed bellow.

4.3.1. Ca^{2+} responses mediated by AMPARs

Previous studies have shown the expression pattern of AMPAR subunits in LSO neurons (Caicedo and Eybalin, 1999; see Figure 3 A INTRODUCTION). The GluR2 subunit, which confers Ca^{2+} impermeability to AMPARs (Hollmann et al., 1991; Verdoorn et al., 1991; review Pellegrini-Giampietro et al., 1997), is present in neonatal LSO neurons and it becomes down-regulated after hearing onset (Caicedo et al., 1998; Caicedo and Eybalin, 1999). Consistent with these studies, results presented here indicate that AMPARs are not calcium permeable early in development (Figure 17). AMPARs impermeable to Ca^{2+} are not very common during development. In general, Ca^{2+}-permeable AMPARs, lacking GluR2, are encountered early in development and are implicated in synaptogenesis, cell migration and formation of neuronal circuitry (review: Konig et al., 2001). Ca^{2+}-impermeable AMPARs are expressed in the adult mammalian central nervous system under physiological conditions and are implicated mostly in mediating fast synaptic transmission (review: Riedel et al., 2003). Thus, developing LSO and other auditory nuclei that express GluR2 (including DCN, MSO and IC: Caicedo and Eybalin, 1999), are somehow special. Indeed, within particular auditory pathways specialized in encoding the temporal properties of sound, the speed of transmission is crucial and thus the function of

AMPARs is critical. Consequently, auditory neurons express unique AMPARs whose structure and biophysical properties are tightly correlated with their function (reviews: Trussell 1997; 1999). For example, the desensitization time constant of auditory AMPARs is less than 2ms (review: Trussell, 1997), much smaller than those of other nonauditory neurons (Partin et al., 1996). To achieve this rapid gating, the ideal receptors should contain the $GluR4_{flop}$ subunit and should lack the GluR2 subunit. Indeed, in the LSO, after hearing onset, (and also in the MNTB), anatomical evidence indicates high expression levels of $GluR4_{flop}$ and low expression levels of GluR2 (Caicedo et al., 1998; Caicedo and Eybalin, 1999; Geiger et al., 1995; Hunter et al., 1993; Sato et al., 1993; review: Trussell, 1997).

What would then be the function of AMPARs impermeable to Ca^{2+} in the neonatal LSO? Early in development they mediate synaptic transmission (Caspary and Faingold 1989; Kotak and Sanes 1996; Wu and Kelly, 1992) triggered by spontaneous activity. At this time when $[Ca^{2+}]_i$ in LSO neurons can be increased by all iGluRs and also by mGluRs, the Ca^{2+} impermeability of AMPARs could represent a way to avoid accumulation of dangerous intracellular calcium levels.

4.3.2. Ca^{2+} responses mediated by kainate receptors

Kainate receptors are expressed in several auditory brainstem nuclei including NM of chick (Lachica et al., 1998), MNTB of developing to adult rat (P2-59; Lohrke and Friauf, 2002) and CN of adult rat (Petralia et al., 1994; 1996; review: Petralia et al., 2000). Previous studies suggested that kainate receptors may be present in developing LSO neurons (Vitten et al., 1999). The present results demonstrate that immature LSO neurons express functional kainate receptors that can increase $[Ca^{2+}]_i$ via activation of VGCCs (Figure 18). These receptors are calcium impermeable and thus most likely composed of the Q/R-edited forms of GluR5 and GluR6 subunits (Bernard and Khrestchatisky, 1994; Burnashev et al., 1995; Paschen et al., 1995; Lee et al., 2001). In support for this, the GluR5 agonist ATPA elicited currents in developing LSO of rat (P2-10: Vitten et al., 1999). The present study did not distinguish whether these receptors are synaptic and/or extrasynaptic, thus it remains to be shown to what extent they participate in

glutamatergic synaptic transmission. Also, it remains to be shown whether kainate receptors undergo developmental changes in the subunit composition similar to AMPARs, and to what extent these changes affect Ca^{2+} permeability of these receptors and consequently their function.

4.3.3. Ca^{2+} responses mediated by NMDARs

The NMDAR is a unique Glu receptor because it is activated by both ligand and voltage; it functions as a coincidence detector between pre- and postsynaptic cells (Mori and Mishina, 1995). NMDARs are highly permeable to calcium (Asher and Nowak, 1986; MacDermott et al., 1986; reviews: Mori and Mishina, 1995; Dingledine et al., 1999) and sensitive to Mg^{2+}. The sensitivity to voltage dependent Mg^{2+} block depends on the incorporation of specific NR2 subunits: NMDAR containing NR2A and NR2B subunits are more sensitive to Mg^{2+} than the NR2C- and NR2D- containing receptors (reviews: Dingledine et al., 1999; Mori and Mishina, 1995; Yamakura and Shimoji, 1999). In this study NMDARs were Mg^{2+} sensitive, thus most likely composed of NR2A and NR2B subunits. In support, previous anatomical data indicate the presence of these subunits in immature LSO neurons (rat: Caicedo and Eybalin, 1999; see Figure 3 B INTRODUCTION).

Early in development, Ca^{2+} entry through NMDARs is thought to play a role in neurite outgrowth (Pearce et al., 1987; Brewer and Cotman, 1989; Matson and Kater, 1989), dendritic growth (in Xenopus tectum: Rajan and Cline, 1998; rat supraoptic nucleus: Chevaleyre et al., 2002), synaptic connectivity (optic tectum of tadpoles: Cline et al., 1987; cat cortex: Kleinschmidt et al., 1987), synapse elimination (developing cerebellum: Rabacchi et al., 1992), synaptic plasticity, and cell death (reviews: West et al., 2001; Wong and Ghosh 2002). Thus, NMDARs could play similar roles in LSO development.

4.3.4. Ca^{2+} responses mediated by mGluRs

Previous studies indicate the presence of group I/II mGluR on postsynaptic LSO neurons (gerbil: Kotak and Sanes, 1995). In this study, activation of group I and group II mGluRs in neonatal LSO neurons induces biphasic Ca^{2+} responses characterized by a peak increase followed by a long lasting plateau increase (Figure 20). Activation of group III mGluRs did not affect $[Ca^{2+}]_i$ (Figure 20), suggesting that these receptors are either not expressed postsynaptically in LSO neurons or are not coupled to intracellular Ca^{2+} pathways. Group I mGluRs are known to activate the PLC dependent intracellular pathway resulting in production of IP3 and $[Ca^{2+}]_i$ increase from the IS (review: Conn and Pin, 1997). The present results indicate that a similar cascade is used in the immature LSO, as PLC inhibition blocked Ca^{2+} responses in a high percentage of cells (Figure 21). These results are in line with studies in other systems, including interneurons in stratum oriens in developing hippocampus of rat (P14-21; Woodhall et al., 1999) or in Purkinje cells in mouse cerebellum (P18-29; Tempia et al., 2001), where similar PLC dependent group I/II mGluRs mediated Ca^{2+} responses were detected.

The biphasic Ca^{2+} responses mediated by group I and II mGluRs are composed of: release from internal stores (Figure 22) and influx from the extracellular milieu (Figure 23). Ca^{2+} release from the internal stores is a prerequisite for the influx component, as stimulation of mGluRs after depleting the internal stores with thapsigargin results in no Ca^{2+} response. However, it only represents about 30% of the peak Ca^{2+} response. The remaining peak response and the entire plateau response are due to Ca^{2+} influx from the extracellular milieu. The channel mediating the influx is different from conventional VGCCs, as blockers of L-, N-, P/Q-type VGCCs have no effect on ACPD-evoked Ca^{2+} responses (Figure 25). Further investigation of the nature of this channel and its contribution to Ca^{2+} responses during development is presented in chapter 5. Similar Ca^{2+} profiles, peak followed by plateau response mediated by group I mGluRs have been observed in dopaminergic neurons of rat Substantia Niagra (Choi et al., 2003).

The responses elicited by group II mGluR agonists were unexpected because group II mGluRs are linked to the adenylate cyclase pathway rather than the PLC-IP_3 pathway. It is unlikely that these responses are due to nonspecific activation of group I mGluRs because $[Ca^{2+}]_i$ also increased upon application of 4C3HPG, which is not only an agonist for group II mGluRs

but also a potent antagonist for group I mGluRs (Hayashi et al., 1994). Although the exact intracellular pathways that underlie group II-elicited calcium responses remain to be investigated, its similarity to group I responses suggests the involvement of IP_3 - dependent calcium mobilization. Recently, group II mGluR-mediated activation of the PLC- IP_3 pathway has been demonstrated in prefrontal cortex neurons (Otani et al., 2002), in which group II mGluRs are critically involved in mediating activity-dependent synaptic plasticity.

In other auditory brainstem nuclei, mGluR expression has been detected early in development and also in adult in chick, rat, gerbil (Zirpel et al., 2000; Schwartz and Eager 1999; Elezgarai et al., 1999, 2001; Jars et al., 1998; review: Petralia et al., 2000). Group I and II mGluRs expression was investigated in CN and MNTB of rat and/or mouse and NM of chick (CN rat: Shigemoto et al., 1992; mouse CN: Bilak and Morest, 1998; Elezgarai et al., 1999, 2001; Jars et al., 1998; DCN: Molitor and Manis, 1997 Schwartz and Eager 1999; Takahashi et al., 1996; NM: Zirpel et al., 2000; review: Petralia, 2000). Their function was not investigated in detail. In NM neurons mGluRs play a role in survival of neurons after deafferentiation. Lethal increases in the $[Ca^{2+}]_i$ caused by deafferentiation (Zirpel et al., 1995a) can be prevented by activation of mGluRs (Zirpel and Rubel, 1996) linked to protein kinase A (PKA) and protein kinase C (PKC) signal transduction pathways (Lachica et al., 1995; Zirpel et al., 1995a,b, 1998). In this study, inhibition of PKC resulted in large increases in resting calcium levels (Figure 24), suggesting a similar protective role for the mGluR-PKC pathway in LSO neurons.

In other systems, mGluRs play a role in survival (review: Holscher et al., 1999), synaptic plasticity (reviews: Con and Pin, 1997; Holscher et al., 1999; Cartmell and Schoepp, 2000), learning and memory (review: Riedel et al., 2003). Also, activation of mGluRs triggers gene expression (cultured rat striatal neurons: Mao and Wang, 2003), and induces morphological changes (spine elongation in dendrites of hippocampus cells: Vanderklish and Edelman, 2002). It is possible that in neonatal LSO neurons mGluRs might serve similar functions.

In conclusion, Ca^{2+} entry routes in neonatal LSO neurons are distinct for each GluR type: AMPA/kainate receptors induce Ca^{2+} influx via activation of VGCCs, NMDARs are Ca^{2+} permeable and group I and group II mGluRs induce biphasic Ca^{2+} responses involving release from internal stores and influx from the extracellular milieu. Given that specific Ca^{2+} entry routes can activate distinct intracellular pathways, it is possible that LSO neurons use these specific pathways for different developmental aspects.

5. CHAPTER 5. DEVELOPMENT OF GROUP I METABOTROPIC GLUTAMATE RECEPTOR-MEDIATED CALCIUM RESPONSES. INVOLVEMENT OF TRP CHANNEL(S)

5.1. INTRODUCTION

Group I mGluRs (mGluR1 and -5) play an important role in survival, neural growth and cell death (Vincent and Maiese, 2000; Hannan et al., 2001; reviews: Bordi and Ugolini, 1999; Hermans and Challiss, 2001; Valenti et al., 2002). Evidence from other systems suggests that the expression pattern of group I mGluRs changes during development (Catania et al., 1994; Romano et al., 1996; Lopez-Bendito et al., 2002). For example, in neocortex and hippocampus the expression levels of mGluR1 increases while the expression of mGluR5 decreases (Catania et al., 1994; Romano et al., 1996; Lopez-Bendito et al., 2002). In addition, these receptors localize differently: during late prenatal development mGluR1 is found mainly in neuropil and mGluR5 mainly in the soma, while during postnatal development the opposite is true (Lopez-Bendito et al., 2002). Although nothing is known about the developmental expression of group I mGluRs in the LSO, it is possible that they undergo developmental changes in their expression levels and/or their cellular localization similar as in cortex. Much less is known about mGluR signaling pathways during development, whether there are developmental changes in these pathways and if so what functional implications they might have. The mechanisms by which group I mGluRs affect $[Ca^{2+}]_i$ is complex and it has been described in chapter 4. In short, group I mGluRs are coupled to $G_{q/11}$ proteins and activate PLC resulting in IP_3 and DAG production. IP_3 diffuses through the cytosol and activates IP_3Rs causing release of calcium from internal stores (review: Conn and Pin, 1997). Ca^{2+} release can activate store-operated channels, possibly members of the

TRP channel family (reviews: Montell, 2001; 2003; Clapham et al., 2001; Zitt et al., 2002; Nilius, 2003; and INTRODUCTION section 1.6). Also DAG, which is membrane-bound lipid, can activate TRP channels. For example, the membrane permeable analogue of DAG, OAG, activates TRPC3 and TRPC6 in CHO-KI cells (Hoffmann et al., 1999); however, it fails to activate I_{BDNF} currents presumably mediated by TRPC3 in pontine nuclei from neonatal rat (Li et. al., 1999). Ca^{2+} signaling triggered by group I mGluRs via release from intracellular stores can activate downstream pathways coupled to activation of caspases, activation of transcription factors and activation of many other signals necessary for regulation of cellular functions such as synaptic plasticity, neuronal excitability or apoptosis (reviews: Berridge, 1995; 2002; Corbett and Michalak, 2000; Bootman et al., 2001; Verkhratsky, 2002; Verkhratsky and Petersen, 2002). Changes in group I mGluRs signaling pathways can affect all these processes. Thus it is of interest to know whether there are developmental changes and what the influences on cellular processes are. To begin addressing these questions, this study investigates Ca^{2+} responses mediated by group I mGluRs in developing LSO neurons.

Results from the previous chapter, indicated that in neonatal LSO neurons (P0-7), group I mGluRs trigger Ca^{2+} release from internal stores and this in turn triggers Ca^{2+} influx through a store-operated Ca^{2+} permeable channel. In this chapter the sources of Ca^{2+} responses mediated by mGluRs and the nature of the store-operated calcium channel are investigated in more detail, expanding the developmental window to P19. This period covers the two important stages in the development of the auditory system: before hearing onset, when neuronal activity is spontaneous and after hearing onset when neuronal activity is sound-driven. The methods used here are Ca^{2+} imaging combined with pharmacology.

5.2. RESULTS

Results presented here are from 1057 neurons in 81 slices prepared from P0-19 animals.

5.2.1. Group I mGluR-mediated responses during development

This section presents a general overview of DHPG elicited responses during development.

Group I mGluR-mediated responses were analyzed in P0-19 slices in n= 739 cells, N= 58 slices, from 57 animals. Data were grouped by age: neonatal P0-5 (n=240 cells, N=7 slices from 7 animals), before hearing onset P9-12 (n=194 cells, N=14 slices from 14 animals), immediately after hearing onset P13-16 (n=191 cells, N=23 slices from 22 animals), and later after hearing onset P17-19 (n=114 cells, N=14 slices from 14 animals).

Resting $[Ca^{2+}]_i$ was in the ranges of 50 – 250 μM and it did not vary significantly during development (Figure 26 A1, ANOVA $p>0.01$; average of all cells 93 ± 2 nM, n= 739). A histogram of all cells grouped by age did not indicate that the four groups form four different populations (Figure 26 A2). Comparison between groups P0-12 and P13-19 showed a statistical significant difference (P0-12: 83 ± 2 nM, n= 432, P13-19 106 ± 3 nM, n= 307, t-test $p< 0.01$). However, a histogram plotting the baseline of all cells in each age group does not indicate two different populations (Figure 26 A3). All cells included in the analysis responded to KCl depolarizations (60mM, 90s). The profile of KCl responses was similar at all ages; peak amplitudes ranged from around 100 nM to saturating responses (>2μM). At younger ages more cells tended to have saturated responses to 60mM KCl (52% at P0-5 compared to 24% at P9-19).

Metabotropic GluR-mediated Ca^{2+} responses changed quantitatively and qualitatively during development. Qualitatively, three types of responses were encountered: increase, no change and decrease of $[Ca^{2+}]_i$ (Figure 26 B). The response type correlated with age. The

percentage of cells that increase $[Ca^{2+}]_i$ diminished from about 95% at P0 to about 50% at P19 (Figure 26 C). At the same time, the percentage of cells responding with decrease in $[Ca^{2+}]_i$ rose from 0% at P0 to about 30 % at P19 (Figure 26 C). Similarly, the percentage of cells responding with no change in $[Ca^{2+}]_i$ rose from about 5% at P0 to about 20% at P19 (Figure 26 C). The distribution of different response types (increase, decrease of $[Ca^{2+}]_i$) in individual slices as a function of age showed that cells that decrease $[Ca^{2+}]_i$ appeared around hearing onset (P12 in mice). Their percentage increased after hearing onset (red circles in Figure 27). At P13-16 in a given slice responses were in general mixed, increase and decrease (black and red symbols in Figure 27), while at other ages responses were either increase or decrease of $[Ca^{2+}]_i$.

These results suggest that Ca^{2+} signaling trough group I mGluRs may involve more than one mechanism. During early development a mechanism resulting in $[Ca^{2+}]_i$ increase prevails, while after hearing onset this mechanism might be replaced by one that decreases $[Ca^{2+}]_i$. To understand the mechanisms underlying these Ca^{2+} responses, DHPG-evoked responses were investigated in more detail. Results are presented separately for the increase and the decrease type of responses.

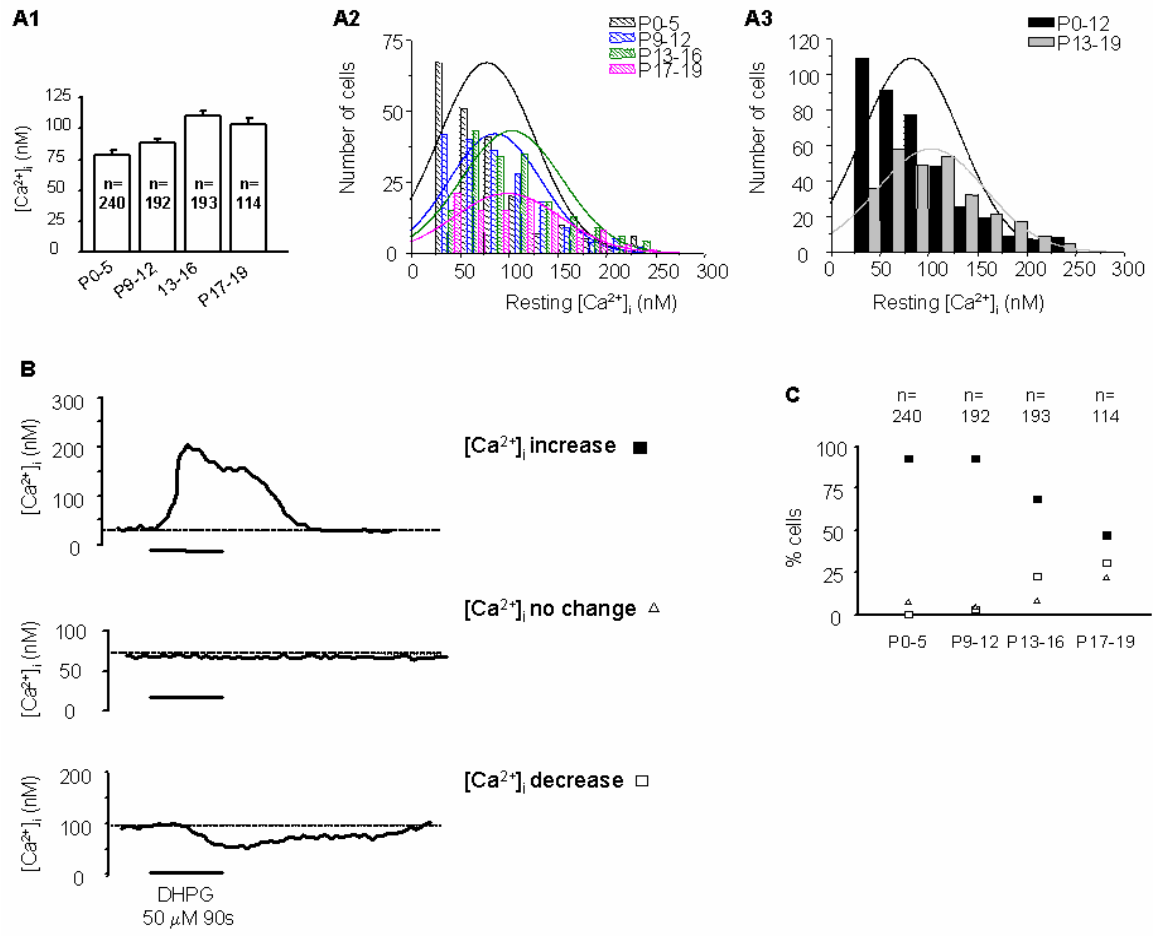

Figure 26. mGluR-mediated Ca^{2+} responses during development.

A1. Resting $[Ca^{2+}]_i$ concentrations are similar across age groups. **A2**. Histograms of resting $[Ca^{2+}]_i$ for each age group. **A3**. Histograms of $[Ca^{2+}]_i$ for cells grouped from P0-12 (black) and P13-19 (grey), illustrating that they are not two different populations. Bin size was 25 nM for A2 and A3. **B**. Three types of DHPG (50μM, 90s)-evoked Ca^{2+} responses are encountered during development: increase, no change and decrease. Examples are from single cells at P0, P14 and P18. Dotted line represents baseline. **C.** Age dependence of group I mGluR-mediated Ca^{2+} responses. During development, the number of cells responding to DHPG with a $[Ca^{2+}]_i$ increase (filled squares) diminishes while the number of cells responding with a $[Ca^{2+}]_i$ decrease (empty squares) or no change (triangles) increases. 100% represents the number of cells responding to KCl (60mM, 90s). Numbers on top represent total number of cells for each age group.

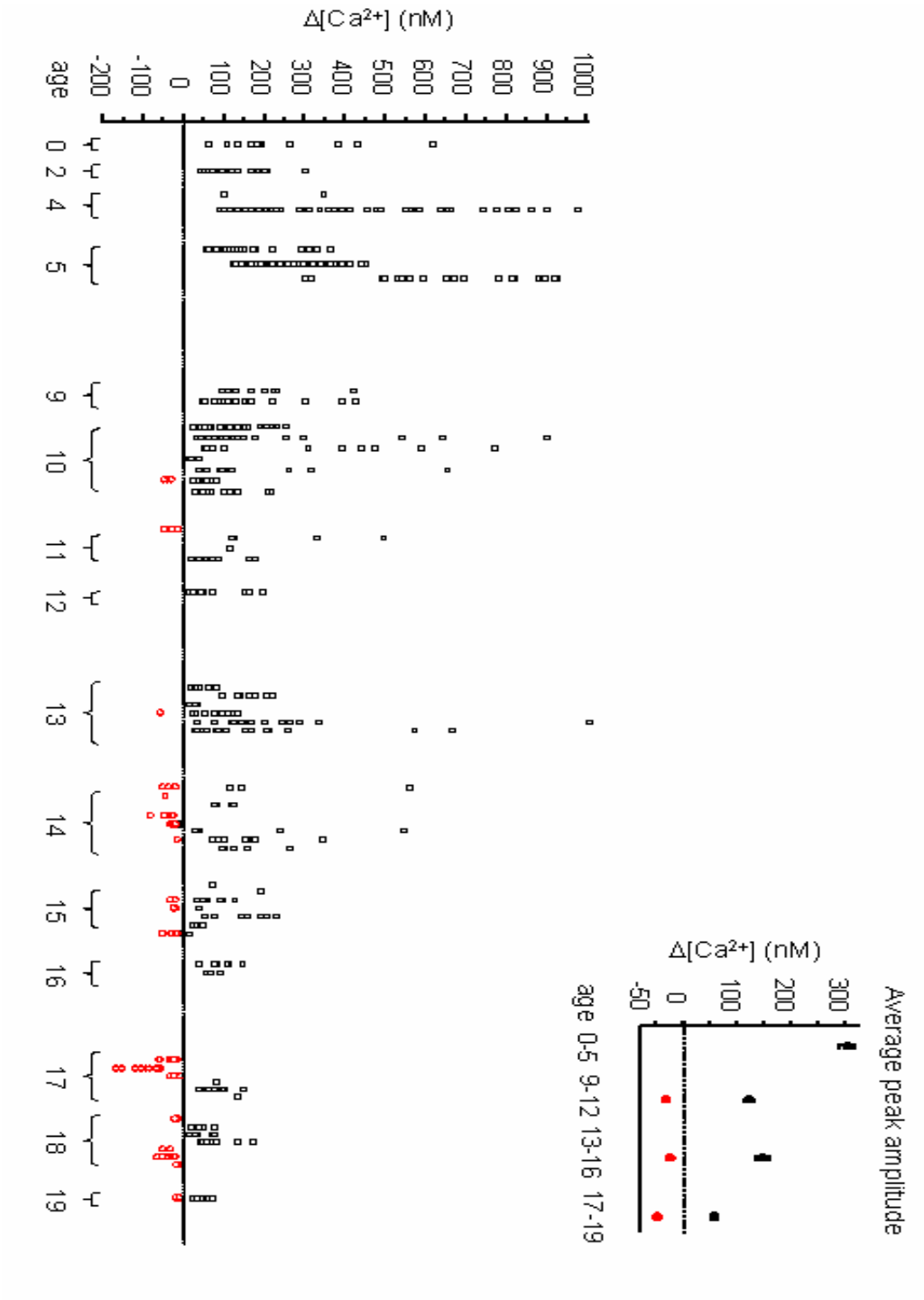
Δ[Ca2+] (nM)
1000
900
800
700
600
500
400
300
200
100
0
-100
-200
age
0 2 4 5 9 10 11 12 13 14 15 16 17 18 19
Average peak amplitude
Δ[Ca2+] (nM)
300
200
100
0
-50
age 0-5 9-12 13-16 17-19

Figure 27. Distribution of peak amplitude of DHPG-induced responses as a function of age in individual slices.

Ca^{2+} responses were elicited by bath application of DHPG (50 μM, 90s). Each square represents a single cell and each column represents an individual slice. Black squares are cells responding with a Ca^{2+} increase; red circles are cells responding with a Ca^{2+} decrease. Cells showing no change in $[Ca^{2+}]_i$ are not plotted. Dotted line indicates 0. Note that the amplitude of the peak response decreases with age. Inset shows average amplitudes grouped by age. Cells that respond with a Ca^{2+} decrease are prominent after hearing onset. n= 222 cells for P0-5 age group; n=184 cells for P9-12 age group, n=177 cells for P13-16 age group, and n=89 cells for P17-19 age group.

5.2.2. Group I mGluR-mediated responses that increase $[Ca^{2+}]_i$ during development

During development mGluRs responses became progressively smaller and their profile changed. There was a transition from a Ca^{2+} profile characterized by a clear peak and a plateau encountered in neonatal cells, to a profile characterized by a peak only (Figure 28). This was quantified by determining the amplitude, area, and duration of the response (as described in the method section 2.10.3). By the end of the third week peak amplitude and area of the responses were reduced by ~80%, duration was reduced by ~60%, and the plateau phase mostly abolished (Figure 29). To further quantify changes in Ca^{2+} profiles, Ca^{2+} responses were classified in three groups: peak and plateau (pp), peak small plateau (psp) and peak no plateau (pnp), as described in method section 2.10.3. Pp responses were characterized by a clear peak and plateau phase, long duration and long decay time constant (Figure 30 A-E and values of parameters characterizing these cells for each age group are given in Table 3). Psp responses were characterized by smaller peak and plateau amplitudes and/or shorter duration of responses. Pnp responses completely missed the plateau phase and also had smaller peak amplitudes, shorter duration and shorter decay time constants. As shown in Figure 30 F in the first postnatal week pp cells were prevalent. Their number decreased starting before hearing onset. At the same time the number of psp cells increased. Around hearing onset there is a mixture of pp, psp and pnp cells and by the end of the 3rd postnatal week the pp and psp cells disappear.

A possible explanation for these results is that the group I mGluR signaling pathway undergoes developmental changes. As shown in Chapter 4, in neonatal neurons the sources of calcium are Ca^{2+} release from the internal stores and Ca^{2+} influx through an unknown channel. This channel might be a member of the TRP family. Because the Ca^{2+} influx is the sole source of the plateau phase, one hypothesis is that the presumed TRP channel is downregulated during development. Thus, in the following experiments the sources of Ca^{2+}during development are further investigated.

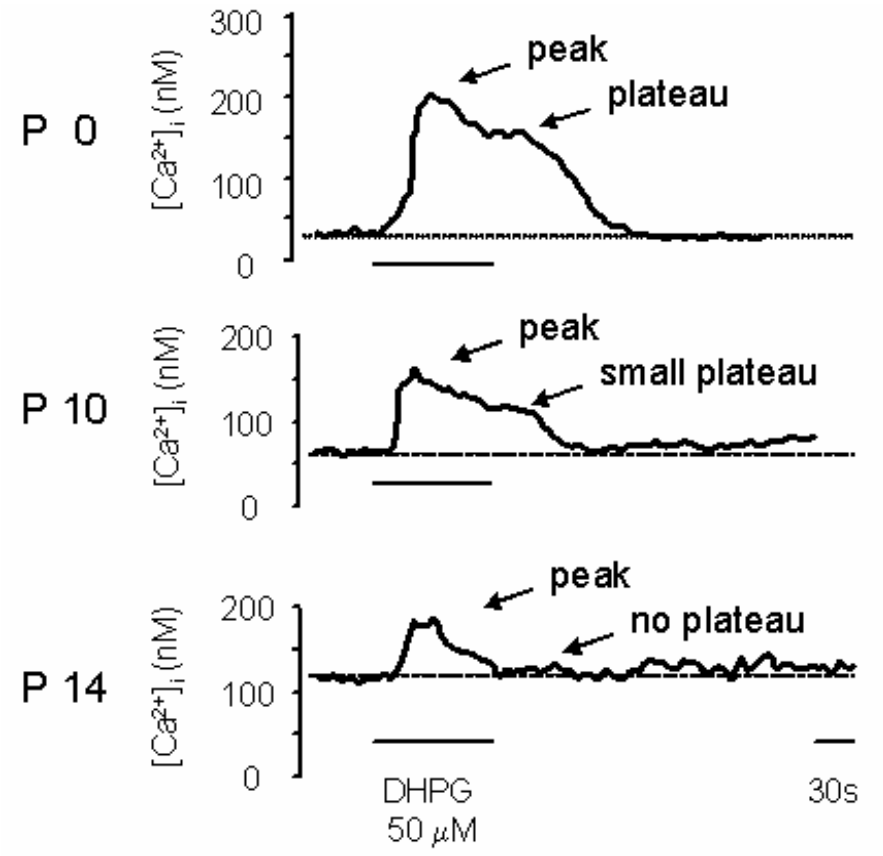

Figure 28. Group I mGluR-mediated Ca^{2+} responses during development.

Ca^{2+} profiles undergo a transition from a peak and plateau to a peak only profile.

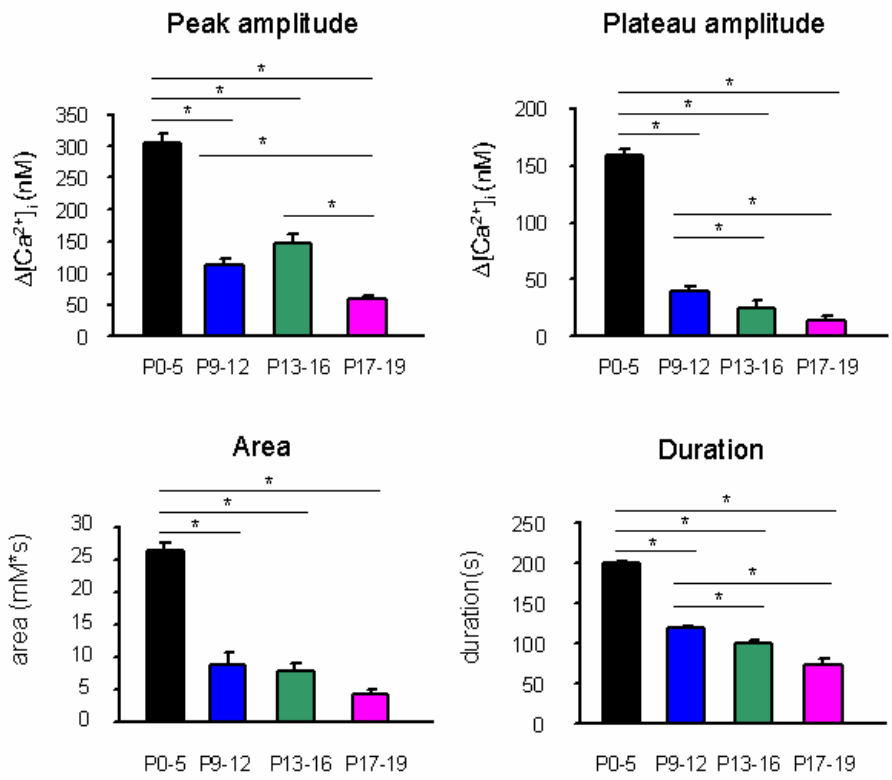

Figure 29. Quantitative changes in Ca^{2+} responses during development.

Summary of all cells that increase $[Ca^{2+}]_i$ in response to DHPG (50 μM, 90s). P0-5 age group includes 222 cells, P9-12: 165 cells, P13-16: 135 cells, and P17-19: 54 cells.

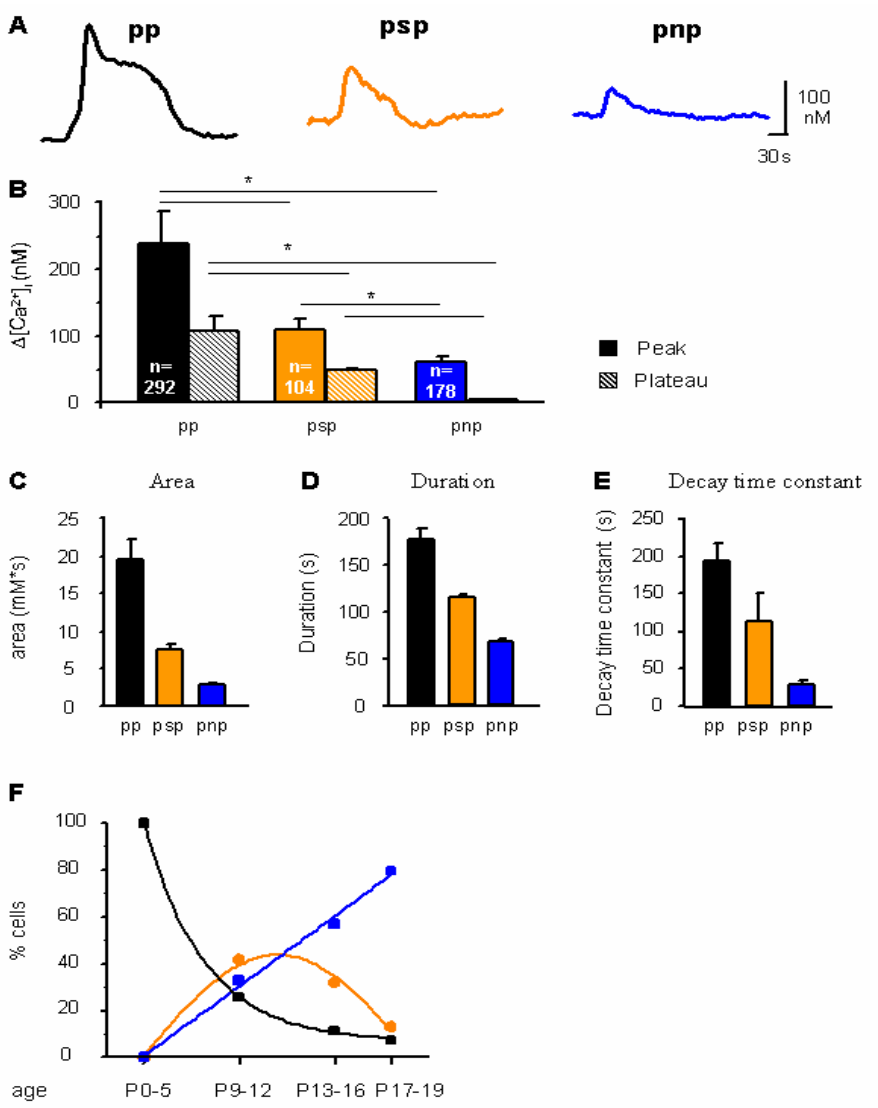

Figure 30. Quantification of parameters for all pp, pnp and psp cells.

A. Examples of pp, psp and pnp responses. **B-E.** Quantification of peak and plateau amplitude (B), area (C), duration (D), decay time constant (E). Responses are pooled across age groups. **F**. Distribution of cells that increase $[Ca^{2+}]_i$ as a function of response type and age. The percentage of pp cells decreases during development while the percentage of pnp cells increases. Number of cells: P0-5 n=222; P9-12 n=165; P13-16 n=135; P17-19 n=54. Data were fitted with single exponentials for pp and pnp cells and with bell-shaped curve function for psp cells. n - number of cells.

Table 3. Parameters describing DHPG-evoked Ca^{2+} responses during development.

Responses were elicited by DHPG (50μM, 90s). N = total number of cells that increase $[Ca^{2+}]_i$; n = number of cells in a certain group; % = percentage of cells in a group from the total number of cells that increase $[Ca^{2+}]_i$. x = indefinite; the plateau amplitude is zero, the ration between the peak and plateau is indefinite. For details for cell classification see methods section 2.10.3.

Response type	pp				psp			pnp		
Age group	P0-5	P9-12	P13-16	P17-19	P9-12	P13-16	P17-19	P9-12	P13-16	P17-19
N	222	178	132	54	178	132	54	178	132	54
n	222	46	15	4	75	42	7	59	75	43
n/N (%)	100	24	11	7	42	32	12	32	57	80
Peak amplitude (nM)	304 ±15	247 ±27	304 ±51	90 ±6	106 ±13	138 ±10	84 ±15	56 ±9	76 ±6	51 ±5
Plateau amplitude (nM)	157 ±7	97 ±11	121 ±20	51 ±3	51 ±4	46 ±6	65 ±13	-	-	-
Duration (s)	190 ±3	157 ±5	167 ±6	215 ±8	129 ±3	122 ±4	172 ±22	65 ±3	76 ±2	65 ±3
Decay time cst (s)	242 ±10	154 ±19	160 ±20	224 ±64	83 ±12	56 ±6	179 ±74	34 ±3	31 ±4	25 ±3
Area (mM*s)	25.9 ±1.0	16.0 ±1.8	26.3 ±4.2	11.6 ±0.3	8.3 ±0.7	9.2 ±0.7	11.9 ±1.5	2.1 ±0.3	3.1 ±0.3	2.5 ±0.4
Ratio peak/plateau	1.88 ±0.04	2.47 ±0.2	3.27 ±0.7	1.8 ±0.2	2.36 ±0.18	4.98 ±0.75	1.3 ±0.2	x	x	x

5.2.3. Developmental changes in the Ca^{2+} sources of group I mGluR-mediated Ca^{2+} increases

To determine the contribution of Ca^{2+} influx, mGluRs were activated in 0 mM external calcium. As shown in Figure 31A (and absolute Ca^{2+}values given in Table 4), the contribution of Ca^{2+} influx from the extracellular medium in pp (P0-5) and psp cells (P9-13, P13-16) was about 70 to 85% of the total Ca^{2+} response quantified by the peak amplitude and the area. In contrast, in pnp cells (P13-16, P17-18) the contribution was much smaller, about 10 to 25%. Extracellular calcium contributed differently to the two components of the response: peak and plateau phase. In the absence of extracellular calcium, the peak response of pp and psp cells was greatly reduced, revealing the contribution of the internal stores, while the plateau response was completely abolished, in pp and psp cells (Figure 31 B). Thus, the internal stores contributed to DHPG-mediated responses at all ages tested while the Ca^{2+} influx component diminished during development. Interestingly, removal of external calcium unmasked Ca^{2+} release from the internal stores in cells that show no response to DHPG (n=7 cells; Figure 31 C), or a decrease of $[Ca^{2+}]_i$ in the presence of extracellular Ca^{2+} (Figure 31 D).

In summary, Ca^{2+} influx from the extracellular medium diminished during development while the release from the internal stores was present in all cells at all ages. This suggests that the mGluR - PLC - IP_3 - internal stores pathway is unaffected by development. Thus, either the link between the internal stores and the channel responsible for Ca^{2+} influx or the channel itself is developmentally downregulated.

As shown in chapter 4, the channel mediating Ca^{2+} influx in the LSO is different from conventional VGCCs and it is dependent on Ca^{2+} release from internal stores. Potential candidates are members of the transient receptor potential channels (TRP) some of which are activated by mobilization of intracellular calcium (review: Clapham et al., 2001). Although specific agonists and antagonists for the large family of TRP channels are currently unavailable, many TRP channels can be blocked by Ni^{2+}, La^{3+} and 2-APB (review: Clapham et al., 2001). Thus, these drugs were tested to verify whether the channel expressed in the LSO neurons is part of the TRP family.

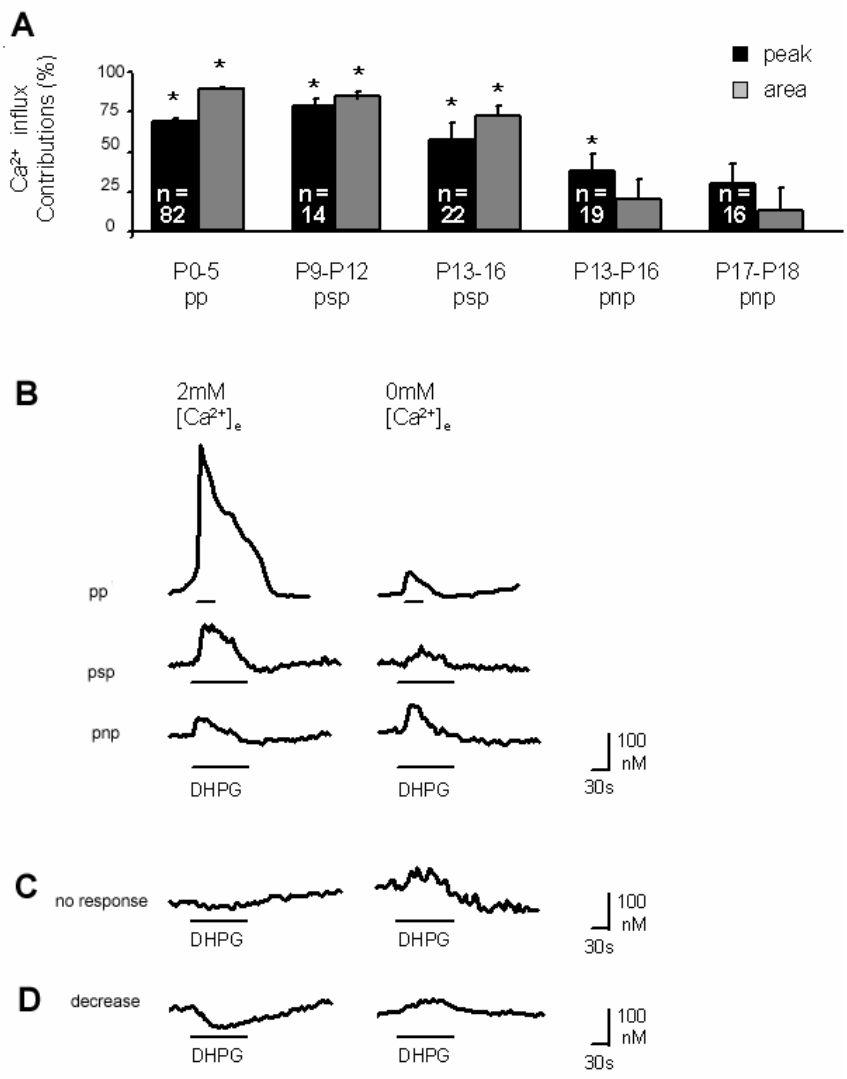

Figure 31. The contribution of Ca^{2+} influx to mGluR-mediated Ca^{2+} responses decreases during development.

A. In pp (P0-5) and psp (P10-11) cells influx of extracellular calcium contributes significantly to the mGluR-mediated response. In pnp (P17-18) cells the contribution is drastically reduced. Asterisks indicate significant contribution ($p < 0.01$; paired t-test). **B-D.** Examples from individual cells of DHPG-elicited responses in 2mM $[Ca^{2+}]_e$ (left traces) and in 0 mM $[Ca^{2+}]_e$ (right traces). In pp (P1) and psp (P10) cells removal of external calcium, reduces the peak response and abolished the plateau phase. The profile of the pnp (P17) response is mostly not affected in 0 Ca^{2+}.

Table 4.Contribution of Ca^{2+} influx to DHPG-elicited Ca^{2+} responses during development.

Asterisk - significant changes, paired t-test $p<0.01$; n-number of cells; %=percentage contribution to Ca^{2+} influx.

	Peak (nM)			Area (mM*s)			n
Age/group	Control	0[Ca^{2+}]e	%	Control	0[Ca^{2+}]e	%	
P0-5 pp	417±19	117±7	68 ± 2 *	19.8±0.6	2.4±0.1	88 ± 1 *	82
P9-12 psp	115±16	22±3	76 ± 4 *	6.6±0.9	0.8±0.03	82 ± 4 *	14
P13-16 psp	109±11	38±8	57±10 *	6.0±0.6	1.5±0.3	72 ± 6 *	22
P13-16 pnp	50±6	33±8	37±10 *	2.7±0.4	2.2±0.3	19± 12	19
P17-19 pnp	48±6	37±9	28±11	2.6±0.4	2.1±0.4	11± 14	16
P14-17 no change in $[Ca^{2+}]_i$	0	29±15	*	0	1.4±0.7	*	7
P14-17 decrease in $[Ca^{2+}]_i$	-23±5	53±15	*	4.6±0.9	2.3±0.6	*	11

5.2.4. Influx of extracellular Ca^{2+} is sensitive to Ni^{2+}

Some store-operated channels and TRP channels are inhibited by millimolar concentration of Ni^{2+} (Villalobos and Garcia-Sancho, 1995). Thus, the sensitivity of DHPG-mediated responses to Ni^{2+} in the LSO was tested. Short application of Ni^{2+} (2 mM for 2 min; Figure 32 A) during the plateau response induced by DHPG (20 μM) transiently decreased the response to the baseline, indicating the contribution of Ni^{2+}-sensitive channels to the entire plateau phase. Short application of Ni^{2+} during the peak response evoked by DHPG resulted in a

significant decrease of the peak amplitude, to about 14 ± 2 % (n = 10 cells, P5; Figure 32 A), indicating the contribution of Ni^{2+}-sensitive channels to the initial peak. Washout of Ni^{2+}, in the continued presence of DHPG resulted in a peak followed by a plateau, suggesting that Ni^{2+} blockade is reversible. In slices pretreated with Ni^{2+}, DHPG responses of pp and psp type (P0-5, P9-13, P13-16) closely resembled responses observed in the absence of the external calcium i.e. the plateau response was abolished and the peak response was greatly reduced (example in Figure 32 B and absolute Ca^{2+} values given in Table 5). DHPG responses of the pnp type (P13-16 and P17-18) were mostly unaffected by Ni^{2+} (example in Figure 32 C). In the same cells, Ni^{2+} reduced Ca^{2+} responses elicited with KCl (60mM, 30s) by about 75% (last column of Table 5), demonstrating that the absence of an effect is not due to the fact that Ni^{2+} might not have worked properly. Quantification of peak and area of responses in control and in the presence of Ni^{2+} indicate that in pp and psp cells the Ni^{2+}-sensitive channel accounts for most or all Ca^{2+} influx from the extracellular space (compare Figure 32 D with Figure 31 A). In pnp cells Ni^{2+}-sensitive channel has no significant contribution. (Figure 32 D)

It is noteworthy that in a small group of pnp cells at P13-16 (n=7 cells, N=3 slices) responses were potentiated approximately 4 fold by Ni^{2+}. These cells were not included in the above analysis and data are shown in the last row of Table 5. These cells could represent different cell types that may possibly express different channel types. The mechanism underlying this effect remains to be investigated.

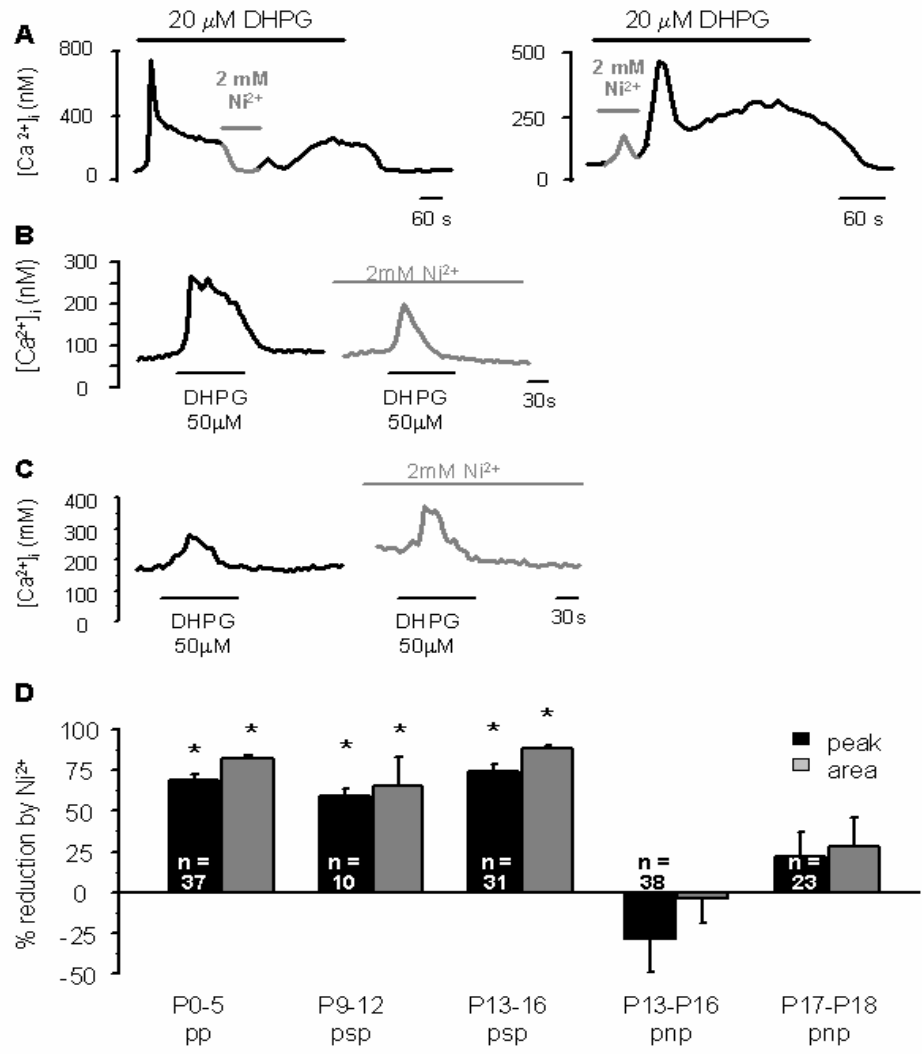

Figure 32. mGluR-mediated Ca^{2+} responses involve calcium influx through Ni^{2+}-sensitive channels.

A. *Left trace*: short application of Ni^{2+} (2 mM, 2 min) during the plateau phase of a calcium response elicited by DHPG (20 μM, 10 min) reduces the response to baseline. *Right trace*: application of Ni^{2+} (2 mM, 2 min) together with DHPG reduces the amplitude of the initial peak response. P5 neuron. **B.** Psp responses are greatly reduced in the presence of Ni^{2+}. Example is from P10 neuron. **C**. Pnp responses are the least affected by Ni^{2+}. Example is from a P15 neuron. **D**. Quantification of the effects of Ni^{2+}. Bar graphs show percentage of peak (black) and area (gray) of the DHPG-evoked response in 2mM Ni^{2+}. Data are grouped by age and response type.

Table 5. Effect of Ni^{2+} on DHPG-evoked Ca^{2+} responses during development.

Asterisk – significant changes; paired t-test $p<0.01$. The last row includes cells that were potentiated by Ni^{2+} and in this case % represents percentage potentiation by Ni^{2+}.

	Peak (nM)			Area (mM*s)				
Age/group	Control	Ni^{2+}	% reduction by Ni^{2+}	Control	Ni^{2+}	% reduction by Ni^{2}	n	% reduction of KCl
P0-5 pp	416 ±40	174± 19	69 ± 3 *	27.3 ±2.6	6.3 ±0.7	80 ± 2 *	37	65±5 *
P9-12 psp	115 ±16	22 ±3	60 ± 4 *	6.6 ±0.9	0.8 ±0.03	66 ± 17 *	10	62±8 *
P13-16 psp	136 ±18	40 ±12	74 ± 3*	11.8 ±1.7	1.4 ±0.5	88 ± 2 *	31	72±6 *
P13-16 pnp	57 ±7	86 ±17	-27 ± 20	2.2 ±0.3	2.2 ±0.3	-3 ± 14	38	66±7 *
P17-19 pnp	48 ±7	27 ±3	22 ± 15	1.8 ±0.2	0.9 ±0.1	27± 18	23	80±2 *
P13-16 psp potentiation	*124 ±22*	*273 ±41*	*429±126 *	*5.1 ±0.9*	*11.6 ±1.7*	*405±200 *	*7*	*73±3 *

5.2.5. DHPG-mediated responses are sensitive to 2-APB

2-APB is a nonspecific blocker of TRP channels acting from the extracellular site. It is also a membrane permeant IP_3 receptor (IP_3R) inhibitor. The effects are dependent on the doses of 2-APB and these doses depend on cell type, species, and age. In general, at lower doses (5-20 μM) 2-APB acts mostly on TRP channels while at higher doses (50-100 μM) it inhibits the

function of IP_3Rs (Ascher-Landsberg et al., 1999; Prakriya and Lewis, 2001; Soulsby and Wojcikiewicz, 2002; review: Bootman et al., 2002). In the hypothesis that the plateau response is mediated by a TRP channel, one can therefore expect that 2-APB at lower concentration inhibits the plateau component more than the peak component.

Figure 33 A shows an example from a single cell (P4) responding to DHPG in the presence of increasing concentrations of 2-APB, illustrating the dose dependent inhibition of plateau and peak components. Controls included washout of 2-APB (for more than 30 minutes) and KCl (60mM, 30s) depolarizations. After washout of 2-APB (50μM) the peak component recovered to 87 ± 3% while the plateau recovered only to 16 ± 2% (n=65 cells), indicating that 2-APB did not kill the cells (Figure 33 B). The almost irreversible inhibition of the plateau phase is consistent with other studies of 2-APB action (Peppiatt et al., 2003).

Because effective doses of 2-APB vary in different cell types (review: Bootman et al., 2002), increasing concentrations of 2-APB (similar to dose-response relations) were tested in each slice and results are presented as average of cells of the same type (i.e. pp, psp, pnp) from all slices in an age group. At concentrations between 2-5 μM, 2-APB potentiated most DHPG responses, typically the peak component (Figure 34 A-G upper panels; see Table 6 for statistical significance of each data point compared to control; paired t-test). This potentiation was approximately1.3 to 3 fold and it was observed at all ages and in all types of responses (pp, psp, pnp). While the mechanism of this 2-APB effect is still unclear, similar observations have been made in Jurkat cells, leukemia cells (Prakriya and Lewis, 2001; review: Bootman et al., 2002), and recently in dopaminergic neurons (Tozzi et. al., 2003). At the other end of the concentration range used, 100μM 2-APB completely abolished the response most likely because of inhibition of IP_3R function. As shown in Figure 34, in pp and psp cells, both peak and plateau are reduced by 10-50 μM 2-APB; nevertheless the effect was more pronounced on the plateau response. This differential effect is better illustrated in Figure 34 panel H, where the percentage reduction of peak and plateau components is plotted for a single 2-APB concentration, 20μM (for actual values see Table 7). In all slices, KCl (60mM, 90s) was also applied in the presence of each 2-APB concentration (Figure 34) as a control for cell healthiness and as a control for the effect of 2-APB. In general, 2-APB had either no effect or increased the amplitude of KCl responses. The effect was mostly random, there was no obvious pattern (i.e. a certain 2-APB concentration causes increase of the response; or after a certain time period the response increases). This

suggests that DHPG and KCl-elicited responses are mediated through different sources and 2-APB does not block VGCCs (Maruyama et al., 1997; Asher-Landsberg et al., 1999; Potocnik and Hill, 2001; review: Bootman et al., 2002). Taken together these results are consistent with the hypothesis that the plateau component is mediated by TRP channels.

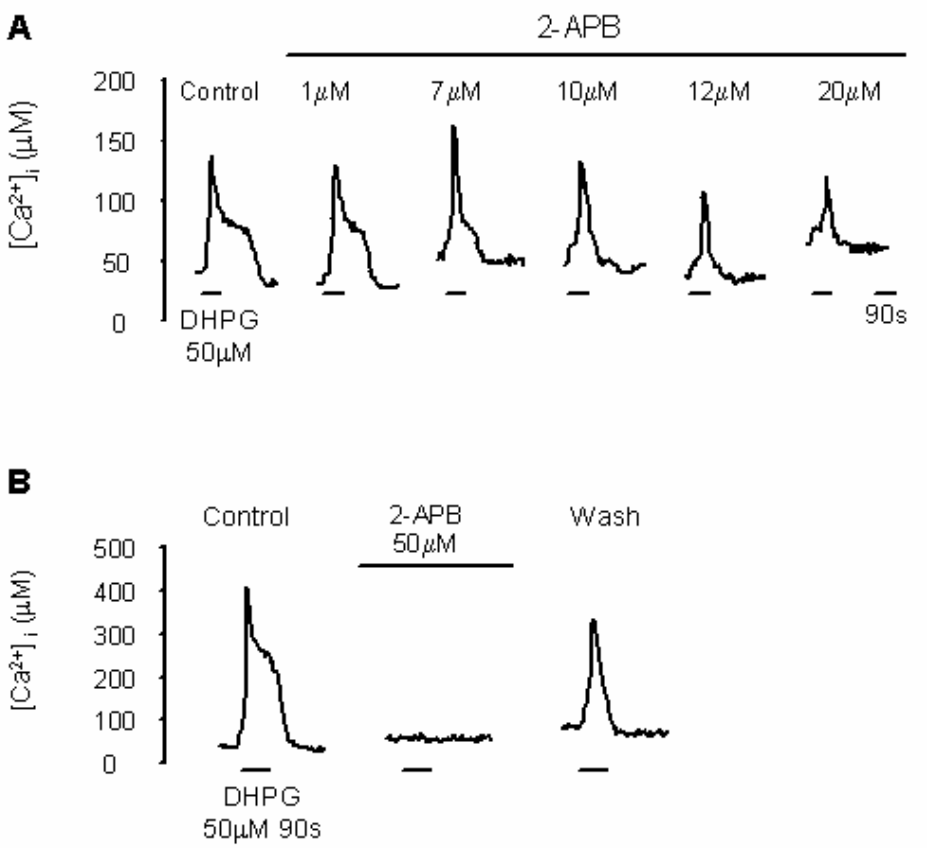

Figure 33. 2-APB effect on DHPG-evoked responses.

Responses are elicited by bath application of DHPG (50 μM, 90s) **A.** Example of the effect of increasing doses of 2-APB on plateau and peak response. Lower doses inhibit the plateau more then the peak. Example is from a P1 cell. **B.** Partial recovery from 2-APB (50 μM) inhibition. Example is from a P4 cell.

Table 6. Statistical significance of 2-APB effect on peak and plateau components of DHPG-elicited Ca^{2+} responses.

Statistical significance tested with ANOVA: ns = not statistically significant, p>0.01; * =statistically significant, p<0.01.

Age		2 μM	5 μM	10 μM	20 μM	50 μM	100 μM	n
P0-5 pp	Peak	ns	ns	ns	*	*	*	125
	Plateau	*	*	*	*	*	*	125
P9-12 pp	peak	*	ns	ns	ns	ns	*	13
	plateau	ns	ns	*	*	*	*	13
P9-12 psp	peak	*	ns	ns	ns	ns	*	38
	plateau	*	*	*	*	*	*	38
P9-12 pnp	peak	*	*	ns	*	ns	*	37
P13-16 pp	peak	ns	ns	ns	ns	*	*	10
	plateau	ns	ns	*	*	*	*	10
P13-16 psp	peak	ns	ns	ns	ns	*	*	16
	plateau	*	*	*	*	*	*	16
P13-16 pnp	peak	*	ns	ns	ns	ns	*	20

Table 7. Percentage reduction of peak and plateau phases of DHPG-elicited Ca^{2+} responses by 20 μM 2-APB.

n= cells; N= slices; Values are mean ± SEM.

	pp				*psp*				*pnp*		
Age	reduction peak (%)	reduction plateau (%)	n	N	reduction peak (%)	reduction plateau (%)	n	N	reduction peak (%)	n	N
P0-5	73.9±3.5	40.2±2.9	125	3							
P9-12	67.5±23.2	25.5±12.7	13	2	77.6±13.9	43.4±10.0	38	4	102.3±30.5	37	3
P13-16	64.0±12.4	4.04±2.9	10	2	60.1±8.0	1.5±1.1	16	2	58.5±16.0	20	2

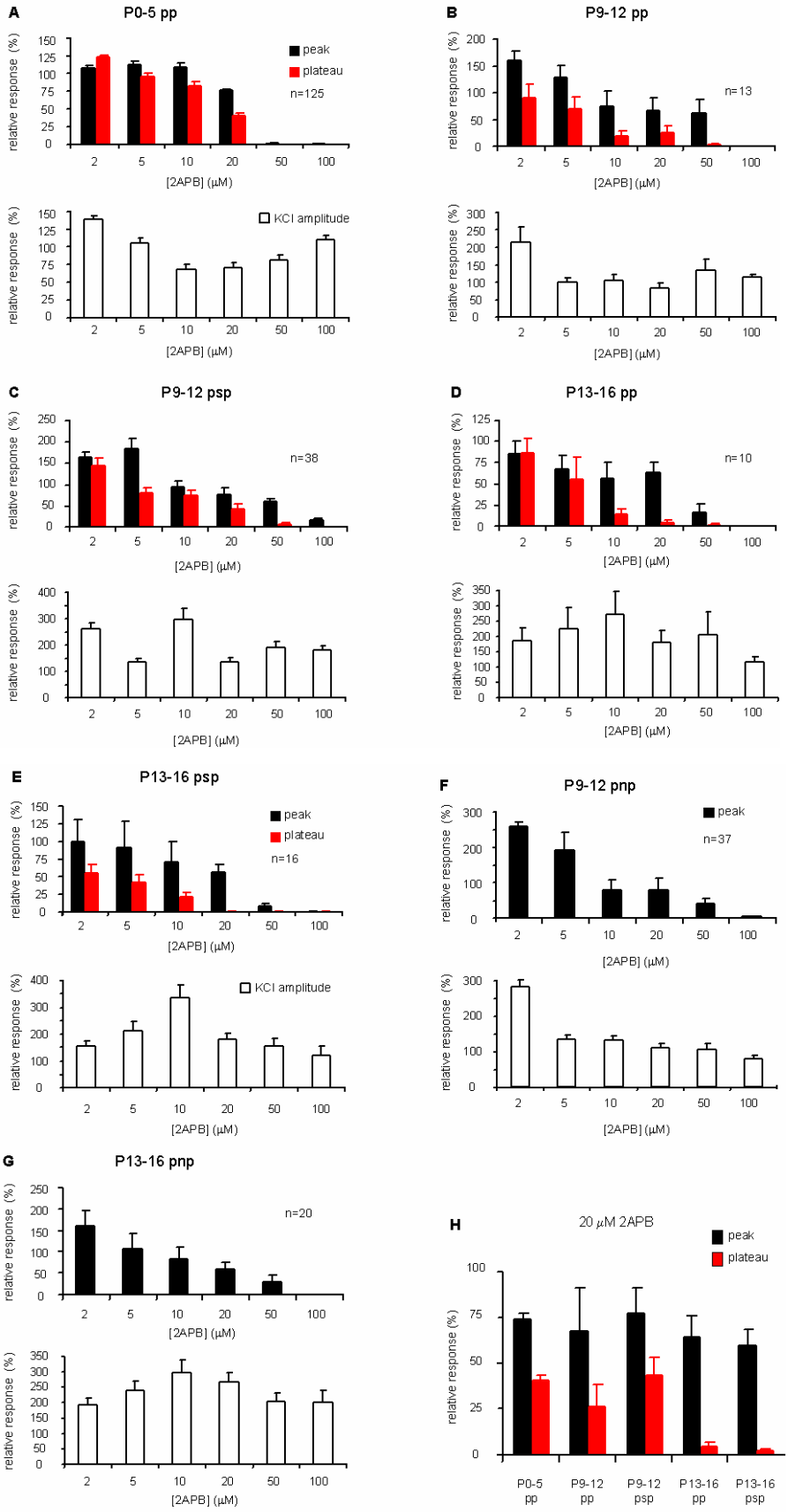
A
P0-5 pp
peak
plateau
n=125
KCl amplitude
B
P9-12 pp
n=13
C
P9-12 psp
n=38
D
P13-16 pp
n=10
E
P13-16 psp
peak
plateau
n=16
KCl amplitude
F
P9-12 pnp
peak
n=37
G
P13-16 pnp
n=20
H
20 μM 2APB
peak
plateau
P0-5 pp
P9-12 pp
P9-12 psp
P13-16 pp
P13-16 psp
relative response (%)
[2APB] (μM)

Figure 34. Peak and plateau components of DHPG-evoked responses are affected differently by 2-APB.

Upper panels in A-G: Peak (black) and plateau (red) of DHPG (50μM, 90s)-evoked responses as a function of 2-APB concentration. *Lower panels in A-G*: Amplitude of KCl-evoked responses for the same cells. **A**. Summary from n=125 P0-5 pp cells. **B**. Summary from n=13 P9-12 pp cells. **C.** Summary from n=38 P9-12 psp cells. **D.** Summary from n=10 P13-16 pp cells. **E.** Summary from n=16 P13-16 psp cells. **F.** Summary from n=37 P9-12 pnp cells. **G**. Summary from n=20 P13-16 pnp cells. **H**. Reduction of the peak and plateau phases of DHPG (50μM, 90s)-evoked responses by 20μM 2-APB for pp and psp cells shown in A-E.

5.2.6. The effect of La^{3+} on DHPG-elicited responses

Most TRPs are inhibited by micromolar concentrations of La^{3+} (Zhu et al., 1998; Kamouchi et al., 1999; Okada et al., 1999; Halaszovich et al., 2000; Inoue et al., 2001; Riccio et al., 2002b; Jung et al., 2002). Some TRPs, in particular TRPC4 & 5 are potentiated by lower concentrations of La^{3+} (~100 μM: Schaefer et al., 2000; 2002; Strubing et al., 2001; Jung et al., 2002). In order to further bring evidence that the channel mediating Ca^{2+} influx upon activation of mGluRs in LSO neurons is part of the TRP family, the sensitivity of DHPG-evoked responses to La^{3+} was tested. DHPG (50 μM, 90s) was applied in the presence of increasing concentrations of La^{3+} (100-2000 μM). Because prolonged applications of La^{3+} resulted in precipitation, only 2-3 concentrations were tested in each slice. Results are summarized by pooling together all cells (within a certain response type and within a certain age group) tested for a particular concentration of La^{3+}.

In neonatal cells (N=4 slices, P2-4), DHPG responses were reduced in a dose-dependent manner and were completely abolished by 1mM La^{3+} (Figure 35 A; and for absolute calcium values see Table 8). 1mM La^{3+} also completely abolished KCl responses (n=49 cells, N=2 slices), consistent with the known effect of La^{3+} on VGCCs (Ozawa et al., 1989).

In older slices (P10 and P15), La^{3+} had different effects depending on the concentrations. DHPG-evoked responses were potentiated up to 4 folds by 100 μM and 500 μM La^{3+}, and not affected by 1mM La^{3+} (Figure 35 B-E). The only exception was in P15 psp cells, where La^{3+} had mostly no effect. 2mM La^{3+} abolished responses but there was precipitation and data were not included in analysis.

In summary, in neonatal cells La^{3+} reduced DHPG responses in a dose-dependent manner, while at later ages La^{3+} potentiated DHPG responses in all cell types. Because La^{3+} has inhibitory and potentiating effects on different TRPs, these results suggest that different TRP subunits might be expressed at different ages in LSO neurons.

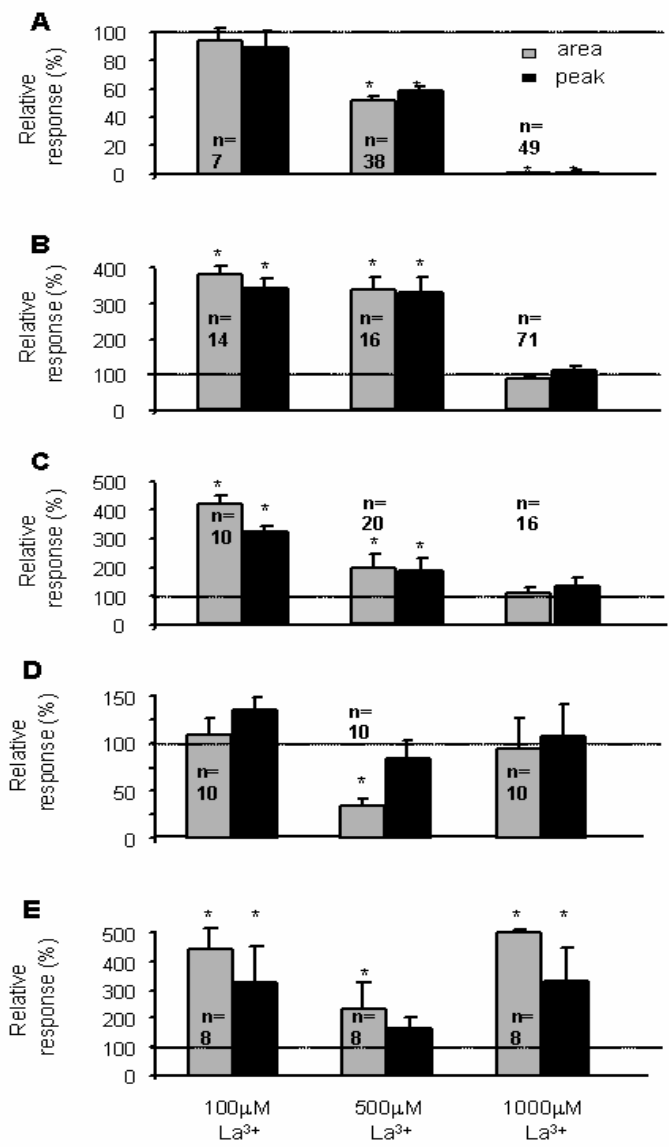

Figure 35. Effect of La^{3+} on mGluR-mediated Ca^{2+} responses during development.

A. In neonatal cells (P0-5) La^{3+} reduced peak (black) and area (gray) of DHPG (50µM, 90s) evoked responses in a dose dependent manner. **B-C.** In P9-12 cells of psp and pnp type lower doses of La^{3+} (100-500 µM) potentiated responses while 1mM had mostly no effect. **D**. In P13-16 psp cells La^{3+} was mostly ineffective in the concentration range tested. **E.** In P13-16 pnp cells La^{3+} potentiated DHPG-evoked responses at all concentrations tested. Dotted line represents 100%.

Table 8. Effect of La^{3+} on DHPG-elicited Ca^{2+} responses.

All responses were elicited by bath application of DHPG (50μM, 90s). n-cells; N-slices; Asterisk – $p<0.01$. % = percentage change after La^{3+}.

		Peak amplitude (nM)			Area (mM*s)				
Age	[La^{3+}] (μM)	control	La^{3+}	%	control	La^{3+}	%	n	N
P0-5 pp	100	466 ±125	358.6 ± 77.5	90.1 ±11.2	33.5 ± 7.4	28.2 ± 4.3	93.5 ±9.2	7	4
	500	225 ± 42	109.2 ± 13	59.3 ±2.6 *	18.4 ±2.6	8.5 ±0.9	51.7 ±3.5 *	38	4
	1000	250 ±31	3.0 ±2.7	1.6 ±1.4 *	27.5 ±2.5	0.097 ± 0.097	0.6 ±0.6 *	49	4
P9-12 psp	100	62 ±20	147 ± 37	331 ±40*	2.4 ± 0.5	6.8 ± 1.7	334 ±35 *	14	5
	500	43 ±10	145 ±36	340 ±28 *	2.0 ±0.6	7.2 ±1.5	379 ±24 *	16	5
	1000	123 ±18	172 ±36	110 ±14	10.3 ±2.0	9.1 ± 1.0	85 ±10	71	5
P9-12 pnp	100	39 ±4	133 ±15	347 ±26 *	1.7 ±0.2	7.2 ±0.8	421 ±30	10	5
	500	49 ±15	78 ±14	206 ±45 *	1.9 ±0.2	3.3 ±0.8	197 ±47 *	20	5
	1000	39 ±3	58 ±13	145 ±30 *	2.3 ±0.3	3.4 ±1.2	105 ±23 *	16	5
P13-16 psp	100	52 ±8	73 ±18	136 ±12	5.3 ±1.0	5.8 ±0.6	108 ±17	10	2

Table 8 (continued).

	500	50 ±5	40 ±9	85 ±19	5.5 ±0.6	2.0 ±0.5	34 ±8 *	10	2
	1000	52 ±8	72 ±15	125 ±7	5.4 ±1.0	5.3 ±1.8	93 ±12	10	2
P13-16 pnp	100	13 ±2	37 ±8	329 ±122 *	1.0 ±0.4	2.1 ±0.5	260 ±116 *	8	2
	500	14 ±2	21 ±4	166 ±39 *	0.9 ±0.2	1.2 0.2	233 ±89 *	8	2
	1000	13 ±2	39 ±13	329 ±120 *	1.0 ±0.4	1.9 ±0.7	240 ±120 *	8	2

5.2.7. Other types of mGluR-mediated Ca^{2+} responses

5.2.7.1. Ca^{2+} decrease: age dependence and pharmacology

DHPG-evoked responses that resulted in a decrease of $[Ca^{2+}]_i$ were encountered predominantly after hearing onset (Figure 27). In general, these responses were smaller in both amplitude and area compared to responses that increase $[Ca^{2+}]_i$ in the same age group (Figure 27 inset).

To determine whether there is a correlation between resting $[Ca^{2+}]_i$ values and the response to DHPG (i.e., increase or decrease of $[Ca^{2+}]_i$), histograms of baseline $[Ca^{2+}]_i$ values for all cells were constructed (Figure 37). Cells that increased and decreased $[Ca^{2+}]_i$ did not appear to fall into two different populations (compare black with hatched bars). Averaging all cells in an age group (Table 9) show that cells from P9-12 and P17-19 had slightly higher resting $[Ca^{2+}]_i$ while cells in P13-16 group showed no significant differences. However, because in the

histograms cells do not fall into two different populations, it is unlikely that cells that have higher baseline are the cells that decrease $[Ca^{2+}]_i$ in response to activation of the mGluR1s.

Table 9. Resting $[Ca^{2+}]_i$ in cells that decrease $[Ca^{2+}]_i$ and in cells that increase $[Ca^{2+}]_i$ in response to DHPG.

	Cells that decrease $[Ca^{2+}]_i$		Cells that increase $[Ca^{2+}]_i$	
Age group	Baseline $[Ca^{2+}]_i$ (nM)	n	Baseline $[Ca^{2+}]_i$ (nM)	n
P9-12	141.9±19	6	84.6±3.6	178
P13-16	97.5±6.7	43	114.0±5.5	132
P17-19	137.9±11	35	70.73±7.2	54

Comparison among the three age groups of cells that decrease $[Ca^{2+}]_i$ shows that the amplitude was slightly smaller for the P13-16 age group (Figure 36; ANOVA followed by Student-Newman-Keuls post hoc test $p<0.01$), while area was similar in all groups.

Intracellular stores contribute to responses that decrease $[Ca^{2+}]_i$ as shown in experiments performed in the absence of external calcium (peak response: control –23 ± 5 nM; $0Ca^{2+}$ 53 ± 15 nM; area: control 4.6 ± 0.9 mM*s, $0Ca^{2+}$: 2.3 ± 0.4 mM*s, n=11 cells, pooled data from P14-18, N= 2 slices; Figure 38). Removal of external calcium Ca^{2+} did not affect resting $[Ca^{2+}]_i$ (before: 80.6±9.3 nM; after: 92.9±11.5 nM; n=11 cells, $p>0.01$, paired t-test).

Ni^{2+} did not affect amplitude or area of DHPG-evoked responses (peak: 118 ± 12 % and area: 141 ± 19 %; n = 37 cells, N = 4 slices, P14-19; paired t-test $p > 0.01$; Figure 39). Baseline calcium slightly increased in the presence of Ni^{2+} (before: 97.2 ± 4 nM; after: 132.6 ± 8.2 nM; n = 37 cells, paired t-test $p < 0.01$). These results suggest that responses that decrease $[Ca^{2+}]_i$ are

not due to closure of a VGCC or a TRP open at rest. Other possibilities include a Na^{2+}/Ca^{2+} exchanger as demonstrated in cerebellar Purkinje cells or neurons in the amygdala (Staub et al., 1992; Mercuri et al., 1993; Linden et al, 1994; Keele, 1997).

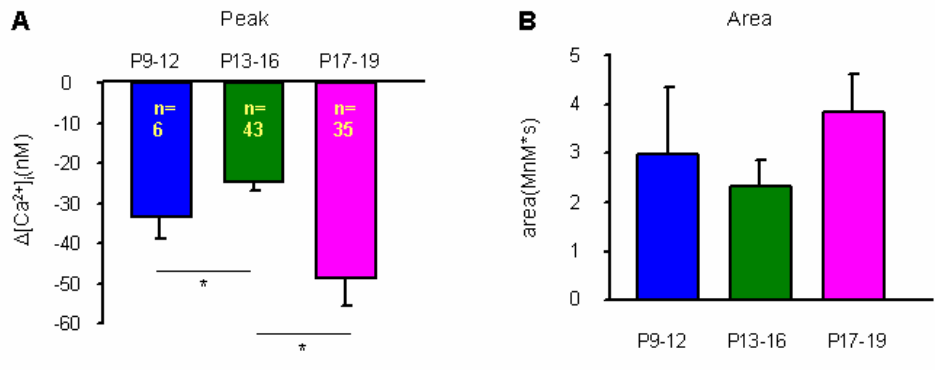

Figure 36. Group I mGluR-elicited responses that decrease $[Ca^{2+}]_i$.

Peak amplitude (**A**) and area (**B**) of DHPG (50μM, 90s)-elicited Ca^{2+} responses as a function of age.

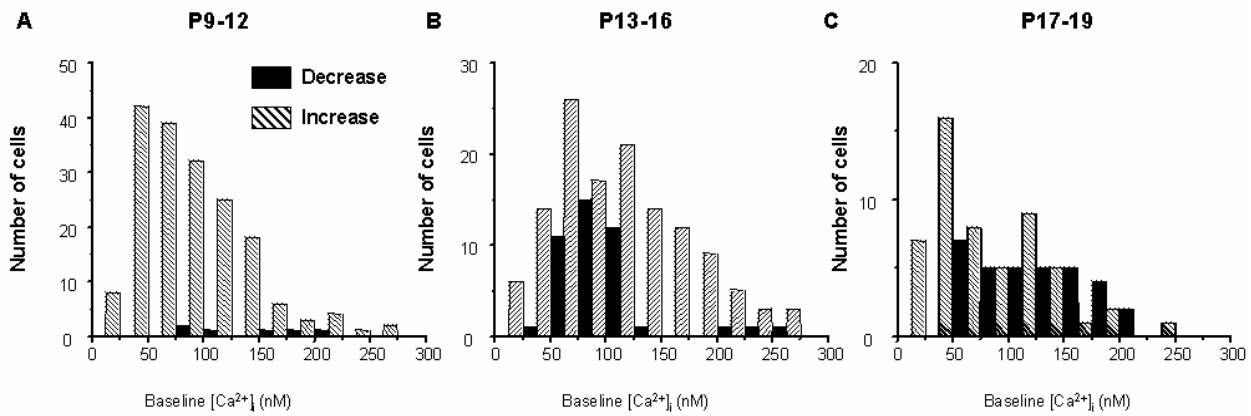

Figure 37. Resting $[Ca^{2+}]_i$ for cells that increase and decrease $[Ca^{2+}]_i$ in response to DHPG.

Histograms of resting $[Ca^{2+}]_i$ values for all cells that increase and decrease $[Ca^{2+}]_i$ in response to DHPG (50mM, 90s). **A**. P9-12 age group. **B**. P13-16 age group. **C**. P17-19 age group. Black represents baseline of cells that decrease $[Ca^{2+}]_i$ and hatched represents baseline of cells that increase $[Ca^{2+}]_i$. Bin size is 25.

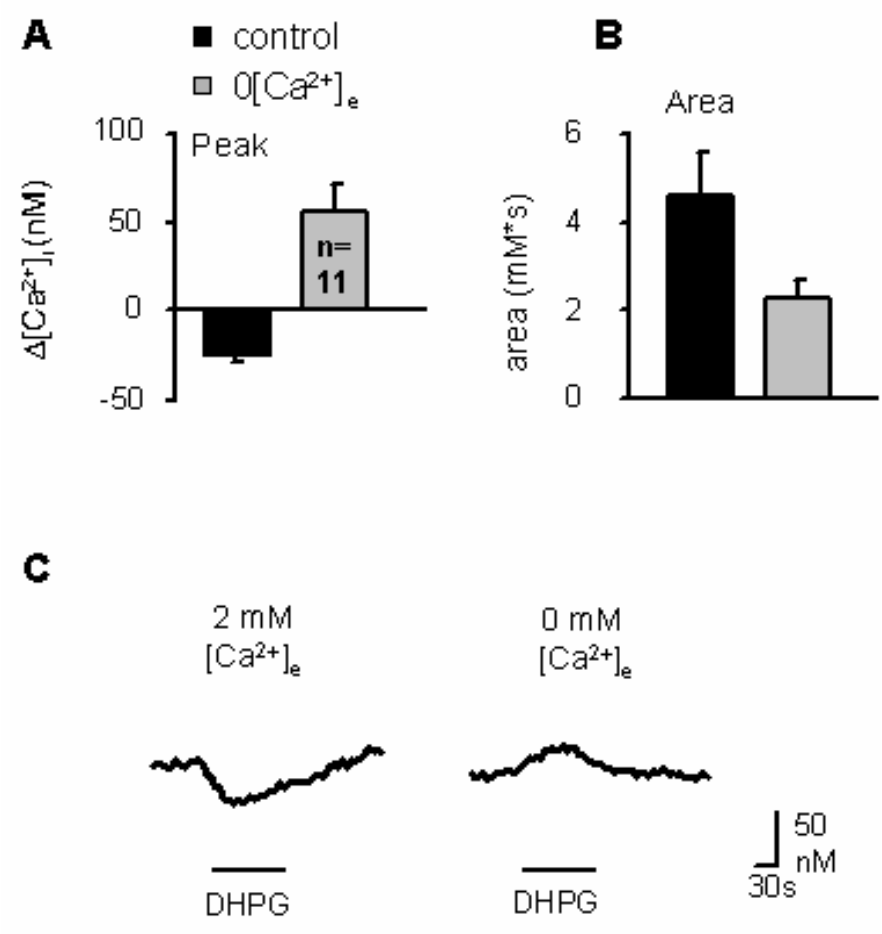

Figure 38. Internal stores contribute to group I mGluR-mediated Ca^{2+} responses in cells that decrease $[Ca^{2+}]_i$.

A. Peak and area of responses in control and after removal of extracellular calcium. Summary from 11 cells at P14-18. **B.** Examples from a P17 neuron, of a DHPG-elicited response in 2mM $[Ca^{2+}]_e$ (left trace) and in 0 mM $[Ca^{2+}]_e$ (right trace).

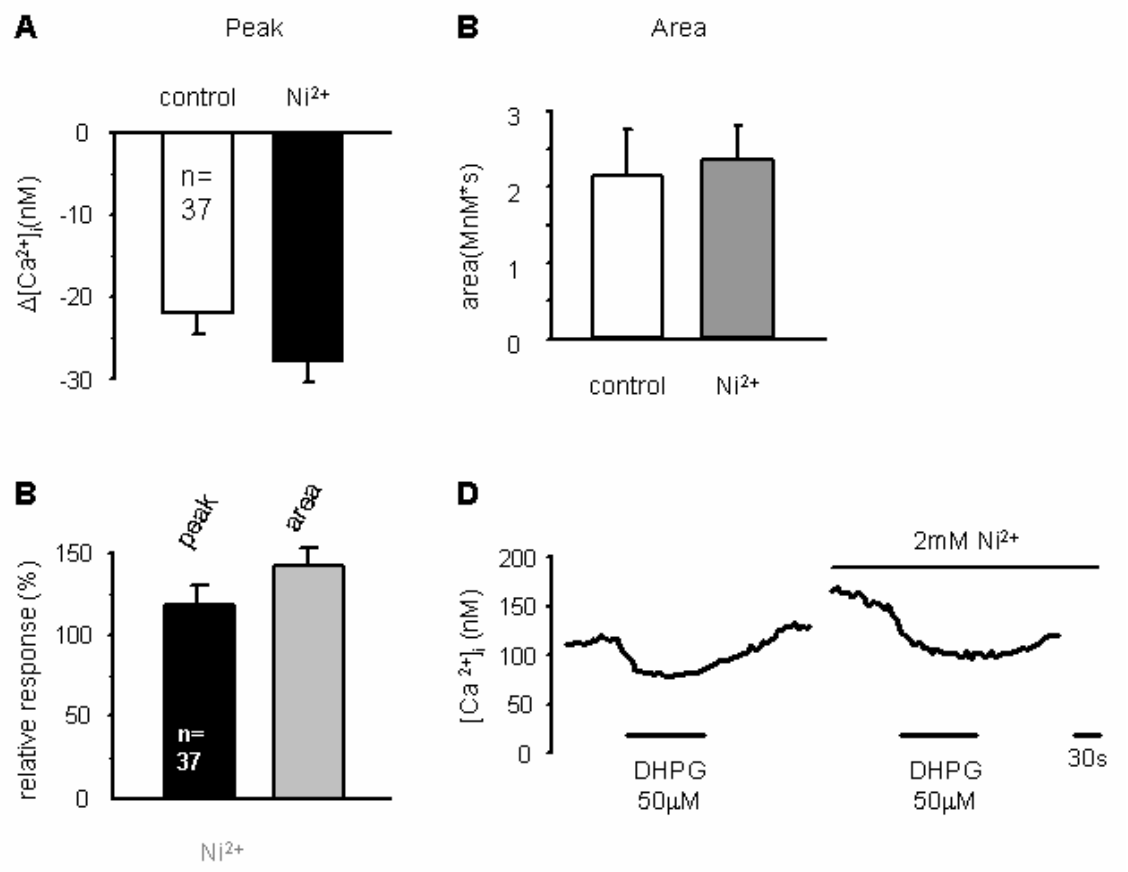

Figure 39. Group I mGluR-mediated responses that decrease $[Ca^{2+}]_i$ are insensitive to Ni^{2+}.

A, B. Peak amplitude and area of DHPG (50μM, 90s)-mediated responses in control and in 2mM Ni^{2+}. **C.** Percentage change of peak (black) and area (gray) of DHPG-mediated responses in 2mM Ni^{2+}. Summary from 37 neurons at P14-17. **D**. Example from a single cell at P15.

5.2.7.2. Oscillations

In a small percentage of LSO neurons, DHPG application induced $[Ca^{2+}]_i$ oscillations in the presence of TTX (1μM). The percentage of oscillating cells increased more than double from P0-5 group to P9-12 group (Fisher's exact test $p<0.05$), then it remained constant (Figure 40 A and Table 10). The frequency of oscillations increased slightly but not significantly as a function of age (Figure 40 B; ANOVA, $p<0.01$). The amplitude varied from approximately 30 nM to 300 nM but there was no obvious systematic correlation with age (examples of large amplitudes are illustrated in Figure 40 C, E and small amplitudes in Figure 40 D, F). In neonatal cells the oscillations lasted mostly as long as the response to the agonist lasted (Figure 40 C) while in older cells, the oscillations tended to outlast the agonist application (Figure 40 D-F).

Table 10. Group I mGluR-mediated $[Ca^{2+}]_i$ oscillations.

Age	# of slices with oscillating cells	Total nr of slices	# of oscillating cells	Total nr of cells	%	F (spikes/s)
P 0-5	10	28	21	709	2.96	0.023±0.002
P 9-12	6	14	13	186	6.98	0.032±0.004
P 13-16	8	25	13	180	7.2	0.033±0.004
P 17-19	4	15	8	115	6.95	0.046±0.011

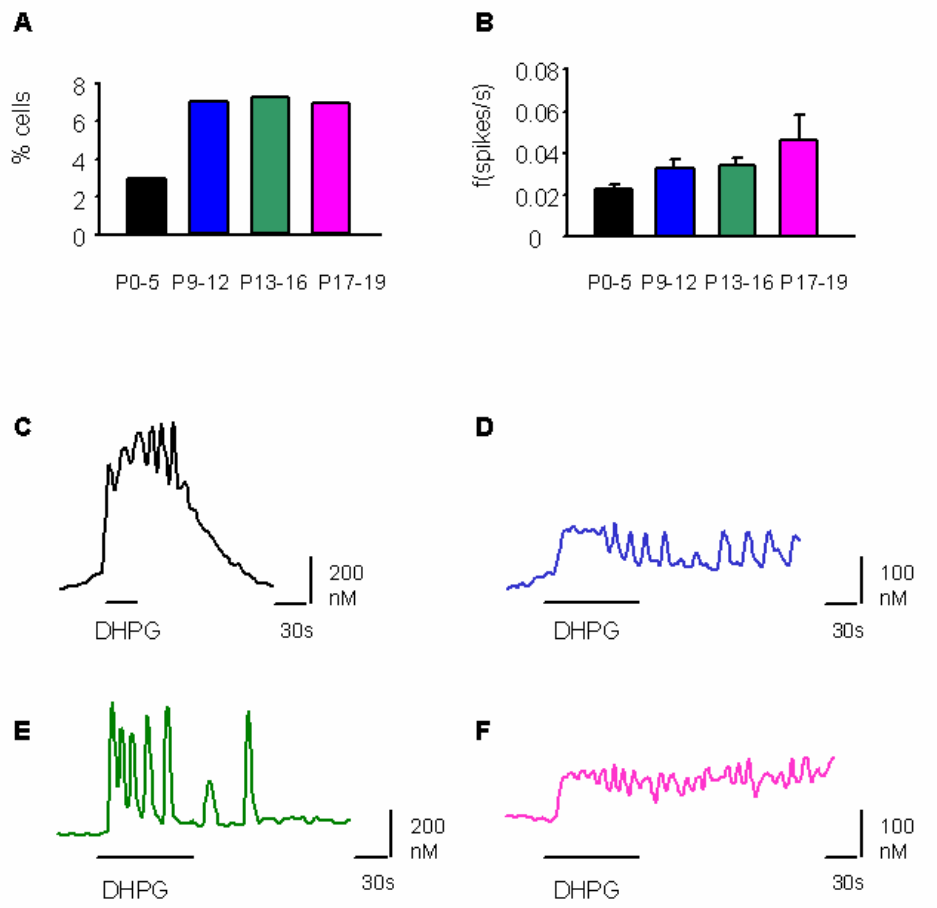

Figure 40. mGluR-mediated $[Ca^{2+}]_i$ oscillations.

A. Percentage of cells that show $[Ca^{2+}]_i$ oscillations in response to DHPG (20-50 μM). **B.** Frequency of oscillations in each age group. **C.** Example of large amplitude oscillations from a P5 cell. **D**. Example of small amplitude oscillations from a P10 cell. **E**. Example of large amplitude oscillations from a P15 cell. **F.** Example of small amplitude oscillations from a P18 cell.

5.3. SUMMARY

1. mGluR-mediated Ca^{2+} responses change during development. Before hearing onset a mechanism that increases $[Ca^{2+}]_i$ prevails while after hearing onset this mechanism is replaced by one that decreases $[Ca^{2+}]_i$ (Figure 26). Ca^{2+} from internal stores contributes to both mechanisms (Figure 31).

2. The amplitude of Ca^{2+} increases diminishes during development, suggesting changes in the mechanism responsible for the increase in $[Ca^{2+}]_i$. The increase mechanism involves Ca^{2+} release from internal stores followed by influx of extracellular Ca^{2+} possibly through a channel from the TRP family. Ni^{2+}, 2-APB and La^{3+} sensitivity of the Ca^{2+} influx early in development is consistent with a TRP channel. This channel contributes to the peak phase and it is the sole source of the plateau phase. This was shown in experiments performed in the absence of external calcium (Figure 31), and experiments in the presence of Ni^{2+} (Figure 32), where the peak was greatly reduced and the plateau phase was abolished. In addition, 2-APB inhibition of the plateau phase is also consistent with the contribution of this channel to the plateau phase (Figure 33). After hearing onset data suggest that the contribution of this channel decreases and it is completely absent in the third postnatal week (Figure 31, Figure 32). Whether the channel is developmentally regulated or the link between internal stores and the channel is affected during development remains to be determined.

3. At older ages, especially after hearing onset, DHPG-elicited responses are potentiated by La^{3+}, suggesting that TRPC4 and -5 may be expressed in the LSO (Figure 35; Schaefer et al., 2000, 2002; Strubing et al., 2001; Jung et al., 2002).

4. In the third postnatal week responses that decrease $[Ca^{2+}]_i$ are encountered. The mechanism responsible for the decrease of $[Ca^{2+}]_i$ cannot be explained by closure of a VGCC open at resting membrane potential as suggested in hippocampus neurons (Magee et al., 1996), because Ni^{2+}, a general blocker of VGCCs, has no effect.

5.4. DISCUSSION

5.4.1. Group I mGluR-evoked responses in neonatal LSO neurons: involvement of TRPC channels

The best characterized pathway by which group I mGluRs increase $[Ca^{2+}]_i$ is through activation of PLC which in turn hydrolyses PIP_2 to DAG and IP_3. DAG can further activate PKC and signaling cascades coupled to this kinase. IP_3 diffuses through the cytosol and activates IP_3Rs located on the internal stores (endoplasmatic reticulum), resulting in calcium release from the internal stores (Conn and Pin, 1997). This in turn activates store-operated channels permeable to calcium that allow calcium influx into the cytosol in order to refill the stores. Candidates for these channels are members of the TRP family (reviews: Clapham, 1996; 2001; Zhu and Birnbaumer, 1998; Hofmann et al., 2000; Zitt et al., 2002; Minke and Cook, 2002). First, members of the TRPC family (TRPC1 to –7) are expressed in the brain (review: Montell, 2001, Garcia and Schilling, 1997; Riccio et al., 2002a). Second, several members of the TRP family including TRPC3 (Zitt et al., 1997; Zhu et al., 1998), TRPC4 (Schaefer et al., 2000), TRPC5 (Okada et al., 1998; Schaefer et al., 2000) and TRPC6 (Boulay et al., 1997) are activated after stimulation of $G_{q/11}$-coupled receptors and can thus be activated by group I mGluRs. In developing LSO neurons, stimulation of group I mGluRs induced Ca^{2+} responses characterized by an initial peak followed by a long-lasting plateau. The pharmacological data presented here are consistent with group I mGluR dependent activation of a TRP channel. In the absence of external calcium, the peak amplitude of these responses was greatly reduced and the plateau phase was abolished, consistent with a store-operated channel (review: Putney, 1997). The activation of this channel was dependent on Ca^{2+} release from internal stores, as shown that after depletion of internal stores with thapsigargin mGluR stimulation failed to induce $[Ca^{2+}]_i$ increases. To date, the activation mechanism of TRP channels is still controversial. A conformational model was proposed for activation of TRPC3. This was based on experiments that suggest direct interaction between TRPC3 and IP_3R, confirmed by in vitro binding studies and identification of two interaction domains in the N-terminus of IP_3R and one in the C-

terminus of TRPC3 (Boulay et al., 1999). Other studies suggest DAG as a mechanism for activation of TRPC3 (in CHO-KI cells: Hoffmann et al., 1999). However, in pontine nuclei in slices from neonatal rat, DAG analogue fail to activate I_{BDNF} currents presumably mediated by TRPC3 (Li et. al., 1999). These contradictory results suggest that the activation mechanisms described in heterologous systems may not be the exact same activation mechanisms found in native cells, most likely due to interaction between TRPs and other proteins (review: Harteneck, 2003).

The TRP family is large and newly discovered, and to date no specific antagonists are available for individual TRP channels. General blockers of store-operated channels, including Ni^{2+} and La^{3+}, have been proved effective (Ni^{2+}: Villalobos and Garcia-Sancho, 1995; La^{3+}: Zhu et al., 1998; Okada et al., 1999; Kamouchi et al., 1999; Halaszovich et al., 2000; Inoue et al., 2001; Riccio et al., 2002; Jung et al., 2002). These unspecific blockers were also affecting the mGluR-mediated Ca^{2+} responses in neonatal LSO neurons. For example, 2mM Ni^{2+} greatly reduced the peak of DHPG evoked response and inhibited completely the plateau. La^{3+} also abolished the response. The concentration of La^{3+} necessary for response inhibition was in the high micromolar range (1000 μM). This suggests TRPC3 as a candidate because in HEK293 cells TRPC3 was inhibited by similarly high concentrations of La^{3+} (Zhu et al., 1996) while other TRPCs and store-operated channels were inhibited by low micromolar concentrations (Aussel et al., 1996; i.e. EC_{50} for TRPC6 is 6.2μM in Jung et al., 2002). 2-APB is another nonspecific inhibitor of TRPs and store-operated channels at low doses (5-20 μM) and an inhibitor of IP_3Rs function at high doses (50-100 μM; Landsberg et al., 1999; Prakriya and Lewis, 2001; Soulsby and Wojcikiewicz, 2002; review: Bootman et al., 2002). Consistent with this, DHPG-mediated responses were inhibited by 2-APB in a dose-dependent manner in developing LSO neurons. Moreover, the plateau response was always blocked by lower concentrations than the peak response, supporting the hypothesis that a TRP channel mediates the plateau.

In summary, the pharmacological data presented here are consistent with a TRP channel, perhaps TRPC3, mediating the DHPG-evoked Ca^{2+} responses in neonatal LSO neurons.

5.4.2. Group I mGluR-evoked responses in developing LSO neurons: downregulation of the TRPC channel

The pharmacological data suggest that the TRPC channel may be developmentally down-regulated. Several lines of evidence suggest this possibility. First, mGlu-mediated Ca^{2+} responses become smaller during development: peak and plateau diminish until the plateau vanishes. The internal stores contribute to DHPG responses throughout the development while the influx component vanishes. Second, Ni^{2+} reduces responses that have a peak and plateau but has no effect on cells that had no plateau, consistent with the idea that the channel may not be present. Third, La^{3+} becomes ineffective. The decrease in the contribution of the TRPC channel takes place around hearing onset (P12 in mice): it starts before P12 and it ends soon after, before P18. It will be interesting to determine whether the downregulation of this channel depends on neuronal activity. As TRPC channels are involved in signal transduction pathways (review: Voets and Nilius, 2003) it may be possible that downregulation of this channel may be involved in discriminating effects triggered by sensory and spontaneous activity.

Among the TRPC subgroup of TRP channels TRPC3 is most likely candidate for mediating Ca^{2+} influx triggered by mGluRs activation, for several reasons. First, it has been shown that TRPC3 is expressed in the brainstem during development from E18 to P20 (Li et al., 1999). This period mirrors the progressive decrease of group I mGluR-mediated Ca^{2+} responses in LSO neurons. Second, as mentioned before, DHPG-evoked responses in neonatal LSO neurons were inhibited by millimolar concentrations of La^{3+} (Figure 35), concentration which is in the range of TRPC3 sensitivity to La^{3+} (Zhu et al., 1996). Third, TRPC3 was suggested as a likely channel for group I mGluR-mediated Ca^{2+} responses in retinal amacrine cells (Sosa et al., 2002). However, immunostaining for the TRPC3 in mouse LSO resulted in no detectable level of expression at any developmental stage (Figure 42, Figure 43, see APENDIX). Further studies are required to identify the exact TRPC channel(s), its role in LSO neurons and the relationship with sensory activity.

After hearing onset either other or additional TRPC channels appear to be expressed in the LSO, as suggested by La^{3+} potentiation of DHPG-evoked responses (Figure 35). The potentiating effect of La^{3+} has been previously observed in other systems and it is attributed to

La^{3+} acting on TRPC4 & 5 (Schaefer et al., 2000; 2002; Strubing et al., 2001; Jung et al., 2002). It was shown that 10 to 1000 μM La^{3+} produces a three-fold increase in TRPC4 & 5 mediated current (Schaefer et al., 2000; 2002; Strubing et al., 2001; Jung et al., 2002), similar to the increases in Ca^{2+} responses described here (Figure 35).

In conclusion, it appears that different TRP subunits are expressed at different stages of LSO development. Further studies are necessary to identify these channels and their functions.

5.4.3. Other mechanisms involved in group I mGluRs mediated Ca^{2+} responses

5.4.3.1. $[Ca^{2+}]_i$ decrease

In the third postnatal week, activation of group I mGluRs decreased $[Ca^{2+}]_i$ in some LSO neurons (Figure 39), suggesting that this may be the case in adult neurons. There was no correlation between the resting calcium values and the response type. Such correlations might suggest that activation of group I mGluRs in cells with higher resting calcium values acts to decrease $[Ca^{2+}]_i$ to prevent accumulation of toxic calcium levels. However, this was not the case. This decrease was not mediated by closure of a VGCC open at rest, as Ni^{2+}, a general blocker of VGCCs (Gu et al., 1994) had no effect. Other mechanisms that could explain the decrease include mGluR-dependent activation of Na^+/Ca^{2+} exchanger (Staub et al., 1992; Mercuri et al., 1993; Linden et al, 1994; Keele, 1997). Electrogenic Na^+/Ca^{2+} exchange brings Na^+ from the extracellular space and extrude intracellular Ca^{2+}, with a Na^+: Ca^{2+} stoichiometry of 3:1 (Kimura et al., 1987; Ehara et al., 1989). In cerebellar Purkinje cells (Staub et al., 1992; Linden et al., 1994), in neurons in the basolateral amygdala (Keele, 1997) and in mesencephalic dopaminergic neurons (Mercuri et al., 1993) this mechanism was activated by group I mGluRs, it required intracellular Ca^{2+}, and it was dependent on extracellular Ca^{2+}. In LSO neurons the response was dependent on external Ca^{2+} (Figure 38) and calcium from the intracellular stores contributed to the response. The requirement of calcium from the intracellular stores for the mechanism inducing DHPG-mediated $[Ca^{2+}]_i$, decreases was not tested in the present experiments. The involvement of an

electrogenic Na^+/Ca^{2+} exchanger could be tested by lowering the extracellular concentration of Na^{2+} to block the transporter.

Functionally, the decrease in $[Ca^{2+}]_i$, could represent a mechanism for protecting against the accumulation of lethal intracellular calcium levels. At this age (>P12), the excitatory input to LSO neurons is presumably strong because of sensory activity. Thus, iGluR-mediated depolarizations could easily lead to high calcium influx through VGCCs. At the same time, AMPARs become Ca^{2+} permeable (Caicedo et al., 1998), providing an additional calcium influx route. Therefore activation of mGluRs might be a mechanism of reducing intracellular calcium levels and preventing calcium toxicity. In support for this, although the mechanism may differ, in chick NM activation of mGluRs prevents accumulation of toxic calcium levels induced by deafferentiation (Zirpel et al., 1995a, b; Zirpel and Rubel, 1996; Zirpel et al., 1998). In these neurons, mGluRs stimulate a second messenger system involving PKA and PKC-mediated inhibition of a VGCC (Zirpel et al., 1995a, b; Zirpel and Rubel, 1996; Lachica et al., 1995; Zirpel et al., 1998).

Similar decreases in $[Ca^{2+}]_i$ were triggered by $GABA_A$ and $GABA_B$ stimulation in LSO neurons after hearing onset (Kullmann et al., 2002), suggesting that mGluR and GABAergic intracellular pathways may converge.

5.4.3.2. $[Ca^{2+}]_i$ oscillations

DHPG-induced $[Ca^{2+}]_i$ oscillations were present in some developing LSO neurons. Although the percentage of cells showing oscillations did not change significantly with age, there was a trend towards higher percentages at older ages. Stimulation of both, mGluR1 and mGluR5, can induce Ca^{2+}oscillations (Kawabata et al., 1998). However, activation of mGluR5 results more often in oscillations while activation of mGluR1 results mostly in a Ca^{2+} response characterized by a peak and plateau (Nakanishi et al., 1998; Kawabata et al., 1998; Nash et al., 2002). Recent studies show that the density of mGluR5 receptors is proportional to the frequency of oscillations (Nash et al., 2002). In LSO neurons, the percentage of cells oscillating increased with age while the frequency increases slightly but not significantly (Figure 40). Thus, results presented here

may indicate an increase in the expression of mGluR5 with age. Further anatomical studies using specific antibodies against mGluR1 and mGluR5 are necessary to confirm this possibility.

Similar mGluR-triggered Ca^{2+} oscillations are encountered in immature neuronal cultures, developing neocortex, developing hippocampus, astrocytes, and heterologous cell cultures (Aniksztejn et al., 1995; Kawabata et al., 1996, 1998; Nakahara et al., 1997; Flint et al., 1999; Woodhall et al., 1999), and are thought to be important in signal transduction, regulation of gene expression and during development for neuronal differentiation (Berridge 1997; Gu and Spitzer, 1997; Berridge et al., 1998; Spitzer, 2000). mGluR-triggered $[Ca^{2+}]_i$ oscillations may serve similar roles in developing LSO neurons.

6. GENERAL DISCUSSION

The present study used Fura-2 Ca^{2+} imaging in brainstem slices to investigate the mechanisms by which glutamatergic inputs from the cochlear nucleus regulate $[Ca^{2+}]_i$ in developing LSO neurons.

In neonatal LSO neurons, iGluRs, group I and group II mGluRs were involved in mediating synaptically elicited calcium responses. Their contribution to $[Ca^{2+}]_i$ increases depended on the stimulus frequency.

AMPA/kainate receptors primarily mediated Ca^{2+} responses elicited by single stimuli and contributed to Ca^{2+} responses elicited by low and high frequency bursts by approximately 75% and 50% respectively. Both AMPAR and kainate receptors were Ca^{2+} impermeable and increased $[Ca^{2+}]_i$ via membrane depolarization and activation of VGCCs.

NMDARs contributed approximately 50% to Ca^{2+} responses independent of the stimulus frequency as long as the stimulus was strong enough to relieve the Mg^{2+} block. Their high contribution to Ca^{2+} responses was consistent with their contribution (30-60%) to EPSPs triggered by stimulation of AVCN-LSO synapses.

mGluRs contributed to Ca^{2+} responses only under high frequency stimulation (>20Hz). Pharmacological dissection revealed that group I mGluR-mediated Ca^{2+} responses had two components: release from internal stores and influx from the extracellular milieu. The influx was mediated by a channel sensitive to Ni^{2+}, La^{3+} and 2-APB, consistent with it being a member of the TRP family. During development, the contribution of this channel decreased and it was lost after hearing onset. This suggests that this channel might be downregulated by auditory experience. The most likely candidate was TRPC3 for several reasons. TRPC3 is expressed in the brainstem during development from E18 to P20 rat (Li et al., 1999) and this period mirrors the decrease of group I mGluR-mediated Ca^{2+} responses in mouse LSO neurons. In addition, DHPG-evoked responses in neonatal LSO neurons were inhibited by millimolar concentrations of La^{3+}, which is in the range of La^{3+} sensitivity of TRPC3 (Zhu et al., 1996). However,

immunostaining for TRPC3 in mouse LSO resulted in no detectable level of expression at any age (see APENDIX). Further studies are required to identify the exact TRPC channel(s), its role in neonatal LSO neurons and its relationship with sensory activity.

After hearing onset additional TRP subunits, TRPC4 and -5 might be present in the LSO as indicated by the potentiation of DHPG-evoked responses by small doses of La^{3+} (Schaefer et al., 2000, 2002; Strubing et al., 2001; Jung et al., 2002).

Group II mGluR mediated $[Ca^{2+}]_i$ increases in developing LSO neurons. Although the intracellular pathways and the role remain to be unveiled by future studies, evidence from other systems suggest that they may be involved in synaptic plasticity. Similar $[Ca^{2+}]_i$ increases were found in prefrontal cortical neurons, where stimulation of group II mGluR induces LTD through activation of the PLC- IP_3 pathway.

In conclusion, distinct temporal patterns of synaptic activity in the LSO activate distinct GluR types and each receptor type employs a distinct Ca^{2+} entry pathway (Figure 41). This could possibly lead to activation of distinct intracellular cascades and distinct gene expression programs (West et al., 2001) that may be involved in distinct developmental aspects.

While the results have been discussed in the context of each chapter, here an attempt is made to examine them in relationship to each other and in relationship with developmental events taking place in the LSO.

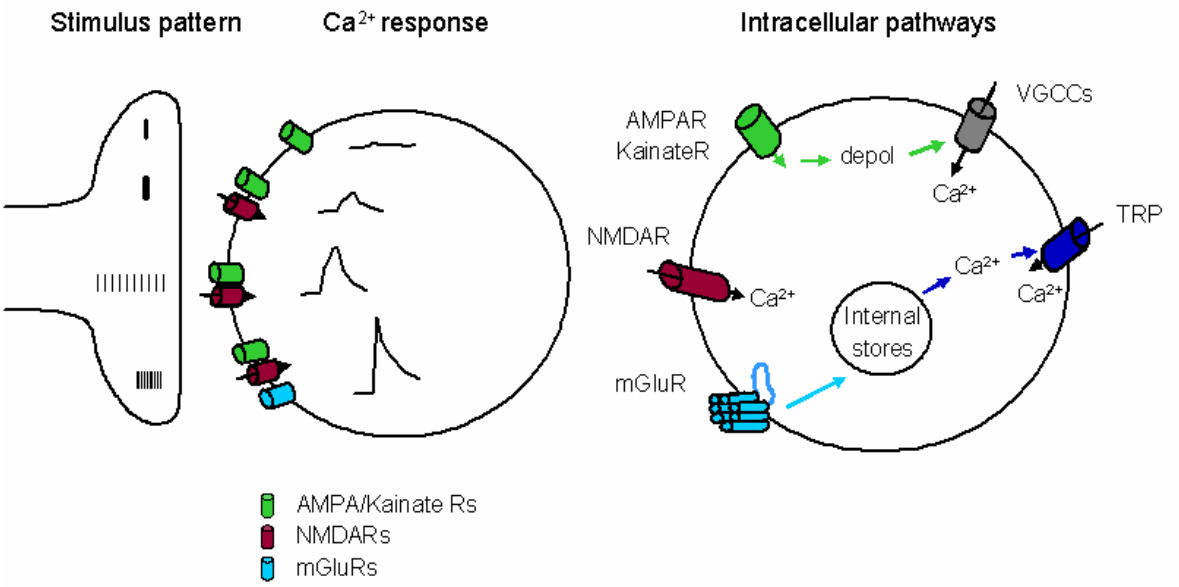

Figure 41. Distinct temporal patterns of synaptic activity triggers Ca^{2+} responses with distinct profiles mediated by distinct sets of GluRs via distinct Ca^{2+} entry pathways.

Figure adapted from Ene et al., 2003.

Technical considerations and alternative methods

In this study, calcium measurements were made exclusively from cell bodies due to the relatively high background staining in bulk-labeled slices and the thin diameter of LSO dendrites, both of which increased the difficulty to reliably detect small fluorescent changes in dendritic segments.

Since in mature LSO neurons most glutamatergic inputs are located on dendrites (Cant and Casseday, 1986; Glendenning et al., 1985), caution must be used in applying calcium measurements obtained from the soma to the dendrites. For example, due to the smaller intracellular volume of dendrites, the same amount of calcium influx will produce a larger increase in $[Ca^{2+}]_i$ in dendrites than in cell bodies. As seen in other neuronal types (Berridge, 1998; Magee et al., 1998), VGCCs and intracellular calcium mobilization mechanisms might be unequally distributed within LSO neurons, resulting in locally distinct calcium responses. Thus,

while this approach allows drawing basic conclusions about specific GluR activation and the Ca^{2+} entry pathways, detailed dendritic calcium imaging combined with electrophysiology are necessary to understand the properties of synapse-specific calcium responses as well as synaptic interaction and integration from the standpoint of local calcium dynamics.

Functional significance

In this part the relevance of GluR-mediated Ca^{2+} responses is discussed in relationship with spontaneous and sound-driven activity, and morphological and functional changes occurring in developing LSO neurons.

Stimulus-dependent recruitment of different classes of GluRs

Distinct temporal patterns of synaptic activity in the LSO activate distinct calcium entry pathways (Figure 41) and, most likely, distinct cellular pathways and gene expression patterns (West et al., 2001). What could they be and how are they connected?

Spontaneous activity is present in the avian and mammalian central auditory pathway prior to hearing onset (Romand and Ehret, 1990; Lippe, 1994; Gummer and Mark, 1994; Kotak and Sanes, 1995; Kros et al., 1998; Glowatzki and Fuchs, 2000; reviews: Rubel et al., 1990; Sanes and Friauf, 2000) and it plays a critical role during development, affecting cell survival (Zirpel et al., 1995a, b; Zirpel and Rubel, 1996; Zirpel et al., 1998), dendritic and axonal growth and refinement (Sanes and Siverls, 1991; Sanes et al., 1992; Sanes and Takacs, 1993; reviews: Rubel et al., 1990; Friauf and Lohmann, 1999; Sanes and Friauf, 2000), that lead to fine-tuning of the mature circuits.

How spontaneous activity is translated into gene expression is not yet understood. Synaptic activity via glutamatergic transmission activates different GluRs types and causes Ca^{2+} influx through different routes (Figure 41). A generally accepted model for activity-regulated gene expression is via Ca^{2+}-dependent activation of the cAMP response element-binding protein (CREB; Yamamoto et al., 1988; Deisseroth, 1996; Kornhauser et al., 2002; reviews: Montminy et al., 1990; Shaywitz and Greenberg, 1999). CREB phosphorylation promotes transcription of genes controlled by the CRE element (Montminy, 1997), many of which may be involved in

neuronal growth and plasticity (e.g., BDNF, CaMKIV, synapsin I, somatostatin, voltage-gated potassium channels, Fos, and Jun; Sauerwald et al., 1990; Mori et al., 1993; Sassone-Corsi, 1995; Shieh et al., 1998; Silva et al., 1998; Lonze et al., 2002). The selection of a certain program of gene expression depends on the sites at which CREB is phosphorylated and/or the length of the phosphorylated CREB (Kornhauser et al., 2002; Impey et al., 2002; review: West et al., 2001). This is determined by several factors including the Ca^{2+} entry route, the pattern and the duration of the stimulus (Bito et al., 1996; 1997; Choe and Wang, 2001; Wu et al., 2001; reviews: Gallin and Greenberg, 1995; Berridge et al, 1998; West et al., 2001).

a) Ca^{2+} entry route

AMPARs. Results from this study demonstrate that in neonatal LSO neurons, AMPA/kainate receptors causes Ca^{2+} entry via activation of VGCCs. Evidence from experiments in organotypic brainstem slice cultures containing LSO and MNTB, indicate that Ca^{2+} entry through VGCCs is necessary for development of normal neuronal morphology and physiology and for the formation of specific topographic connections from MNTB to LSO (Lohmann et al., 1998; Lohrke et al., 1998). Evidence from other systems indicates that depolarizations that activate VGCCs and induce Ca^{2+} influx promote dendritic growth in cortical slice cultures (Redmond et al., 2002). The mechanism of Ca^{2+} action is not completely understood. It is mediated via CaMKIV, a calcium/calmodulin-regulated serine/threonine kinase and phosphorylation of CREB which in turn controls the expression of the neurotrophin BDNF (Shieh et al., 1998; review: Wong and Ghosh, 2002). BDNF is involved in a variety of processes during development, including neuronal growth and differentiation, survival and synaptic plasticity (review: Huang and Reichardt, 2001). In the LSO, BDNF and its receptor TrkB are expressed starting around the first postnatal week; they peak around hearing onset and reach adult levels in the third postnatal week (rat: Hafidi, 1999; gerbil: Tierney et al., 2001; Hafidi et al., 1996). This period mirrors the period of dendritic growth which peaks before hearing onset (quantified by dendritic length and branching points: Sanes et al., 1992). Taken together these studies suggest that Ca^{2+} influx due to activation of AMPARs may be involved in BDNF-mediated cytoarchitectural and functional changes.

NMDARs. In neonatal LSO neurons, NMDARs have a significant contribution to Ca^{2+} responses. Accumulating evidence from different systems indicate that Ca^{2+} entry through NMDARs affects many cellular processes including neuronal survival (review: Hardingham and

Bading 2003), dendritic growth and refinement (Rajan and Cline, 1998; Chevaleyre et al., 2002), synapse elimination (Rabacchi et al., 1992) and synaptic plasticity (reviews: Goodman and Shatz, 1993; Malenka and Nicoll, 1993; Constantine-Paton and Cline, 1998). For example, Ca^{2+} entry through NMDARs is thought to account for the some of the neuroprotective effects of neuronal activity during development, as in vivo blockade of NMDARs causes extensive apoptosis in many brain regions (Ikonomidou et al., 1999; rat dentate gyrus: Gould et al., 1994; cerebellum: Monti and Contestabile, 2000). The mechanisms by which Ca^{2+} entry via NMDARs has a protective effect are not yet clear. There is evidence that Ca^{2+} influx via NMDARs can trigger pro-survival genes including the nuclear factor kappa B (NF-kB; Lipsky et al., 2001; Mattson et al., 2000) or BDNF (Hardingham et al., 2002; reviews: West et al., 2001; Hardingham and Bading, 2003; review BDNF: Huang and Reichardt, 2001).

Ca^{2+} entry through NMDARs is also involved in dendritic growth as pharmacological blockade of NMDARs markedly reduces dendritic growth in Xenopus optical tectum neurons (Rajan and Cline, 1998). The underlying mechanisms may involve CREB as NMDARs activation in hippocampal cultured neurons trigger robust CREB phosphorylation at Ser-133 (Sala et al., 2000). Interestingly, this is developmentally regulated such that younger neurons (<7DIV) are able to drive robust CREB expression while older neurons are unable (Sala et al., 2000). This suggests that NMDARs activate CREB at critical stages during development, i.e. at the time when synapses are established and strengthened or eliminated (Sala et al., 2000). Although it involves CREB phosphorylation this pathway is different from the pathway activated by Ca^{2+} entry through L-type VGCCs as immediate early genes were differentially activated by these distinct Ca^{2+} entry pathways (Bading et al., 1993; review: Gallin and Greenberg, 1995).
Taken together it is possible that Ca^{2+} influx via NMDARs serves protective and instructive roles in developing LSO neurons.

mGluRs. In developing LSO neurons mGluR-mediated increases of $[Ca^{2+}]_i$ involve release of Ca^{2+} from intracellular stores. Studies in developing retinal ganglion cells show that blocking Ca^{2+} release from internal stores results in rapid retraction of dendrites (Lohmann et al., 2002). Thus, it is possible that mGluRs serve a role in dendritic maintenance and this could also be the case in developing LSO neurons. In addition to Ca^{2+} release from internal stores mGluR-mediated Ca^{2+} increases also involve Ca^{2+} entry from the extracellular space, possibly through TRP channels. TRPC channels have low conductance (review: Clapham, et al., 2001) and

therefore can operate over longer time scales without swamping the cell with too much calcium. This property together with their ubiquitous tissue expression suggests that they may serve critical functions. For example, it has been suggested that TRPC3 may be involved in activity-dependent changes that occur in early development of the brain (Li et al., 1999). In pontine nuclei, TRPC3 expression is found in a narrow window during development (rat E18-P20) and the expression parallels that of the transmembrane receptor protein tyrosine kinase TrkB (Li et al., 1999). Application of BDNF activates a current most likely mediated by TRPC3 (Li et al., 1999). Since BDNF is critically involved in survival and synaptic plasticity (review: Huang and Reichardt, 2001) it is possible that some of its effects are mediated by Ca^{2+} influx through TRPC3.

In the LSO, pharmacological data indicate the participation of TRPC channel(s) to Ca^{2+} influx triggered by group I mGluRs, suggesting that similar intracellular cascades may contribute to LSO development.

b) Pattern and duration of stimulus

In vivo recordings from different auditory brainstem nuclei have shown that spontaneous activity prior to hearing is sustained and rhythmic, consisting of brief bursts interrupted by periods of quiescence (Lippe, 1994; Kotak and Sanes, 1995; reviews: Rubel et al., 1990; Sanes and Friauf, 2000). The mean spontaneous activity is low, around 0.4 spikes/s, though the discharge rate in a burst varies around a mean of 37 spikes/s and it can go up to 180 spikes/s (gerbil IC at P9-13: Kotak and Sanes, 1995). The functional meaning of this pattern is not understood. Similar patterns, i.e. burst-like synaptic activity are present in other developing sensory systems and they are thought to play an important role during development (review: Cline, 2001).

Results of the present study demonstrate that distinct temporal patterns of synaptic activity in the LSO activate distinct calcium entry routes resulting in distinct Ca^{2+} response profiles (Figure 41). Cells use sophisticated machinery to decipher the information encoded into the duration and the frequency of Ca^{2+} transients. For example, different frequencies of Ca^{2+} oscillations are optimal for the expression of different genes. In lymphocytes oscillations of $[Ca^{2+}]_i$ at low frequency activate the transcription factor NF-kB whereas oscillations at high frequency activate the transcription factor NF-AT (Dolmetsch et al., 1998; Li et al., 1998;

review: Berridge et al., 2000). Also, IP_3-dependent $[Ca^{2+}]_i$ oscillations were more effective in promoting gene transcription than prolonged increases in $[Ca^{2+}]_i$ (Li et al., 1998). Ca^{2+} oscillations are common in developing systems where they are implicated in many vital processes (reviews: Berridge et al., 1998; 2003) including neuronal migration (Komuro and Rakic, 1996), differentiation (Gu and Spitzer, 1994; review: Spitzer, 2000), axonal growth (Hong et al., 2000) and development of neurotransmitter phenotype (Ciccolini et al., 2003). In developing LSO neurons Ca^{2+} oscillations were triggered by activation of group I mGluRs, suggesting that these receptors may play similar roles in developing LSO neurons. Studies in cultured rat striatal neurons show that group I mGluR-mediated Ca^{2+} responses can trigger immediate early gene expression (Mao and Wang, 2003). Moreover, specificity of gene programs is achieved using different Ca^{2+} profiles such that Ca^{2+} oscillations elicited by mGluR5 trigger a different extracellular signal-regulated kinase (ERK) cascade than that triggered by peak/plateau Ca^{2+} increases elicited by mGluR1 (Thandi et al., 2002). ERK mediated cascades are regarded as key regulating factors in gene expression, cell proliferation, differentiation and cell survival (review: Chang and Karin, 2001), suggesting that mGluRs play critical roles in altering gene expression.

In LSO neurons group I mGluRs elicited Ca^{2+} responses whose duration decreased during development. In hippocampal neurons, lengthening the stimulus duration prolongs residual nuclear phosphorylated CREB and also produces an increase in the expression of CRE-regulated gene products c-Fos and SS-14 (Bito et al., 1996). Thus, it is possible that the developmental changes in group I mGluR-mediated Ca^{2+} responses in LSO neurons result in similar changes in gene expression pattern.

In summary, evidence from many systems suggests that Ca^{2+} entry through distinct entry routes can activate distinct cellular pathways and distinct gene expression (West et al., 2001). Similar processes can take place in developing LSO neurons. Although the exact nature of these intracellular events remains to be shown, these results are consistent with the idea that different patterns of afferent activity serve distinct developmental roles, highlighting the importance of the temporal pattern of spontaneous activity and Ca^{2+} signaling in the immature auditory system.

LSO development and Ca^{2+} requirement

Evidence from different systems suggests that during development neurons require greater Ca^{2+} fluxes and higher $[Ca^{2+}]_i$ then after they mature, to facilitate survival, synapse formation, synapse refinement, dendritic growth and remodeling and other intracellular functions (reviews: Franklin and Johnson, 1992; Ghosh and Greenberg, 1995; Spitzer, 1995; Spitzer et al., 1995). This seems to be also true for LSO neurons. Prior to hearing onset, activation of iGluRs and mGluRs increases $[Ca^{2+}]_i$. In addition, glycinergic/GABAergic input is depolarizing and can increase $[Ca^{2+}]_i$ (Kandler and Friauf, 1995a; Kullmann et al., 2002). Thus, LSO neurons seem to be exposed to high Ca^{2+} fluxes. How do they protect themselves against toxicity? Anatomical studies indicate that LSO neurons express different calcium binding proteins (calretinin, calbindin and parvalbumin) at different times in their development (Friauf, 1993; 1994; Lohmann and Friauf, 1996). Calretinin is expressed from E20 to P8. Calbindin is prominent during early postnatal development E20-P11, while parvalbumin expression starts around P8 and increases until around P28 when adult levels are reached. Thus, in the first postnatal week calretinin and calbindin overlap suggesting that this is a period when the neurons have a strong demand for calcium buffering. This period corresponds to the period when maximal Ca^{2+} fluxes can be elicited via glutamatergic and glycinergic/GABAergic inputs to the LSO (Ene et al., 2003; Kullmann et al., 2002).

This high Ca^{2+} demand period before hearing onset coincides with an array of morphological and functional changes that take place in the LSO, events that shape the system in order to make it ready for high speed/high fidelity transmission necessary for sound transduction. The dendritic growth of LSO neurons peaks before hearing onset (quantified by dendritic length and branching points: Sanes et al., 1992) and refinement of both dendrites and axonal arbors starts before hearing onset. Most of the functional refinement of MNTB inputs takes place before hearing onset, as a high percentage of functional inhibitory synapses (~75%) from the MNTB are eliminated (Kim and Kandler, 2003). Although there is nothing known about the growth and refinement of AVCN-LSO synapses it is very likely that it occurs around the same time as suggested by in vivo recordings from LSO neurons at the onset of hearing (Sanes and Rubel, 1988). These studies found that several parameters including sound detection threshold and

frequency selectivity of both excitatory and inhibitory inputs were equally poor at hearing onset, suggesting that maturation of both inputs has similar time course (Sanes and Rubel, 1988).

After hearing onset, it seems that the requirement for Ca^{2+} diminishes. Glycinergic/GABAergic inputs become hyperpolarizing and decrease $[Ca^{2+}]_i$ (Kandler and Friauf, 1995a; Kullmann et al., 2002). mGluRs become less effective in elevating $[Ca^{2+}]_i$ as the influx of calcium through TRPC channel(s) diminishes. There are still developmental changes during this period. Refinement of the dendritic tree takes place during the third postnatal week (gerbil: Sanes et al., 1992; rat: Rietzel and Friauf, 1998). Functionally, there is a fine-tuning of LSO neuronal properties. The ability of LSO neurons to encode sound intensity, as characterized by the dynamic range (dB) and maximum possible output (discharge rate), mature during the third postnatal week (Sanes and Rubel, 1988). Binaural properties such as topographical alignment exemplified by the degree of matching of characteristic frequencies of excitatory and inhibitory inputs also mature during this time (Sanes and Rubel, 1988). These events are mostly dependent on sound-driven activity. For example, dendritic remodeling is impaired in the absence of sensory neuronal activity: monaural deprivation results in shortening of laminar nucleus dendrites that correspond to the plugged ear (Gray et al., 1982; Smith et al., 1983). Taken together these studies highlight the importance of Ca^{2+} and neuronal activity for development of auditory neurons.

In summary, an array of events that shape and fine-tune LSO circuitry take place during postnatal development. These include growth and refinement of synaptic connections, elimination of functional synapses and maturation of functional properties (Sanes and Rubel, 1988; Sanes and Siverls, 1991; Sanes et al., 1992; Sanes and Takacs, 1993; Rietzel and Friauf, 1998; Caicedo and Eybalin, 1999; Korada and Schwartz, 1999; Kim and Kandler, 2003; reviews: Rubel et al., 1990; Sanes and Walsh, 1998; Cant, 1998; Sanes and Friauf, 2000). These processes are accomplished through an interplay of spontaneous and sound-driven activity, glutamatergic and glycinergic/GABAergic synaptic transmission and Ca^{2+} signaling. The present study investigated the mechanisms by which glutamatergic inputs from the cochlear nucleus regulate $[Ca^{2+}]_i$ in developing LSO neurons and revealed that distinct temporal patterns of synaptic activity in the LSO activate distinct GluR types and distinct Ca^{2+} entry pathways. This could lead to activation of distinct intracellular cascades and distinct gene expression programs (West et al., 2001) that may be involved in distinct developmental aspects. Thus, this study

provides a direction for future research to investigate the molecular and genetic mechanisms underlying the array of events that take place during development not only in the auditory system but also in other sensory systems.

APPENDIX A

IMMUNOSTAINING FOR TRPC3

INTRODUCTION

Pharmacological data suggested a TRPC channel as the channel mediating the influx of calcium triggered by mGluRs activation. The most likely candidate was TRPC3 because it is transiently expressed in brainstem neurons (Li et al., 1999) during a period of development that mirrors the changes in mGluR-mediated Ca^{2+} responses. Moreover, it has been suggested as the channel mediating group I mGluR-evoked Ca^{2+} responses in retinal amacrine cells (Sosa et al., 2002).

To determine the expression of TRPC3 in the LSO, antibody staining was performed in tissue from neonatal to adult mice and rats.

MATERIALS AND METHODS

Animals were anesthetized by hypothermia (P0-7) and with isofluorane (>P7), and perfused through the left ventricle with 0.1M PBS at room temperature (RT), followed by 4% PFA with 4% sucrose in PB (4 ºC; perfusion rate 2.5-3 ml/min; pump from Fisher Scientific). The brains were removed, postfixed for 4h at 4 ºC and placed in 30% sucrose overnight (until they sank completely; at 4 ºC). Sections (30 - 40μm) were cut using a freezing microtome

(American Optical Company, Buffalo, NY) and collected in 0.1M PBS as free-floating sections. To minimize variations in staining from one experiment to another, tissue was collected at different days, cryoprotected after sectioning (in 40% ethylene glycol and 1% polyvinylpyrolidone in 0.1 M Acetate buffer, pH 6.5; storage at -20 ºC) and processed for TRPC3 immunostaining all at a later time. Sections were washed with 0.1M PBS, incubated in blocker (PBS / 5% goat serum or 4% non-fat milk / 0.15% Triton X-100/ 0.05 % Tween 20) for 2h at RT and then incubated in primary Ab for 2h at RT followed by overnight incubation at 4 ºC. Primary antibody, rabbit-anti-mouse TRPC3 (polyclonal; gift from Dr. W.P. Schilling; Case Western University) was diluted to 1:1000 in blocker. On the next day, sections were washed with 0.1M PBS and incubated in biotinylated anti-rabbit secondary Ab raised in goat (Jackson Laboratories, USA; dilution 1:250 in blocker) for 2h at RT. After that a standard detection protocol was used. In short, sections were incubated in avidin biotin peroxidase complex (ABC Elite, Vector Laboratories, USA), followed by incubation in 3, 3'-diaminobenzidine tetrachloride and 0.015% hydrogen peroxide. Finally, sections were washed with 0.1M PBS, mounted on gelatin subbed slides, dried overnight and coversliped using DPX (Fluka).

Controls included sections in which the primary Ab was omitted and sections from the ventral tegmental area (VTA) where TRPC3 was found to be strongly expressed. Images were acquired using an upright microscope (Nikon) equipped with 10x (NA 0.25), 20x (NA: 0.5) and 40x (NA: 0.75) air objectives.

In the initial studies a commercially available antibody (Alomone labs) was used. This Ab produced unspecific staining. In subsequent studies, a new TRPC3 antibody obtained from Dr W.P. Schilling (Goel et al., 2002) was used. The results presented here show data using the new antibody.

RESULTS

Results are from mice aged between P5 and adult: 4 P5, 3 P10-11, 3 P15-16 and 1 adult (>6 weeks). At least two sections per animal were stained with primary antibody and at least one

section per animal served as control. Immunostaining was also performed in sections containing LSO from 2 rats at P12, one of which was performed by Dr. Land.

In mouse LSO tissue TRPC3 expression was not detected at any developmental stage (Figure 42). At the same time TRPC3 expression was clearly evident in VTA (last column in Figure 42). Also in rat P12 TRPC3 expression was detected throughout the LSO (Figure 43 from Dr. Land).

The results of these experiments suggest that mouse LSO neurons do not express TRPC3 or that the expression level is bellow the detection threshold of the method used here. Alternatively, as TRPCs associate with other proteins to form a signaling complex, it could be that the epitope was masked by one of these proteins.

CONCLUSIONS

Present immunohistochemistry data do not support the hypothesis that TRPC3 is the channel mediating DHPG-induced Ca^{2+} influx in developing LSO neurons. Future studies are necessary to determine which TRP channels are expressed in LSO neurons and their developmental expression pattern.

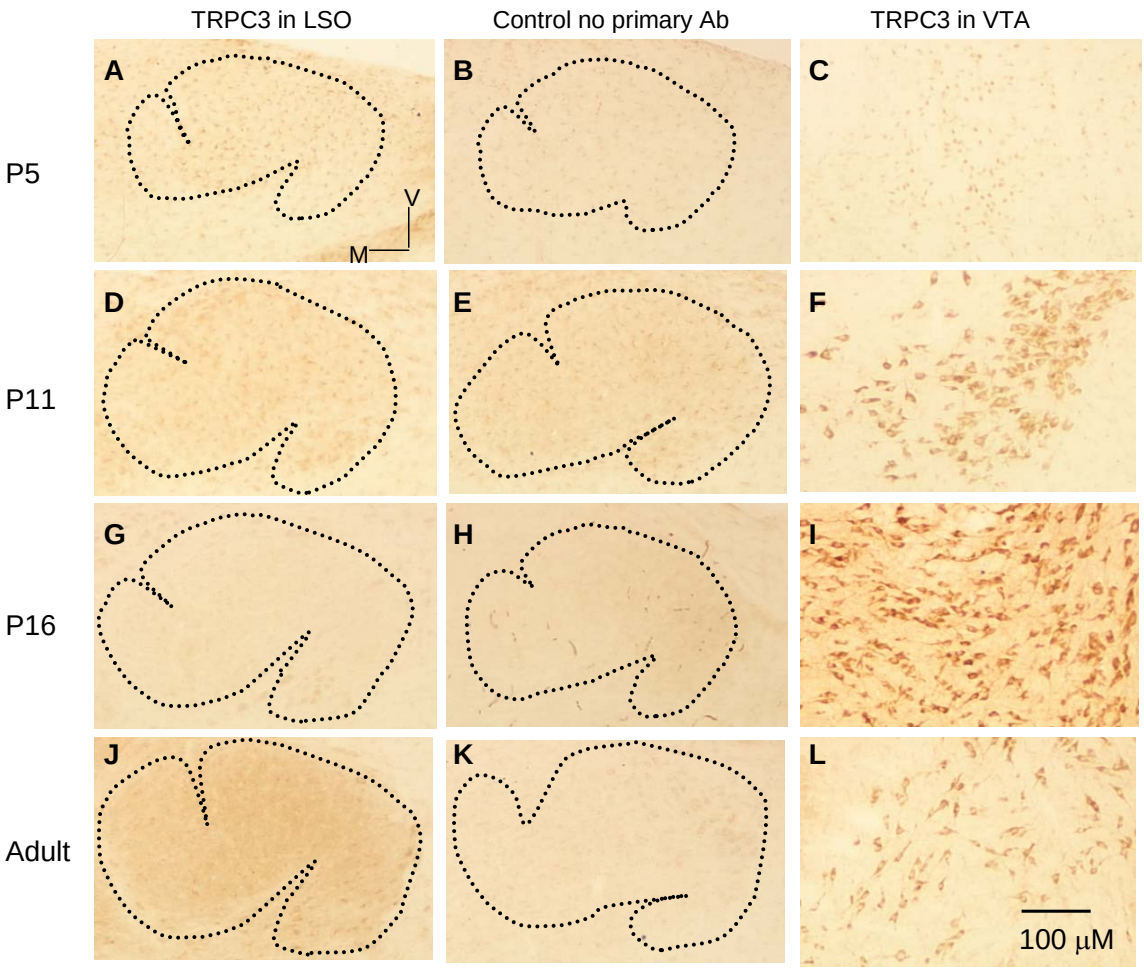

Figure 42. Immunostaining for TRPC3 in mouse.

Panels A, D, G, J: TRPC3 expression in the LSO at P5, P11, P16 and adult, respectively. *Panels B, E, H, K*: Negative controls in which the primary Ab was omitted. *Panels C, F, I, L*: Positive control tissue from the ventral tegmental area (VTA). Dotted line outlines the LSO. V-ventral; M-medial.

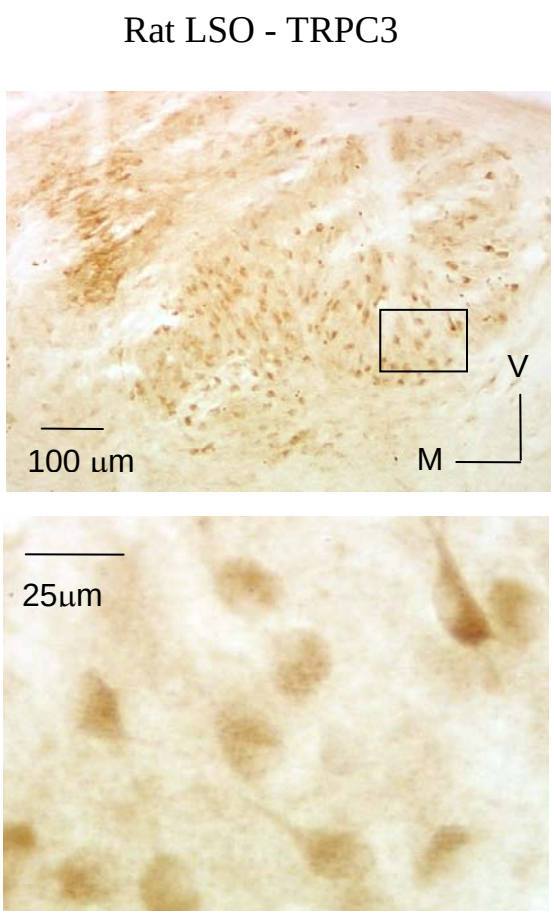

Figure 43. Immunostaining for TRPC3 in rat.

A. P12 rat LSO. **B.** Higher magnification of the area underlined in A. V-ventral; M-medial. TRPC3 immunostaining illustrated in this figure was performed by Dr. Land.

APENDIX B

ABBREVIATIONS

AC = adenylate cyclase

ACPD = 1S, 3R,-aminocyclopentane-trans-dicarboxylate

AMPA = α-amino-3-hydroxy-5-methyl-4-isoxazole propionate

AMPAR= AMPA receptor

APV = 2-Amino-5-phosphonopentanoic acid

AVCN = anteroventral cochlear nucleus

BDNF = brain-derived-neurotrophic factor

Bic = Bicuculline

$[Ca^{2+}]_i$ = intracellular calcium concentration

CaMKII = Ca^{2+}/calmodulin dependent protein kinase II

CaMKIV = Ca^{2+}/calmodulin dependent protein kinase IV

CA= cochlea ablation

CCE = capacitive calcium entry

CHO = Chinese Hamster Ovary

CN = cochlear nucleus

CNQX = 6-Cyano-7-nitroquinoxaline-2,3-dione disodium

CRAC = calcium-release-activated current

CREB= cAMP-response-element-binding-protein

DAG = diacylglycerol

DHPG=(S)-3,5-dihydroxyphenylglycine

ER = endoplasmatic reticulum

ERK = extracellular signal-regulated kinase

Glu= glutamate

GluR = glutamate receptor

GYKI =1-(4-Aminophenyl)-4-methyl-7,8-methylenedioxy-5H-2,3-benzodiazepine hydrochloride

IC = inferior colliculus

IP3= inositol-1,4,5-trisphosphate

IS = internal stores

KA=kainic acid

LSO = lateral superior olivary nucleus

L-AP4 = L (+)-2-amino-4-posphonobutyric acid

MCPG = α-Methyl-4-carboxyphenylglycine

mGluR=metabotropic glutamate receptor

MNTB = medial nucleus of trapezoidal body

NMDA = N-Methyl-D-Aspartate

NMDAR = NMDA receptor

OAG = 1-oleoyl-2-acetyl-*sn*-glycerol

PtdIns4P = phosphatidylinositol-4-phosphate

PIP_2 = phosphatidylinositol-4,5-bisphosphate

PLC = phospholipase C

RT = room temperature

SD = standard deviation

SEM = standard error of the mean

SOC = store operated channels

Stry = Strychnine

TM = transmembranare spanning subunit

TRP=transient receptor potential

TRPC=transient receptor potential canonic

TTX = tetrodotoxin

VAS = via ventral acoustic stria

4C3HPG = 4-carboxy-3-hydroxyphenylglycine

2- APB = 2-aminoethoxydiphenylborane

BIBLIOGRAPHY

1. Abe K, Araki T, Kawagoe J, Aoki M, Kogure K (1992) Phospholipid metabolism and second messenger system after brain ischemia. Adv Exp Med Biol 318: 183-195.

2. Alagarsamy S, Sorensen SD, Conn PJ (2001) Coordinate regulation of metabotropic glutamate receptors. Curr Opin Neurobiol 11: 357-362.

3. Aniksztejn L, Sciancalepore M, Ben Ari Y, Cherubini E (1995) Persistent current oscillations produced by activation of metabotropic glutamate receptors in immature rat CA3 hippocampal neurons. J Neurophysiol 73: 1422-1429.

4. Anwyl R (1999) Metabotropic glutamate receptors: electrophysiological properties and role in plasticity. Brain Res Brain Res Rev 29: 83-120.

5. Ascher-Landsberg J, Saunders T, Elovitz M, Phillippe M (1999) The effects of 2-aminoethoxydiphenyl borate, a novel inositol 1,4, 5-trisphosphate receptor modulator on myometrial contractions. Biochem Biophys Res Commun 264: 979-982.

6. Ascher P, Nowak L (1986) A patch-clamp study of excitatory amino acid activated channels. Adv Exp Med Biol 203: 507-511.

7. Aussel C, Marhaba R, Pelassy C, Breittmayer JP (1996) Submicromolar La3+ concentrations block the calcium release-activated channel, and impair CD69 and CD25 expression in CD3- or thapsigargin-activated Jurkat cells. Biochem J 313 (Pt 3): 909-913.

8. Baba A, Yasui T, Fujisawa S, Yamada RX, Yamada MK, Nishiyama N, Matsuki N, Ikegaya Y (2003) Activity-evoked capacitative Ca2+ entry: implications in synaptic plasticity. J Neurosci 23: 7737-7741.

9. Bading H, Ginty DD, Greenberg ME (1993) Regulation of gene expression in hippocampal neurons by distinct calcium signaling pathways. Science 260: 181-186.

10. Batchelor AM, Garthwaite J (1997) Frequency detection and temporally dispersed synaptic signal association through a metabotropic glutamate receptor pathway. Nature 385: 74-77.

11. Bernard A, Khrestchatisky M (1994) Assessing the extent of RNA editing in the TMII regions of GluR5 and GluR6 kainate receptors during rat brain development. J Neurochem 62: 2057-2060.

12. Bernard A, Ferhat L, Dessi F, Charton G, Represa A, Ben Ari Y, Khrestchatisky M (1999) Q/R editing of the rat GluR5 and GluR6 kainate receptors in vivo and in vitro: evidence for independent developmental, pathological and cellular regulation. Eur J Neurosci 11: 604-616.

13. Berridge MJ (1995) Capacitative calcium entry. Biochem J 312 (Pt 1): 1-11.

14. Berridge MJ (1995) Inositol trisphosphate and calcium signaling. Ann N Y Acad Sci 766: 31-43.

15. Berridge MJ (1997) Elementary and global aspects of calcium signalling. J Physiol 499 (Pt 2): 291-306.

16. Berridge MJ (1998) Neuronal calcium signaling. Neuron 21: 13-26.

17. Berridge MJ, Bootman MD, Lipp P (1998) Calcium--a life and death signal. Nature 395: 645-648.

18. Berridge MJ, Lipp P, Bootman MD (2000) The versatility and universality of calcium signalling. Nat Rev Mol Cell Biol 1: 11-21.

19. Berridge MJ (2002) The endoplasmic reticulum: a multifunctional signaling organelle. Cell Calcium 32: 235-249.

20. Berridge MJ, Bootman MD, Roderick HL (2003) Calcium signalling: dynamics, homeostasis and remodelling. Nat Rev Mol Cell Biol 4: 517-529.

21. Betz WJ, Bewick GS (1993) Optical monitoring of transmitter release and synaptic vesicle recycling at the frog neuromuscular junction. J Physiol 460: 287-309.

22. Bilak SR, Morest DK (1998) Differential expression of the metabotropic glutamate receptor mGluR1alpha by neurons and axons in the cochlear nucleus: in situ hybridization and immunohistochemistry. Synapse 28: 251-270.

23. Bito H, Deisseroth K, Tsien RW (1996) CREB phosphorylation and dephosphorylation: a Ca(2+)- and stimulus duration-dependent switch for hippocampal gene expression. Cell 87: 1203-1214.

24. Bito H, Deisseroth K, Tsien RW (1997) Ca2+-dependent regulation in neuronal gene expression. Curr Opin Neurobiol 7: 419-429.

25. Bleakman D, Lodge D (1998) Neuropharmacology of AMPA and kainate receptors. Neuropharmacology 37: 1187-1204.

26. Bleasdale JE, Bundy GL, Bunting S, Fitzpatrick FA, Huff RM, Sun FF, Pike JE (1989) Inhibition of phospholipase C dependent processes by U-73, 122. Adv Prostaglandin Thromboxane Leukot Res 19: 590-593.

27. Bollmann JH, Helmchen F, Borst JG, Sakmann B (1998) Postsynaptic Ca2+ influx mediated by three different pathways during synaptic transmission at a calyx-type synapse. J Neurosci 18: 10409-10419.

28. Bootman MD, Collins TJ, Peppiatt CM, Prothero LS, MacKenzie L, de Smet P, Travers M, Tovey SC, Seo JT, Berridge MJ, Ciccolini F, Lipp P (2001) Calcium signalling--an overview. Semin Cell Dev Biol 12: 3-10.

29. Bootman MD, Collins TJ, MacKenzie L, Roderick HL, Berridge MJ, Peppiatt CM (2002) 2-aminoethoxydiphenyl borate (2-APB) is a reliable blocker of store-operated Ca2+ entry but an inconsistent inhibitor of InsP3-induced Ca2+ release. FASEB J 16: 1145-1150.

30. Bordi F, Ugolini A (1999) Group I metabotropic glutamate receptors: implications for brain diseases. Prog Neurobiol 59: 55-79.

31. Borges K, Dingledine R (1998) AMPA receptors: molecular and functional diversity. Prog Brain Res 116: 153-170.

32. Born DE, Rubel EW (1985) Afferent influences on brain stem auditory nuclei of the chicken: neuron number and size following cochlea removal. J Comp Neurol 231: 435-445.

33. Boudreau JC, Tsuchitani C (1968) Binaural interaction in the cat superior olive S segment. J Neurophysiol 31: 442-454.

34. Boulay G, Zhu X, Peyton M, Jiang M, Hurst R, Stefani E, Birnbaumer L (1997) Cloning and expression of a novel mammalian homolog of Drosophila transient receptor potential (Trp) involved in calcium entry secondary to activation of receptors coupled by the Gq class of G protein. J Biol Chem 272: 29672-29680.

35. Boulay G, Brown DM, Qin N, Jiang M, Dietrich A, Zhu MX, Chen Z, Birnbaumer M, Mikoshiba K, Birnbaumer L (1999) Modulation of Ca(2+) entry by polypeptides of the inositol 1,4, 5-trisphosphate receptor (IP3R) that bind transient receptor potential (TRP): evidence for roles of TRP and IP3R in store depletion-activated Ca(2+) entry. Proc Natl Acad Sci U S A 96: 14955-14960.

36. Brunjes PC (1994) Unilateral naris closure and olfactory system development. Brain Res Brain Res Rev 19: 146-160.

37. Bruno V, Battaglia G, Copani A, Casabona G, Storto M, Di GG, V, Ngomba R, Nicoletti F (1998) Metabotropic glutamate receptors and neurodegeneration. Prog Brain Res 116: 209-221.

38. Burnashev N, Zhou Z, Neher E, Sakmann B (1995) Fractional calcium currents through recombinant GluR channels of the NMDA, AMPA and kainate receptor subtypes. J Physiol 485 (Pt 2): 403-418.

39. Caicedo A, Kungel M, Pujol R, Friauf E (1998) Glutamate-induced Co2+ uptake in rat auditory brainstem neurons reveals developmental changes in Ca2+ permeability of glutamate receptors. Eur J Neurosci 10: 941-954.

40. Caicedo A, Eybalin M (1999) Glutamate receptor phenotypes in the auditory brainstem and mid-brain of the developing rat. Eur J Neurosci 11: 51-74.

41. Cant NB (1998) Development of the auditory system. In Webster, B., Popper, A.N., Fay, R.R.(eds), Springer Verlag, New York, p 315-415.

42. Cant NB, Casseday JH (1986) Projections from the anteroventral cochlear nucleus to the lateral and medial superior olivary nuclei. J Comp Neurol 247: 457-476.

43. Cartmell J, Schoepp DD (2000) Regulation of neurotransmitter release by metabotropic glutamate receptors. J Neurochem 75: 889-907.

44. Caspary DM, Faingold CL (1989) Non-N-methyl-D-aspartate receptors may mediate ipsilateral excitation at lateral superior olivary synapses. Brain Res 503: 83-90.

45. Casteels R, Droogmans G (1981) Exchange characteristics of the noradrenaline-sensitive calcium store in vascular smooth muscle cells or rabbit ear artery. J Physiol 317: 263-279.

46. Catania MV, Landwehrmeyer GB, Testa CM, Standaert DG, Penney JB, Jr., Young AB (1994) Metabotropic glutamate receptors are differentially regulated during development. Neuroscience 61: 481-495.

47. Catania MV, Bellomo M, Giorgi-Gerevini V, Seminara G, Giuffrida R, Romeo R, De Blasi A, Nicoletti F (2001) Endogenous activation of group-I metabotropic glutamate receptors is required for differentiation and survival of cerebellar Purkinje cells. J Neurosci 21: 7664-7673.

48. Caterina MJ, Schumacher MA, Tominaga M, Rosen TA, Levine JD, Julius D (1997) The capsaicin receptor: a heat-activated ion channel in the pain pathway. Nature 389: 816-824.

49. Catterall WA (2000) Structure and regulation of voltage-gated Ca2+ channels. Annu Rev Cell Dev Biol 16: 521-555.

50. Chang L, Karin M (2001) Mammalian MAP kinase signalling cascades. Nature 410: 37-40.

51. Chevaleyre V, Moos FC, Desarmenien MG (2002) Interplay between presynaptic and postsynaptic activities is required for dendritic plasticity and synaptogenesis in the supraoptic nucleus. J Neurosci 22: 265-273.

52. Chittajallu R, Braithwaite SP, Clarke VR, Henley JM (1999) Kainate receptors: subunits, synaptic localization and function. Trends Pharmacol Sci 20: 26-35.

53. Choe ES, Wang JQ (2002) CaMKII regulates amphetamine-induced ERK1/2 phosphorylation in striatal neurons. Neuroreport 13: 1013-1016.

54. Choi YM, Kim SH, Uhm DY, Park MK (2003) Glutamate-mediated [Ca2+]c dynamics in spontaneously firing dopamine neurons of the rat substantia nigra pars compacta. J Cell Sci 116: 2665-2675.

55. Ciccolini F, Collins TJ, Sudhoelter J, Lipp P, Berridge MJ, Bootman MD (2003) Local and global spontaneous calcium events regulate neurite outgrowth and onset of GABAergic phenotype during neural precursor differentiation. J Neurosci 23: 103-111.

56. Clapham DE (1996) TRP is cracked but is CRAC TRP? Neuron 16: 1069-1072.

57. Clapham DE, Runnels LW, Strubing C (2001) The TRP ion channel family. Nat Rev Neurosci 2: 387-396.

58. Cline HT, Debski EA, Constantine-Paton M (1987) N-methyl-D-aspartate receptor antagonist desegregates eye-specific stripes. Proc Natl Acad Sci U S A 84: 4342-4345.

59. Cline HT (2001) Dendritic arbor development and synaptogenesis. Curr Opin Neurobiol 11: 118-126.

60. Conlee JW, Parks TN (1981) Age- and position-dependent effects of monaural acoustic deprivation in nucleus magnocellularis of the chicken. J Comp Neurol 202: 373-384.

61. Conlee JW, Parks TN (1983) Late appearance and deprivation-sensitive growth of permanent dendrites in the avian cochlear nucleus (nuc. magnocellularis). J Comp Neurol 217: 216-226.

62. Conn PJ, Pin JP (1997) Pharmacology and functions of metabotropic glutamate receptors. Annu Rev Pharmacol Toxicol 37: 205-237.

63. Constantine-Paton M, Cline HT, Debski E (1990) Patterned activity, synaptic convergence, and the NMDA receptor in developing visual pathways. Annu Rev Neurosci 13: 129-154.

64. Constantine-Paton M, Cline HT (1998) LTP and activity-dependent synaptogenesis: the more alike they are, the more different they become. Curr Opin Neurobiol 8: 139-148.

65. Corbett EF, Michalak M (2000) Calcium, a signaling molecule in the endoplasmic reticulum? Trends Biochem Sci 25: 307-311.

66. Corriveau RA (1999) Electrical activity and gene expression in the development of vertebrate neural circuits. J Neurobiol 41: 148-157.

67. Cosens DJ, Manning A (1969) Abnormal electroretinogram from a Drosophila mutant. Nature 224: 285-287.

68. Crowley JC, Katz LC (2000) Early development of ocular dominance columns. Science 290: 1321-1324.

69. Dale LB, Babwah AV, Bhattacharya M, Kelvin DJ, Ferguson SS (2001) Spatial-temporal patterning of metabotropic glutamate receptor-mediated inositol 1,4,5-triphosphate, calcium, and protein kinase C oscillations: protein kinase C-dependent receptor phosphorylation is not required. J Biol Chem 276: 35900-35908.

70. De Blasi A, Conn PJ, Pin J, Nicoletti F (2001) Molecular determinants of metabotropic glutamate receptor signaling. Trends Pharmacol Sci 22: 114-120.

71. Deisseroth K, Bito H, Tsien RW (1996) Signaling from synapse to nucleus: postsynaptic CREB phosphorylation during multiple forms of hippocampal synaptic plasticity. Neuron 16: 89-101.

72. Dingledine R, Borges K, Bowie D, Traynelis SF (1999) The glutamate receptor ion channels. Pharmacol Rev 51: 7-61.

73. Dolmetsch RE, Xu K, Lewis RS (1998) Calcium oscillations increase the efficiency and specificity of gene expression. Nature 392: 933-936.

74. Duncan WC, Jr., Johnson KA, Wehr TA (1998) Decreased sensitivity to light of the photic entrainment pathway during chronic clorgyline and lithium treatments. J Biol Rhythms 13: 330-346.

75. Durham D, Rubel EW (1985) Afferent influences on brain stem auditory nuclei of the chicken: changes in succinate dehydrogenase activity following cochlea removal. J Comp Neurol 231: 446-456.

76. Ehara T, Matsuoka S, Noma A (1989) Measurement of reversal potential of Na+-Ca2+ exchange current in single guinea-pig ventricular cells. J Physiol 410: 227-249.

77. Ehret G (1976) Development of absolute auditory thresholds in the house mouse (Mus musculus). J Am Audiol Soc 1: 179-184.

78. Ehrlich I, Ilic V, Lohmann C, Friauf E (1998) Development of glycinergic transmission in organotypic cultures from auditory brain stem. Neuroreport 9: 2785-2790.

79. Ehrlich I, Lohrke S, Friauf E (1999) Shift from depolarizing to hyperpolarizing glycine action in rat auditory neurones is due to age-dependent Cl- regulation. J Physiol 520 Pt 1: 121-137.

80. Elezgarai I, Benitez R, Mateos JM, Lazaro E, Osorio A, Azkue JJ, Bilbao A, Lingenhoehl K, Van Der PH, Hampson DR, Kuhn R, Knopfel T, Grandes P (1999) Developmental expression of the group III metabotropic glutamate receptor mGluR4a in the medial nucleus of the trapezoid body of the rat. J Comp Neurol 411: 431-440.

81. Elezgarai I, Bilbao A, Mateos JM, Azkue JJ, Benitez R, Osorio A, Diez J, Puente N, Donate-Oliver F, Grandes P (2001) Group II metabotropic glutamate receptors are differentially expressed in the medial nucleus of the trapezoid body in the developing and adult rat. Neuroscience 104: 487-498.

82. Ene FA, Kullmann PH, Gillespie DC, Kandler K (2003) Glutamatergic calcium responses in the developing lateral superior olive: receptor types and their specific activation by synaptic activity patterns. J Neurophysiol 90: 2581-2591.

83. Favreau P, Le Gall F, Benoit E, Molgo J (1999) A review on conotoxins targeting ion channels and acetylcholine receptors of the vertebrate neuromuscular junction. Acta Physiol Pharmacol Ther Latinoam 49: 257-267.

84. Feng AS, Rogowski BA (1980) Effects of monaural and binaural occlusion on the morphology of neurons in the medial superior olivary nucleus of the rat. Brain Res 189: 530-534.

85. Flint AC, Dammerman RS, Kriegstein AR (1999) Endogenous activation of metabotropic glutamate receptors in neocortical development causes neuronal calcium oscillations. Proc Natl Acad Sci U S A 96: 12144-12149.

86. Franklin JL, Johnson EM, Jr. (1992) Suppression of programmed neuronal death by sustained elevation of cytoplasmic calcium. Trends Neurosci 15: 501-508.

87. Friauf E (1993) Transient appearance of calbindin-D28k-positive neurons in the superior olivary complex of developing rats. J Comp Neurol 334: 59-74.

88. Friauf E (1994) Distribution of calcium-binding protein calbindin-D28k in the auditory system of adult and developing rats. J Comp Neurol 349: 193-211.

89. Friauf E, Lohmann C (1999) Development of auditory brainstem circuitry. Activity-dependent and activity-independent processes. Cell Tissue Res 297: 187-195.

90. Friauf E, Aragon C, Lohrke S, Westenfelder B, Zafra F (1999) Developmental expression of the glycine transporter GLYT2 in the auditory system of rats suggests involvement in synapse maturation. J Comp Neurol 412: 17-37.

91. Friauf E, Aragon C, Lohrke S, Westenfelder B, Zafra F (1999) Developmental expression of the glycine transporter GLYT2 in the auditory system of rats suggests involvement in synapse maturation. J Comp Neurol 412: 17-37.

92. Gallin WJ, Greenberg ME (1995) Calcium regulation of gene expression in neurons: the mode of entry matters. Curr Opin Neurobiol 5: 367-374.

93. Gallo V, Zhou JM, McBain CJ, Wright P, Knutson PL, Armstrong RC (1996) Oligodendrocyte progenitor cell proliferation and lineage progression are regulated by glutamate receptor-mediated K+ channel block. J Neurosci 16: 2659-2670.

94. Garcia RL, Schilling WP (1997) Differential expression of mammalian TRP homologues across tissues and cell lines. Biochem Biophys Res Commun 239: 279-283.

95. Garden GA, Canady KS, Lurie DI, Bothwell M, Rubel EW (1994) A biphasic change in ribosomal conformation during transneuronal degeneration is altered by inhibition of mitochondrial, but not cytoplasmic protein synthesis. J Neurosci 14: 1994-2008.

96. Geiger JR, Melcher T, Koh DS, Sakmann B, Seeburg PH, Jonas P, Monyer H (1995) Relative abundance of subunit mRNAs determines gating and Ca2+ permeability of AMPA receptors in principal neurons and interneurons in rat CNS. Neuron 15: 193-204.

97. Ghosh A, Ginty DD, Bading H, Greenberg ME (1994) Calcium regulation of gene expression in neuronal cells. J Neurobiol 25: 294-303.

98. Ghosh A, Greenberg ME (1995) Calcium signaling in neurons: molecular mechanisms and cellular consequences. Science 268: 239-247.

99. Glendenning KK, Hutson KA, Nudo RJ, Masterton RB (1985) Acoustic chiasm II: Anatomical basis of binaurality in lateral superior olive of cat. J Comp Neurol 232: 261-285.

100. Glowatzki E, Fuchs PA (2000) Cholinergic synaptic inhibition of inner hair cells in the neonatal mammalian cochlea. Science 288: 2366-2368.

101. Goel M, Sinkins WG, Schilling WP (2002) Selective association of TRPC channel subunits in rat brain synaptosomes. J Biol Chem 277: 48303-48310.

102. Goodman CS, Shatz CJ (1993) Developmental mechanisms that generate precise patterns of neuronal connectivity. Cell 72 Suppl: 77-98.

103. Gould E, Cameron HA, McEwen BS (1994) Blockade of NMDA receptors increases cell death and birth in the developing rat dentate gyrus. J Comp Neurol 340: 551-565.

104. Gray L, Smith Z, Rubel EW (1982) Developmental and experimental changes in dendritic symmetry in n. laminaris of the chick. Brain Res 244: 360-364.

105. Grynkiewicz G, Poenie M, Tsien RY (1985) A new generation of Ca2+ indicators with greatly improved fluorescence properties. J Biol Chem 260: 3440-3450.

106. Gu X, Olson EC, Spitzer NC (1994) Spontaneous neuronal calcium spikes and waves during early differentiation. J Neurosci 14: 6325-6335.

107. Gu X, Spitzer NC (1995) Distinct aspects of neuronal differentiation encoded by frequency of spontaneous Ca2+ transients. Nature 375: 784-787.

108. Gummer AW, Mark RF (1994) Patterned neural activity in brain stem auditory areas of a prehearing mammal, the tammar wallaby (Macropus eugenii). Neuroreport 5: 685-688.

109. Hafidi A, Moore T, Sanes DH (1996) Regional distribution of neurotrophin receptors in the developing auditory brainstem. J Comp Neurol 367: 454-464.

110. Hafidi A (1999) Distribution of BDNF, NT-3 and NT-4 in the developing auditory brainstem. Int J Dev Neurosci 17: 285-294.

111. Halaszovich CR, Zitt C, Jungling E, Luckhoff A (2000) Inhibition of TRP3 channels by lanthanides. Block from the cytosolic side of the plasma membrane. J Biol Chem 275: 37423-37428.

112. Hannan AJ, Blakemore C, Katsnelson A, Vitalis T, Huber KM, Bear M, Roder J, Kim D, Shin HS, Kind PC (2001) PLC-beta1, activated via mGluRs, mediates activity-dependent differentiation in cerebral cortex. Nat Neurosci 4: 282-288.

113. Hardie RC, Minke B (1992) The trp gene is essential for a light-activated Ca2+ channel in Drosophila photoreceptors. Neuron 8: 643-651.

114. Hardie RC, Minke B (1993) Novel Ca2+ channels underlying transduction in Drosophila photoreceptors: implications for phosphoinositide-mediated Ca2+ mobilization. Trends Neurosci 16: 371-376.

115. Hardie RC, Minke B (1995) Phosphoinositide-mediated phototransduction in Drosophila photoreceptors: the role of Ca2+ and trp. Cell Calcium 18: 256-274.

116. Hardie RC (1996) Calcium signalling: setting store by calcium channels. Curr Biol 6: 1371-1373.

117. Hardingham GE, Fukunaga Y, Bading H (2002) Extrasynaptic NMDARs oppose synaptic NMDARs by triggering CREB shut-off and cell death pathways. Nat Neurosci 5: 405-414.

118. Hardingham GE, Bading H (2003) The Yin and Yang of NMDA receptor signalling. Trends Neurosci 26: 81-89.

119. Harteneck C, Plant TD, Schultz G (2000) From worm to man: three subfamilies of TRP channels. Trends Neurosci 23: 159-166.

120. Harteneck C (2003) Proteins modulating TRP channel function. Cell Calcium 33: 303-310.

121. Hayashi Y, Sekiyama N, Nakanishi S, Jane DE, Sunter DC, Birse EF, Udvarhelyi PM, Watkins JC (1994) Analysis of agonist and antagonist activities of phenylglycine derivatives for different cloned metabotropic glutamate receptor subtypes. J Neurosci 14: 3370-3377.

122. Helfert RH, Schwartz IR (1987) Morphological features of five neuronal classes in the gerbil lateral superior olive. Am J Anat 179: 55-69.

123. Hermans E, Challiss RA (2001) Structural, signalling and regulatory properties of the group I metabotropic glutamate receptors: prototypic family C G-protein-coupled receptors. Biochem J 359: 465-484.

124. Hofmann T, Obukhov AG, Schaefer M, Harteneck C, Gudermann T, Schultz G (1999) Direct activation of human TRPC6 and TRPC3 channels by diacylglycerol. Nature 397: 259-263.

125. Hofmann T, Schaefer M, Schultz G, Gudermann T (2000) Transient receptor potential channels as molecular substrates of receptor-mediated cation entry. J Mol Med 78: 14-25.

126. Hollmann M, Hartley M, Heinemann S (1991) Ca2+ permeability of KA-AMPA--gated glutamate receptor channels depends on subunit composition. Science 252: 851-853.

127. Holscher C, Gigg J, O'Mara SM (1999) Metabotropic glutamate receptor activation and blockade: their role in long-term potentiation, learning and neurotoxicity. Neurosci Biobehav Rev 23: 399-410.

128. Hong K, Nishiyama M, Henley J, Tessier-Lavigne M, Poo M (2000) Calcium signalling in the guidance of nerve growth by netrin-1. Nature 403: 93-98.

129. Hoth M, Penner R (1992) Depletion of intracellular calcium stores activates a calcium current in mast cells. Nature 355: 353-356.

130. Huang EJ, Reichardt LF (2001) Neurotrophins: roles in neuronal development and function. Annu Rev Neurosci 24: 677-736.

131. Huang EP (1998) Synaptic transmission: spillover at central synapses. Curr Biol 8: R613-R615.

132. Hubel DH, Wiesel TN (1970) Stereoscopic vision in macaque monkey. Cells sensitive to binocular depth in area 18 of the macaque monkey cortex. Nature 225: 41-42.

133. Huerta PT, Lisman JE (1995) Bidirectional synaptic plasticity induced by a single burst during cholinergic theta oscillation in CA1 in vitro. Neuron 15: 1053-1063.

134. Hunter C, Petralia RS, Vu T, Wenthold RJ (1993) Expression of AMPA-selective glutamate receptor subunits in morphologically defined neurons of the mammalian cochlear nucleus. J Neurosci 13: 1932-1946.

135. Hyde GE, Durham D (1990) Cytochrome oxidase response to cochlea removal in chicken auditory brainstem neurons. J Comp Neurol 297: 329-339.

136. Hyde GE, Durham D (1994) Increased deafferentation-induced cell death in chick brainstem auditory neurons following blockade of mitochondrial protein synthesis with chloramphenicol. J Neurosci 14: 291-300.

137. Hyde GE, Durham D (1994) Rapid increase in mitochondrial volume in nucleus magnocellularis neurons following cochlea removal. J Comp Neurol 339: 27-48.

138. Ikonomidou C, Bosch F, Miksa M, Bittigau P, Vockler J, Dikranian K, Tenkova TI, Stefovska V, Turski L, Olney JW (1999) Blockade of NMDA receptors and apoptotic neurodegeneration in the developing brain. Science 283: 70-74.

139. Impey S, Fong AL, Wang Y, Cardinaux JR, Fass DM, Obrietan K, Wayman GA, Storm DR, Soderling TR, Goodman RH (2002) Phosphorylation of CBP mediates transcriptional activation by neural activity and CaM kinase IV. Neuron 34: 235-244.

140. Inoue R, Okada T, Onoue H, Hara Y, Shimizu S, Naitoh S, Ito Y, Mori Y (2001) The transient receptor potential protein homologue TRP6 is the essential component of vascular alpha(1)-adrenoceptor-activated Ca(2+)-permeable cation channel. Circ Res 88: 325-332.

141. Irvine DR(1992) Physiology of the auditory brainstem. In Pooper AN and Fay RR (eds): The mammalian auditory pathway: Neurophysiology.New York: Springer, pp153-231.

142. Isaacson JS (2000) Spillover in the spotlight. Curr Biol 10: R475-R477.

143. Ito I, Kohda A, Tanabe S, Hirose E, Hayashi M, Mitsunaga S, Sugiyama H (1992) 3,5-Dihydroxyphenyl-glycine: a potent agonist of metabotropic glutamate receptors. Neuroreport 3: 1013-1016.

144. Jaarsma D, Dino MR, Ohishi H, Shigemoto R, Mugnaini E (1998) Metabotropic glutamate receptors are associated with non-synaptic appendages of unipolar brush cells in rat cerebellar cortex and cochlear nuclear complex. J Neurocytol 27: 303-327.

145. Jhaveri S, Morest DK (1982) Neuronal architecture in nucleus magnocellularis of the chicken auditory system with observations on nucleus laminaris: a light and electron microscope study. Neuroscience 7: 809-836.

146. Jhaveri S, Morest DK (1982) Sequential alterations of neuronal architecture in nucleus magnocellularis of the developing chicken: a Golgi study. Neuroscience 7: 837-853.

147. Jung S, Strotmann R, Schultz G, Plant TD (2002) TRPC6 is a candidate channel involved in receptor-stimulated cation currents in A7r5 smooth muscle cells. Am J Physiol Cell Physiol 282: C347-C359.

148. Kamouchi M, Philipp S, Flockerzi V, Wissenbach U, Mamin A, Raeymaekers L, Eggermont J, Droogmans G, Nilius B (1999) Properties of heterologously expressed hTRP3 channels in bovine pulmonary artery endothelial cells. J Physiol 518 Pt 2: 345-358.

149. Kandler K, Friauf E (1993) Pre- and postnatal development of efferent connections of the cochlear nucleus in the rat. J Comp Neurol 328: 161-184.

150. Kandler K, Friauf E (1995) Development of glycinergic and glutamatergic synaptic transmission in the auditory brainstem of perinatal rats. J Neurosci 15: 6890-6904.

151. Kandler K, Friauf E (1995) Development of electrical membrane properties and discharge characteristics of superior olivary complex neurons in fetal and postnatal rats. Eur J Neurosci 7: 1773-1790.

152. Kandler K, Kullmann PH, Ene FA, Kim G (2002) Excitatory action of an immature glycinergic/GABAergic sound localization pathway. Physiol Behav 77: 583-587.

153. Kanzaki M, Zhang YQ, Mashima H, Li L, Shibata H, Kojima I (1999) Translocation of a calcium-permeable cation channel induced by insulin-like growth factor-I. Nat Cell Biol 1: 165-170.

154. Kao JP (1994) Practical aspects of measuring [Ca2+] with fluorescent indicators. Methods Cell Biol 40: 155-181.

155. Katz LC, Shatz CJ (1996) Synaptic activity and the construction of cortical circuits. Science 274: 1133-1138.

156. Kawabata S, Tsutsumi R, Kohara A, Yamaguchi T, Nakanishi S, Okada M (1996) Control of calcium oscillations by phosphorylation of metabotropic glutamate receptors. Nature 383: 89-92.

157. Kawabata S, Kohara A, Tsutsumi R, Itahana H, Hayashibe S, Yamaguchi T, Okada M (1998) Diversity of calcium signaling by metabotropic glutamate receptors. J Biol Chem 273: 17381-17385.

158. Keele NB, Arvanov VL, Shinnick-Gallagher P (1997) Quisqualate-preferring metabotropic glutamate receptor activates Na(+)-Ca2+ exchange in rat basolateral amygdala neurones. J Physiol 499 (Pt 1): 87-104.

159. Keele NB, Neugebauer V, Shinnick-Gallagher P (1999) Differential effects of metabotropic glutamate receptor antagonists on bursting activity in the amygdala. J Neurophysiol 81: 2056-2065.

160. Kim G, Kandler K (2003) Elimination and strengthening of glycinergic/GABAergic connections during tonotopic map formation. Nat Neurosci 6: 282-290.

161. Kimura J, Miyamae S, Noma A (1987) Identification of sodium-calcium exchange current in single ventricular cells of guinea-pig. J Physiol 384: 199-222.

162. Kiselyov K, Xu X, Mozhayeva G, Kuo T, Pessah I, Mignery G, Zhu X, Birnbaumer L, Muallem S (1998) Functional interaction between InsP3 receptors and store-operated Htrp3 channels. Nature 396: 478-482.

163. Kitzes LM, Kageyama GH, Semple MN, Kil J (1995) Development of ectopic projections from the ventral cochlear nucleus to the superior olivary complex induced by neonatal ablation of the contralateral cochlea. J Comp Neurol 353: 341-363.

164. Kleinschmidt A, Bear MF, Singer W (1987) Blockade of "NMDA" receptors disrupts experience-dependent plasticity of kitten striate cortex. Science 238: 355-358.

165. Kleinschmidt A, Bear MF, Singer W (1987) Blockade of "NMDA" receptors disrupts experience-dependent plasticity of kitten striate cortex. Science 238: 355-358.

166. Konig N, Poluch S, Estabel J, Durand M, Drian MJ, Exbrayat JM (2001) Synaptic and non-synaptic AMPA receptors permeable to calcium. Jpn J Pharmacol 86: 1-17.

167. Korada S, Schwartz IR (1999) Development of GABA, glycine, and their receptors in the auditory brainstem of gerbil: a light and electron microscopic study. J Comp Neurol 409: 664-681.

168. Kornhauser JM, Cowan CW, Shaywitz AJ, Dolmetsch RE, Griffith EC, Hu LS, Haddad C, Xia Z, Greenberg ME (2002) CREB transcriptional activity in neurons is regulated by multiple, calcium-specific phosphorylation events. Neuron 34: 221-233.

169. Kotak VC, Sanes DH (1995) Synaptically evoked prolonged depolarizations in the developing auditory system. J Neurophysiol 74: 1611-1620.

170. Kotak VC, Sanes DH (1996) Developmental influence of glycinergic transmission: regulation of NMDA receptor-mediated EPSPs. J Neurosci 16: 1836-1843.

171. Kotak VC, Sanes DH (1997) Deafferentation weakens excitatory synapses in the developing central auditory system. Eur J Neurosci 9: 2340-2347.

172. Kotak VC, Korada S, Schwartz IR, Sanes DH (1998) A developmental shift from GABAergic to glycinergic transmission in the central auditory system. J Neurosci 18: 4646-4655.

173. Kros CJ, Ruppersberg JP, Rusch A (1998) Expression of a potassium current in inner hair cells during development of hearing in mice. Nature 394: 281-284.

174. Kullmann DM, Asztely F, Walker MC (2000) The role of mammalian ionotropic receptors in synaptic plasticity: LTP, LTD and epilepsy. Cell Mol Life Sci 57: 1551-1561.

175. Kullmann PH, Kandler K (2001) Glycinergic/GABAergic synapses in the lateral superior olive are excitatory in neonatal C57Bl/6J mice. Brain Res Dev Brain Res 131: 143-147.

176. Kullmann PH, Ene FA, Kandler K (2002) Glycinergic and GABAergic calcium responses in the developing lateral superior olive. Eur J Neurosci 15: 1093-1104.

177. Lachica EA, Rubsamen R, Zirpel L, Rubel EW (1995) Glutamatergic inhibition of voltage-operated calcium channels in the avian cochlear nucleus. J Neurosci 15: 1724-1734.

178. Lachica EA, Rubsamen R, Zirpel L, Rubel EW (1995) Glutamatergic inhibition of voltage-operated calcium channels in the avian cochlear nucleus. J Neurosci 15: 1724-1734.

179. Lachica EA, Kato BM, Lippe WR, Rubel EW (1998) Glutamatergic and GABAergic agonists increase [Ca2+]i in avian cochlear nucleus neurons. J Neurobiol 37: 321-337.

180. Lee CJ, Kong H, Manzini MC, Albuquerque C, Chao MV, MacDermott AB (2001) Kainate receptors expressed by a subpopulation of developing nociceptors rapidly switch from high to low Ca2+ permeability. J Neurosci 21: 4572-4581.

181. Leissring MA, Akbari Y, Fanger CM, Cahalan MD, Mattson MP, LaFerla FM (2000) Capacitative calcium entry deficits and elevated luminal calcium content in mutant presenilin-1 knockin mice. J Cell Biol 149: 793-798.

182. Lepple-Wienhues A, Cahalan MD (1996) Conductance and permeation of monovalent cations through depletion-activated Ca2+ channels (ICRAC) in Jurkat T cells. Biophys J 71: 787-794.

183. Lerma J (2003) Roles and rules of kainate receptors in synaptic transmission. Nat Rev Neurosci 4: 481-495.

184. Leypold BG, Yu CR, Leinders-Zufall T, Kim MM, Zufall F, Axel R (2002) Altered sexual and social behaviors in trp2 mutant mice. Proc Natl Acad Sci U S A 99: 6376-6381.

185. Li HS, Xu XZ, Montell C (1999) Activation of a TRPC3-dependent cation current through the neurotrophin BDNF. Neuron 24: 261-273.

186. Li W, Llopis J, Whitney M, Zlokarnik G, Tsien RY (1998) Cell-permeant caged InsP3 ester shows that Ca2+ spike frequency can optimize gene expression. Nature 392: 936-941.

187. Liman ER, Corey DP, Dulac C (1999) TRP2: a candidate transduction channel for mammalian pheromone sensory signaling. Proc Natl Acad Sci U S A 96: 5791-5796.

188. Linden DJ, Smeyne M, Connor JA (1994) Trans-ACPD, a metabotropic receptor agonist, produces calcium mobilization and an inward current in cultured cerebellar Purkinje neurons. J Neurophysiol 71: 1992-1998.

189. Lippe WR (1994) Rhythmic spontaneous activity in the developing avian auditory system. J Neurosci 14: 1486-1495.

190. Lipsky RH, Xu K, Zhu D, Kelly C, Terhakopian A, Novelli A, Marini AM (2001) Nuclear factor kappaB is a critical determinant in N-methyl-D-aspartate receptor-mediated neuroprotection. J Neurochem 78: 254-264.

191. Lisman JE (1997) Bursts as a unit of neural information: making unreliable synapses reliable. Trends Neurosci 20: 38-43.

192. Lo KJ, Luk HN, Chin TY, Chueh SH (2002) Store depletion-induced calcium influx in rat cerebellar astrocytes. Br J Pharmacol 135: 1383-1392.

193. Lohmann C, Friauf E (1996) Distribution of the calcium-binding proteins parvalbumin and calretinin in the auditory brainstem of adult and developing rats. J Comp Neurol 367: 90-109.

194. Lohmann C, Ilic V, Friauf E (1998) Development of a topographically organized auditory network in slice culture is calcium dependent. J Neurobiol 34: 97-112.

195. Lohmann C, Myhr KL, Wong RO (2002) Transmitter-evoked local calcium release stabilizes developing dendrites. Nature 418: 177-181.

196. Lohrke S, Kungel M, Friauf E (1998) Electrical membrane properties of trapezoid body neurons in the rat auditory brain stem are preserved in organotypic slice cultures. J Neurobiol 36: 395-409.

197. Lohrke S, Friauf E (2002) Developmental distribution of the glutamate receptor subunits KA2, GluR6/7, and delta 1/2 in the rat medial nucleus of the trapezoid body. A quantitative image analysis. Cell Tissue Res 308: 19-33.

198. Lonze BE, Riccio A, Cohen S, Ginty DD (2002) Apoptosis, axonal growth defects, and degeneration of peripheral neurons in mice lacking CREB. Neuron 34: 371-385.

199. Lopez-Bendito G, Shigemoto R, Fairen A, Lujan R (2002) Differential distribution of group I metabotropic glutamate receptors during rat cortical development. Cereb Cortex 12: 625-638.

200. LoTurco JJ, Owens DF, Heath MJ, Davis MB, Kriegstein AR (1995) GABA and glutamate depolarize cortical progenitor cells and inhibit DNA synthesis. Neuron 15: 1287-1298.

201. Ma CL, Kelly JB, Wu SH (2002) AMPA and NMDA receptors mediate synaptic excitation in the rat's inferior colliculus. Hear Res 168: 25-34.

202. MacDermott AB, Mayer ML, Westbrook GL, Smith SJ, Barker JL (1986) NMDA-receptor activation increases cytoplasmic calcium concentration in cultured spinal cord neurones. Nature 321: 519-522.

203. Magee J, Hoffman D, Colbert C, Johnston D (1998) Electrical and calcium signaling in dendrites of hippocampal pyramidal neurons. Annu Rev Physiol 60: 327-346.

204. Magee JC, Avery RB, Christie BR, Johnston D (1996) Dihydropyridine-sensitive, voltage-gated Ca2+ channels contribute to the resting intracellular Ca2+ concentration of hippocampal CA1 pyramidal neurons. J Neurophysiol 76: 3460-3470.

205. Maiese K, Ahmad I, TenBroeke M, Gallant J (1999) Metabotropic glutamate receptor subtypes independently modulate neuronal intracellular calcium. J Neurosci Res 55: 472-485.

206. Malenka RC, Nicoll RA (1993) NMDA-receptor-dependent synaptic plasticity: multiple forms and mechanisms. Trends Neurosci 16: 521-527.

207. Mao L, Wang JQ (2003) Group I metabotropic glutamate receptor-mediated calcium signalling and immediate early gene expression in cultured rat striatal neurons. Eur J Neurosci 17: 741-750.

208. Martin LJ, Blackstone CD, Huganir RL, Price DL (1992) Cellular localization of a metabotropic glutamate receptor in rat brain. Neuron 9: 259-270.

209. Maruyama T, Kanaji T, Nakade S, Kanno T, Mikoshiba K (1997) 2APB, 2-aminoethoxydiphenyl borate, a membrane-penetrable modulator of Ins(1,4,5)P3-induced Ca2+ release. J Biochem (Tokyo) 122: 498-505.

210. Mattson MP (1988) Neurotransmitters in the regulation of neuronal cytoarchitecture. Brain Res 472: 179-212.

211. Mattson MP, Culmsee C, Yu Z, Camandola S (2000) Roles of nuclear factor kappaB in neuronal survival and plasticity. J Neurochem 74: 443-456.

212. Mayer ML, Westbrook GL, Guthrie PB (1984) Voltage-dependent block by Mg2+ of NMDA responses in spinal cord neurones. Nature 309: 261-263.

213. Mercuri NB, Stratta F, Calabresi P, Bernardi G (1993) Neurotensin induces an inward current in rat mesencephalic dopaminergic neurons. Neurosci Lett 153: 192-196.

214. Minke B, Selinger Z (1996) The roles of trp and calcium in regulating photoreceptor function in Drosophila. Curr Opin Neurobiol 6: 459-466.

215. Minke B, Cook B (2002) TRP channel proteins and signal transduction. Physiol Rev 82: 429-472.

216. Molitor SC, Manis PB (1997) Evidence for functional metabotropic glutamate receptors in the dorsal cochlear nucleus. J Neurophysiol 77: 1889-1905.

217. Montell C, Rubin GM (1989) Molecular characterization of the Drosophila trp locus: a putative integral membrane protein required for phototransduction. Neuron 2: 1313-1323.

218. Montell C (2001) Physiology, phylogeny, and functions of the TRP superfamily of cation channels. Sci STKE 2001: RE1.

219. Montell C (2003) The venerable inveterate invertebrate TRP channels. Cell Calcium 33: 409-417.

220. Monti B, Contestabile A (2000) Blockade of the NMDA receptor increases developmental apoptotic elimination of granule neurons and activates caspases in the rat cerebellum. Eur J Neurosci 12: 3117-3123.

221. Montminy M (1997) Transcriptional regulation by cyclic AMP. Annu Rev Biochem 66: 807-822.

222. Montminy MR, Gonzalez GA, Yamamoto KK (1990) Regulation of cAMP-inducible genes by CREB. Trends Neurosci 13: 184-188.

223. Moore DR, Kitzes LM (1985) Projections from the cochlear nucleus to the inferior colliculus in normal and neonatally cochlea-ablated gerbils. J Comp Neurol 240: 180-195.

224. Moore DR, Kowalchuk NE (1988) Auditory brainstem of the ferret: effects of unilateral cochlear lesions on cochlear nucleus volume and projections to the inferior colliculus. J Comp Neurol 272: 503-515.

225. Moore DR (1990) Auditory brainstem of the ferret: early cessation of developmental sensitivity of neurons in the cochlear nucleus to removal of the cochlea. J Comp Neurol 302: 810-823.

226. Moore DR (1993) Auditory brainstem responses in ferrets following unilateral cochlear removal. Hear Res 68: 28-34.

227. Moore DR, King AJ, McAlpine D, Martin RL, Hutchings ME (1993) Functional consequences of neonatal unilateral cochlear removal. Prog Brain Res 97: 127-133.

228. Moore DR, Rogers NJ, O'Leary SJ (1998) Loss of cochlear nucleus neurons following aminoglycoside antibiotics or cochlear removal. Ann Otol Rhinol Laryngol 107: 337-343.

229. Mori H, Mishina M (1995) Structure and function of the NMDA receptor channel. Neuropharmacology 34: 1219-1237.

230. Mori Y, Matsubara H, Folco E, Siegel A, Koren G (1993) The transcription of a mammalian voltage-gated potassium channel is regulated by cAMP in a cell-specific manner. J Biol Chem 268: 26482-26493.

231. Mostafapour SP, Cochran SL, Del Puerto NM, Rubel EW (2000) Patterns of cell death in mouse anteroventral cochlear nucleus neurons after unilateral cochlea removal. J Comp Neurol 426: 561-571.

232. Nakahara K, Okada M, Nakanishi S (1997) The metabotropic glutamate receptor mGluR5 induces calcium oscillations in cultured astrocytes via protein kinase C phosphorylation. J Neurochem 69: 1467-1475.

233. Nakajima Y, Iwakabe H, Akazawa C, Nawa H, Shigemoto R, Mizuno N, Nakanishi S (1993) Molecular characterization of a novel retinal metabotropic glutamate receptor mGluR6 with a high agonist selectivity for L-2-amino-4-phosphonobutyrate. J Biol Chem 268: 11868-11873.

234. Nakanishi S, Nakajima Y, Masu M, Ueda Y, Nakahara K, Watanabe D, Yamaguchi S, Kawabata S, Okada M (1998) Glutamate receptors: brain function and signal transduction. Brain Res Brain Res Rev 26: 230-235.

235. Narasimhan K, Pessah IN, Linden DJ (1998) Inositol-1,4,5-trisphosphate receptor-mediated Ca mobilization is not required for cerebellar long-term depression in reduced preparations. J Neurophysiol 80: 2963-2974.

236. Nash MS, Schell MJ, Atkinson PJ, Johnston NR, Nahorski SR, Challiss RA (2002) Determinants of metabotropic glutamate receptor-5-mediated Ca2+ and inositol 1,4,5-trisphosphate oscillation frequency. Receptor density versus agonist concentration. J Biol Chem 277: 35947-35960.

237. Neher E, Augustine GJ (1992) Calcium gradients and buffers in bovine chromaffin cells. J Physiol 450: 273-301.

238. Nilius B (2003) Calcium-impermeable monovalent cation channels: a TRP connection? Br J Pharmacol 138: 5-7.

239. Nordeen KW, Killackey HP, Kitzes LM (1983) Ascending projections to the inferior colliculus following unilateral cochlear ablation in the neonatal gerbil, Meriones unguiculatus. J Comp Neurol 214: 144-153.

240. Nowak L, Bregestovski P, Ascher P, Herbet A, Prochiantz A (1984) Magnesium gates glutamate-activated channels in mouse central neurones. Nature 307: 462-465.

241. Oancea E, Meyer T (1998) Protein kinase C as a molecular machine for decoding calcium and diacylglycerol signals. Cell 95: 307-318.

242. Oancea E, Teruel MN, Quest AF, Meyer T (1998) Green fluorescent protein (GFP)-tagged cysteine-rich domains from protein kinase C as fluorescent indicators for diacylglycerol signaling in living cells. J Cell Biol 140: 485-498.

243. Okada T, Inoue R, Yamazaki K, Maeda A, Kurosaki T, Yamakuni T, Tanaka I, Shimizu S, Ikenaka K, Imoto K, Mori Y (1999) Molecular and functional characterization of a novel mouse transient receptor potential protein homologue TRP7. Ca(2+)-permeable cation channel that is constitutively activated and enhanced by stimulation of G protein-coupled receptor. J Biol Chem 274: 27359-27370.

244. Okamoto N, Hori S, Akazawa C, Hayashi Y, Shigemoto R, Mizuno N, Nakanishi S (1994) Molecular characterization of a new metabotropic glutamate receptor mGluR7 coupled to inhibitory cyclic AMP signal transduction. J Biol Chem 269: 1231-1236.

245. Ollo C, Schwartz IR (1979) The superior olivary complex in C57BL/6 mice. Am J Anat 155: 349-373.

246. Otani S, Daniel H, Takita M, Crepel F (2002) Long-term depression induced by postsynaptic group II metabotropic glutamate receptors linked to phospholipase C and intracellular calcium rises in rat prefrontal cortex. J Neurosci 22: 3434-3444.

247. Ozawa S, Tsuzuki K, Iino M, Ogura A, Kudo Y (1989) Three types of voltage-dependent calcium current in cultured rat hippocampal neurons. Brain Res 495: 329-336.

248. Parekh AB, Terlau H, Stuhmer W (1993) Depletion of InsP3 stores activates a Ca2+ and K+ current by means of a phosphatase and a diffusible messenger. Nature 364: 814-818.

249. Parekh AB, Penner R (1997) Store depletion and calcium influx. Physiol Rev 77: 901-930.

250. Parks TN (1997) Effects of early deafness on development of brain stem auditory neurons. Ann Otol Rhinol Laryngol Suppl 168: 37-43.

251. Parks TN (2000) The AMPA receptors of auditory neurons. Hear Res 147: 77-91.

252. Partin KM, Patneau DK, Winters CA, Mayer ML, Buonanno A (1993) Selective modulation of desensitization at AMPA versus kainate receptors by cyclothiazide and concanavalin A. Neuron 11: 1069-1082.

253. Partin KM, Fleck MW, Mayer ML (1996) AMPA receptor flip/flop mutants affecting deactivation, desensitization, and modulation by cyclothiazide, aniracetam, and thiocyanate. J Neurosci 16: 6634-6647.

254. Paschen W, Schmitt J, Dux E, Djuricic B (1995) Temporal analysis of the upregulation of GluR5 mRNA editing with age: regional evaluation. Brain Res Dev Brain Res 86: 359-363.

255. Pasic TR, Rubel EW (1989) Rapid changes in cochlear nucleus cell size following blockade of auditory nerve electrical activity in gerbils. J Comp Neurol 283: 474-480.

256. Pasic TR, Moore DR, Rubel EW (1994) Effect of altered neuronal activity on cell size in the medial nucleus of the trapezoid body and ventral cochlear nucleus of the gerbil. J Comp Neurol 348: 111-120.

257. Paternain AV, Vicente A, Nielsen EO, Lerma J (1996) Comparative antagonism of kainate-activated kainate and AMPA receptors in hippocampal neurons. Eur J Neurosci 8: 2129-2136.

258. Peinado A (2001) Immature neocortical neurons exist as extensive syncitial networks linked by dendrodendritic electrical connections. J Neurophysiol 85: 620-629.

259. Pellegrini-Giampietro DE, Bennett MV, Zukin RS (1992) Are Ca(2+)-permeable kainate/AMPA receptors more abundant in immature brain? Neurosci Lett 144: 65-69.

260. Pellegrini-Giampietro DE, Gorter JA, Bennett MV, Zukin RS (1997) The GluR2 (GluR-B) hypothesis: Ca(2+)-permeable AMPA receptors in neurological disorders. Trends Neurosci 20: 464-470.

261. Peppiatt CM, Collins TJ, MacKenzie L, Conway SJ, Holmes AB, Bootman MD, Berridge MJ, Seo JT, Roderick HL (2003) 2-Aminoethoxydiphenyl borate (2-APB) antagonises inositol 1,4,5-trisphosphate-induced calcium release, inhibits calcium pumps and has a use-dependent and slowly reversible action on store-operated calcium entry channels. Cell Calcium 34: 97-108.

262. Peterlin ZA, Kozloski J, Mao BQ, Tsiola A, Yuste R (2000) Optical probing of neuronal circuits with calcium indicators. Proc Natl Acad Sci U S A 97: 3619-3624.

263. Petralia RS, Wang YX, Wenthold RJ (1994) Histological and ultrastructural localization of the kainate receptor subunits, KA2 and GluR6/7, in the rat nervous system using selective antipeptide antibodies. J Comp Neurol 349: 85-110.

264. Petralia RS, Wang YX, Zhao HM, Wenthold RJ (1996) Ionotropic and metabotropic glutamate receptors show unique postsynaptic, presynaptic, and glial localizations in the dorsal cochlear nucleus. J Comp Neurol 372: 356-383.

265. Petralia RS, Rubio ME, Wang YX, Wenthold RJ (2000) Differential distribution of glutamate receptors in the cochlear nuclei. Hear Res 147: 59-69.

266. Philipp S, Cavalie A, Freichel M, Wissenbach U, Zimmer S, Trost C, Marquart A, Murakami M, Flockerzi V (1996) A mammalian capacitative calcium entry channel homologous to Drosophila TRP and TRPL. EMBO J 15: 6166-6171.

267. Philipp S, Hambrecht J, Braslavski L, Schroth G, Freichel M, Murakami M, Cavalie A, Flockerzi V (1998) A novel capacitative calcium entry channel expressed in excitable cells. EMBO J 17: 4274-4282.

268. Pin JP, Duvoisin R (1995) The metabotropic glutamate receptors: structure and functions. Neuropharmacology 34: 1-26.

269. Potocnik SJ, Hill MA (2001) Pharmacological evidence for capacitative Ca(2+) entry in cannulated and pressurized skeletal muscle arterioles. Br J Pharmacol 134: 247-256.

270. Prakriya M, Lewis RS (2001) Potentiation and inhibition of Ca(2+) release-activated Ca(2+) channels by 2-aminoethyldiphenyl borate (2-APB) occurs independently of IP(3) receptors. J Physiol 536: 3-19.

271. Prothero LS, Mathie A, Richards CD (2000) Purinergic and muscarinic receptor activation activates a common calcium entry pathway in rat neocortical neurons and glial cells. Neuropharmacology 39: 1768-1778.

272. Putney JW, Jr. (1976) Stimulation of 45Ca influx in rat parotid gland by carbachol. J Pharmacol Exp Ther 199: 526-537.

273. Putney JW, Jr. (1976) Biphasic modulation of potassium release in rat parotid gland by carbachol and phenylephrine. J Pharmacol Exp Ther 198: 375-384.

274. Putney JW, Jr. (1986) A model for receptor-regulated calcium entry. Cell Calcium 7: 1-12.

275. Putney JW, Jr. (1990) Capacitative calcium entry revisited. Cell Calcium 11: 611-624.

276. Putney JW, Jr. (1997) Type 3 inositol 1,4,5-trisphosphate receptor and capacitative calcium entry. Cell Calcium 21: 257-261.

277. Rabacchi S, Bailly Y, Delhaye-Bouchaud N, Mariani J (1992) Involvement of the N-methyl D-aspartate (NMDA) receptor in synapse elimination during cerebellar development. Science 256: 1823-1825.

278. Rajan I, Cline HT (1998) Glutamate receptor activity is required for normal development of tectal cell dendrites in vivo. J Neurosci 18: 7836-7846.

279. Rajendra S, Lynch JW, Schofield PR (1997) The glycine receptor. Pharmacol Ther 73: 121-146.

280. Randriamampita C, Tsien RY (1993) Emptying of intracellular Ca2+ stores releases a novel small messenger that stimulates Ca2+ influx. Nature 364: 809-814.

281. Ranganathan R, Malicki DM, Zuker CS (1995) Signal transduction in Drosophila photoreceptors. Annu Rev Neurosci 18: 283-317.

282. Redmond L, Kashani AH, Ghosh A (2002) Calcium regulation of dendritic growth via CaM kinase IV and CREB-mediated transcription. Neuron 34: 999-1010.

283. Rhode WS, Greenberg S (1992) The mammalian Auditory Pathways: Neurophysiology. In Webster, B., Popper, A.N., Fay, R.R. (eds) Springer Verlag, New York.

284. Riccio A, Medhurst AD, Mattei C, Kelsell RE, Calver AR, Randall AD, Benham CD, Pangalos MN (2002) mRNA distribution analysis of human TRPC family in CNS and peripheral tissues. Brain Res Mol Brain Res 109: 95-104.

285. Riccio A, Mattei C, Kelsell RE, Medhurst AD, Calver AR, Randall AD, Davis JB, Benham CD, Pangalos MN (2002) Cloning and functional expression of human short TRP7, a candidate protein for store-operated Ca2+ influx. J Biol Chem 277: 12302-12309.

286. Riedel G, Platt B, Micheau J (2003) Glutamate receptor function in learning and memory. Behav Brain Res 140: 1-47.

287. Rietzel HJ, Friauf E (1998) Neuron types in the rat lateral superior olive and developmental changes in the complexity of their dendritic arbors. J Comp Neurol 390: 20-40.

288. Romand R, Ehret G (1990) Development of tonotopy in the inferior colliculus. I. Electrophysiological mapping in house mice. Brain Res Dev Brain Res 54: 221-234.

289. Romano C, van den Pol AN, O'Malley KL (1996) Enhanced early developmental expression of the metabotropic glutamate receptor mGluR5 in rat brain: protein, mRNA splice variants, and regional distribution. J Comp Neurol 367: 403-412.

290. Rubel EW, Smith ZD, Steward O (1981) Sprouting in the avian brainstem auditory pathway: dependence on dendritic integrity. J Comp Neurol 202: 397-414.

291. Rubel EW, Parks TN (1988) Organization and development of the avian brain-stem auditory system. In Edelman GM, Gall WE, Cowan WM (eds) Auditory Function: Neurological Bases of Hearing. New York: John Wiley and Sons, pp 3-92.

292. Rubel EW, Hyson RL, Durham D (1990) Afferent regulation of neurons in the brain stem auditory system. J Neurobiol 21: 169-196.

293. Russell FA, Moore DR (1995) Afferent reorganisation within the superior olivary complex of the gerbil: development and induction by neonatal, unilateral cochlear removal. J Comp Neurol 352: 607-625.

294. Russell FA, Moore DR (1999) Effects of unilateral cochlear removal on dendrites in the gerbil medial superior olivary nucleus. Eur J Neurosci 11: 1379-1390.

295. Sala C, Rudolph-Correia S, Sheng M (2000) Developmentally regulated NMDA receptor-dependent dephosphorylation of cAMP response element-binding protein (CREB) in hippocampal neurons. J Neurosci 20: 3529-3536.

296. Sanes DH, Walsh E J (1998) Development of the auditory system. In Webster, B., Popper, A.N., Fay, R.R.(eds), Spinger Verlag, New York, 271-315.

297. Sanes DH, Constantine-Paton M (1983) Altered activity patterns during development reduce neural tuning. Science 221: 1183-1185.

298. Sanes DH, Constantine-Paton M (1985) The sharpening of frequency tuning curves requires patterned activity during development in the mouse, Mus musculus. J Neurosci 5: 1152-1166.

299. Sanes DH, Rubel EW (1988) The ontogeny of inhibition and excitation in the gerbil lateral superior olive. J Neurosci 8: 682-700.

300. Sanes DH, Siverls V (1991) Development and specificity of inhibitory terminal arborizations in the central nervous system. J Neurobiol 22: 837-854.

301. Sanes DH, Song J, Tyson J (1992) Refinement of dendritic arbors along the tonotopic axis of the gerbil lateral superior olive. Brain Res Dev Brain Res 67: 47-55.

302. Sanes DH, Takacs C (1993) Activity-dependent refinement of inhibitory connections. Eur J Neurosci 5: 570-574.

303. Sanes DH, Friauf E (2000) Development and influence of inhibition in the lateral superior olivary nucleus. Hear Res 147: 46-58.

304. Sassone-Corsi P (1995) Transcription factors responsive to cAMP. Annu Rev Cell Dev Biol 11: 355-377.

305. Sato K, Kiyama H, Tohyama M (1993) The differential expression patterns of messenger RNAs encoding non-N-methyl-D-aspartate glutamate receptor subunits (GluR1-4) in the rat brain. Neuroscience 52: 515-539.

306. Sato K, Nakagawa H, Kuriyama H, Altschuler RA (1999) Differential distribution of N-methyl-D-aspartate receptor-2 subunit messenger RNA in the rat superior olivary complex. Neuroscience 89: 839-853.

307. Sauerwald A, Hoesche C, Oschwald R, Kilimann MW (1990) The 5'-flanking region of the synapsin I gene. A G+C-rich. J Biol Chem 265: 14932-14937.

308. Schaefer M, Plant TD, Obukhov AG, Hofmann T, Gudermann T, Schultz G (2000) Receptor-mediated regulation of the nonselective cation channels TRPC4 and TRPC5. J Biol Chem 275: 17517-17526.

309. Schaefer M, Plant TD, Stresow N, Albrecht N, Schultz G (2002) Functional differences between TRPC4 splice variants. J Biol Chem 277: 3752-3759.

310. Scheenen WJ, Makings LR, Gross LR, Pozzan T, Tsien RY (1996) Photodegradation of indo-1 and its effect on apparent Ca2+ concentrations. Chem Biol 3: 765-774.

311. Schmid S, Guthmann A, Ruppersberg JP, Herbert H (2001) Expression of AMPA receptor subunit flip/flop splice variants in the rat auditory brainstem and inferior colliculus. J Comp Neurol 430: 160-171.

312. Schwartz IR, Eager PR (1999) Glutamate receptor subunits in neuronal populations of the gerbil lateral superior olive. Hear Res 137: 77-90.

313. Shatz CJ (1990) Impulse activity and the patterning of connections during CNS development. Neuron 5: 745-756.

314. Shatz CJ (1996) Emergence of order in visual system development. Proc Natl Acad Sci U S A 93: 602-608.

315. Shaywitz AJ, Greenberg ME (1999) CREB: a stimulus-induced transcription factor activated by a diverse array of extracellular signals. Annu Rev Biochem 68: 821-861.

316. Shieh PB, Hu SC, Bobb K, Timmusk T, Ghosh A (1998) Identification of a signaling pathway involved in calcium regulation of BDNF expression. Neuron 20: 727-740.

317. Shigemoto R, Nakanishi S, Mizuno N (1992) Distribution of the mRNA for a metabotropic glutamate receptor (mGluR1) in the central nervous system: an in situ hybridization study in adult and developing rat. J Comp Neurol 322: 121-135.

318. Silva AJ, Kogan JH, Frankland PW, Kida S (1998) CREB and memory. Annu Rev Neurosci 21: 127-148.

319. Simpson PB, Challiss RA, Nahorski SR (1995) Divalent cation entry in cultured rat cerebellar granule cells measured using Mn2+ quench of fura 2 fluorescence. Eur J Neurosci 7: 831-840.

320. Sinkins WG, Estacion M, Schilling WP (1998) Functional expression of TrpC1: a human homologue of the Drosophila Trp channel. Biochem J 331 (Pt 1): 331-339.

321. Smith ZD, Gray L, Rubel EW (1983) Afferent influences on brainstem auditory nuclei of the chicken: n. laminaris dendritic length following monaural conductive hearing loss. J Comp Neurol 220: 199-205.

322. Soong TW, Stea A, Hodson CD, Dubel SJ, Vincent SR, Snutch TP (1993) Structure and functional expression of a member of the low voltage-activated calcium channel family. Science 260: 1133-1136.

323. Sosa R, Hoffpauir B, Rankin ML, Bruch RC, Gleason EL (2002) Metabotropic glutamate receptor 5 and calcium signaling in retinal amacrine cells. J Neurochem 81: 973-983.

324. Soulsby MD, Wojcikiewicz RJ (2002) 2-Aminoethoxydiphenyl borate inhibits inositol 1,4,5-trisphosphate receptor function, ubiquitination and downregulation, but acts with variable characteristics in different cell types. Cell Calcium 32: 175-181.

325. Spitzer NC (1995) Spontaneous activity: functions of calcium transients in neuronal differentiation. Perspect Dev Neurobiol 2: 379-386.

326. Spitzer NC, Olson E, Gu X (1995) Spontaneous calcium transients regulate neuronal plasticity in developing neurons. J Neurobiol 26: 316-324.

327. Spitzer NC, Lautermilch NJ, Smith RD, Gomez TM (2000) Coding of neuronal differentiation by calcium transients. Bioessays 22: 811-817.

328. Staub C, Vranesic I, Knopfel T (1992) Responses to Metabotropic Glutamate Receptor Activation in Cerebellar Purkinje Cells: Induction of an Inward Current. Eur J Neurosci 4: 832-839.

329. Steward O, Rubel EW (1985) Afferent influences on brain stem auditory nuclei of the chicken: cessation of amino acid incorporation as an antecedent to age-dependent transneuronal degeneration. J Comp Neurol 231: 385-395.

330. Stowers L, Holy TE, Meister M, Dulac C, Koentges G (2002) Loss of sex discrimination and male-male aggression in mice deficient for TRP2. Science 295: 1493-1500.

331. Strubing C, Krapivinsky G, Krapivinsky L, Clapham DE (2001) TRPC1 and TRPC5 form a novel cation channel in mammalian brain. Neuron 29: 645-655.

332. Takahashi T, Forsythe ID, Tsujimoto T, Barnes-Davies M, Onodera K (1996) Presynaptic calcium current modulation by a metabotropic glutamate receptor. Science 274: 594-597.

333. Takumi Y, Bergersen L, Landsend AS, Rinvik E, Ottersen OP (1998) Synaptic arrangement of glutamate receptors. Prog Brain Res 116: 105-121.

334. Takumi Y, Matsubara A, Rinvik E, Ottersen OP (1999) The arrangement of glutamate receptors in excitatory synapses. Ann N Y Acad Sci 868: 474-482.

335. Tanabe Y, Nomura A, Masu M, Shigemoto R, Mizuno N, Nakanishi S (1993) Signal transduction, pharmacological properties, and expression patterns of two rat metabotropic glutamate receptors, mGluR3 and mGluR4. J Neurosci 13: 1372-1378.

336. Tanaka H, Grooms SY, Bennett MV, Zukin RS (2000) The AMPAR subunit GluR2: still front and center-stage. Brain Res 886: 190-207.

337. Tarnawa I, Farkas S, Berzsenyi P, Pataki A, Andrasi F (1989) Electrophysiological studies with a 2,3-benzodiazepine muscle relaxant: GYKI 52466. Eur J Pharmacol 167: 193-199.

338. Telgkamp P, Backus KH, Deitmer JW (1996) Blockade of AMPA receptors by nickel in cultured rat astrocytes. Glia 16: 140-146.

339. Tempia F, Alojado ME, Strata P, Knopfel T (2001) Characterization of the mGluR(1)-mediated electrical and calcium signaling in Purkinje cells of mouse cerebellar slices. J Neurophysiol 86: 1389-1397.

340. Thandi S, Blank JL, Challiss RA (2002) Group-I metabotropic glutamate receptors, mGlu1a and mGlu5a, couple to extracellular signal-regulated kinase (ERK) activation via distinct, but overlapping, signalling pathways. J Neurochem 83: 1139-1153.

341. Thandi S, Blank JL, Challiss RA (2002) Group-I metabotropic glutamate receptors, mGlu1a and mGlu5a, couple to extracellular signal-regulated kinase (ERK) activation via distinct, but overlapping, signalling pathways. J Neurochem 83: 1139-1153.

342. Thompson AM, Schofield BR (2000) Afferent projections of the superior olivary complex. Microsc Res Tech 51: 330-354.

343. Tierney TS, Russell FA, Moore DR (1997) Susceptibility of developing cochlear nucleus neurons to deafferentation-induced death abruptly ends just before the onset of hearing. J Comp Neurol 378: 295-306.

344. Tierney TS, Doubell P, Xia G, Moore DR (2001) Development of brain-derived neurotrophic factor and neurotrophin-3 immunoreactivity in the lower auditory brainstem of the postnatal gerbil. Eur J Neurosci 14: 785-793.

345. Tozzi A, Bengtson CP, Longone P, Carignani C, Fusco FR, Bernardi G, Mercuri NB (2003) Involvement of transient receptor potential-like channels in responses to mGluR-I activation in midbrain dopamine neurons. European Journal of Neuroscience 18: 2133-2145.

346. Trune DR (1982) Influence of neonatal cochlear removal on the development of mouse cochlear nucleus: II. Dendritic morphometry of its neurons. J Comp Neurol 209: 425-434.

347. Trune DR (1982) Influence of neonatal cochlear removal on the development of mouse cochlear nucleus: I. Number, size, and density of its neurons. J Comp Neurol 209: 409-424.

348. Trussell LO (1997) Cellular mechanisms for preservation of timing in central auditory pathways. Curr Opin Neurobiol 7: 487-492.

349. Trussell LO (1999) Synaptic mechanisms for coding timing in auditory neurons. Annu Rev Physiol 61: 477-496.

350. Tsavaler L, Shapero MH, Morkowski S, Laus R (2001) Trp-p8, a novel prostate-specific gene, is up-regulated in prostate cancer and other malignancies and shares high homology with transient receptor potential calcium channel proteins. Cancer Res 61: 3760-3769.

351. Vaca L, Sinkins WG, Hu Y, Kunze DL, Schilling WP (1994) Activation of recombinant trp by thapsigargin in Sf9 insect cells. Am J Physiol 267: C1501-C1505.

352. Valenti O, Conn PJ, Marino MJ (2002) Distinct physiological roles of the Gq-coupled metabotropic glutamate receptors Co-expressed in the same neuronal populations. J Cell Physiol 191: 125-137.

353. Van der LH, Woolsey TA (1973) Somatosensory cortex: structural alterations following early injury to sense organs. Science 179: 395-398.

354. Vanderklish PW, Edelman GM (2002) Dendritic spines elongate after stimulation of group 1 metabotropic glutamate receptors in cultured hippocampal neurons. Proc Natl Acad Sci U S A 99: 1639-1644.

355. Verdoorn TA, Burnashev N, Monyer H, Seeburg PH, Sakmann B (1991) Structural determinants of ion flow through recombinant glutamate receptor channels. Science 252: 1715-1718.

356. Verkhratsky A (2002) The endoplasmic reticulum and neuronal calcium signalling. Cell Calcium 32: 393-404.

357. Verkhratsky A, Petersen OH (2002) The endoplasmic reticulum as an integrating signalling organelle: from neuronal signalling to neuronal death. Eur J Pharmacol 447: 141-154.

358. Villalobos C, Garcia-Sancho J (1995) Capacitative Ca2+ entry contributes to the Ca2+ influx induced by thyrotropin-releasing hormone (TRH) in GH3 pituitary cells. Pflugers Arch 430: 923-935.

359. Vincent AM, Maiese K (2000) The metabotropic glutamate system promotes neuronal survival through distinct pathways of programmed cell death. Exp Neurol 166: 65-82.

360. Vitten H, Friauf E, Peich L, Lohrke S (1999) Kainate mediated currents in lateral superior olive neurons of the rat. Soc. Neurosci. Abstr., 392.16.

361. Voets T, Nilius B (2003) TRPs make sense. J Membr Biol 192: 1-8.

362. West AE, Chen WG, Dalva MB, Dolmetsch RE, Kornhauser JM, Shaywitz AJ, Takasu MA, Tao X, Greenberg ME (2001) Calcium regulation of neuronal gene expression. Proc Natl Acad Sci U S A 98: 11024-11031.

363. Westenbroek RE, Sakurai T, Elliott EM, Hell JW, Starr TV, Snutch TP, Catterall WA (1995) Immunochemical identification and subcellular distribution of the alpha 1A subunits of brain calcium channels. J Neurosci 15: 6403-6418.

364. Westenbroek RE, Hoskins L, Catterall WA (1998) Localization of Ca2+ channel subtypes on rat spinal motor neurons, interneurons, and nerve terminals. J Neurosci 18: 6319-6330.

365. Wong RO, Ghosh A (2002) Activity-dependent regulation of dendritic growth and patterning. Nat Rev Neurosci 3: 803-812.

366. Woodhall G, Gee CE, Robitaille R, Lacaille JC (1999) Membrane potential and intracellular Ca2+ oscillations activated by mGluRs in hippocampal stratum oriens/alveus interneurons. J Neurophysiol 81: 371-382.

367. Wu H, Shen HW, Wu TF, Brass LF, Sung KC (2002) Extracellular Signal-Regulated Kinases and G Protein-Coupled Receptors in Megakaryocytic Human Erythroleukemia Cells: Selective Activation, Differential Regulation, and Dissociation from Mitogenesis. J Pharmacol Exp Ther 300: 339-345.

368. Wu SH, Kelly JB (1992) Synaptic pharmacology of the superior olivary complex studied in mouse brain slice. J Neurosci 12: 3084-3097.

369. Wu SH, Kelly JB (1994) Physiological evidence for ipsilateral inhibition in the lateral superior olive: synaptic responses in mouse brain slice. Hear Res 73: 57-64.

370. Wu SH, Fu XW (1998) Glutamate receptors underlying excitatory synaptic transmission in the rat's lateral superior olive studied in vitro. Hear Res 122: 47-59.

371. Yamakura T, Shimoji K (1999) Subunit- and site-specific pharmacology of the NMDA receptor channel. Prog Neurobiol 59: 279-298.

372. Yamamoto KK, Gonzalez GA, Biggs WH, III, Montminy MR (1988) Phosphorylation-induced binding and transcriptional efficacy of nuclear factor CREB. Nature 334: 494-498.

373. Yokoyama CT, Westenbroek RE, Hell JW, Soong TW, Snutch TP, Catterall WA (1995) Biochemical properties and subcellular distribution of the neuronal class E calcium channel alpha 1 subunit. J Neurosci 15: 6419-6432.

374. Yoo AS, Cheng I, Chung S, Grenfell TZ, Lee H, Pack-Chung E, Handler M, Shen J, Xia W, Tesco G, Saunders AJ, Ding K, Frosch MP, Tanzi RE, Kim TW (2000) Presenilin-mediated modulation of capacitative calcium entry. Neuron 27: 561-572.

375. Yoon J, Ben Ami HC, Hong YS, Park S, Strong LL, Bowman J, Geng C, Baek K, Minke B, Pak WL (2000) Novel mechanism of massive photoreceptor degeneration caused by mutations in the trp gene of Drosophila. J Neurosci 20: 649-659.

376. Yuste R, Katz LC (1991) Control of postsynaptic Ca2+ influx in developing neocortex by excitatory and inhibitory neurotransmitters. Neuron 6: 333-344.

377. Zhu X, Jiang M, Peyton M, Boulay G, Hurst R, Stefani E, Birnbaumer L (1996) trp, a novel mammalian gene family essential for agonist-activated capacitative Ca2+ entry. Cell 85: 661-671.

378. Zhu X, Jiang M, Birnbaumer L (1998) Receptor-activated Ca2+ influx via human Trp3 stably expressed in human embryonic kidney (HEK)293 cells. Evidence for a non-capacitative Ca2+ entry. J Biol Chem 273: 133-142.

379. Zhu X, Birnbaumer L (1998) Calcium Channels Formed by Mammalian Trp Homologues. News Physiol Sci 13: 211-217.

380. Zirpel L, Lachica EA, Lippe WR (1995) Deafferentation increases the intracellular calcium of cochlear nucleus neurons in the embryonic chick. J Neurophysiol 74: 1355-1357.

381. Zirpel L, Lachica EA, Rubel EW (1995) Activation of a metabotropic glutamate receptor increases intracellular calcium concentrations in neurons of the avian cochlear nucleus. J Neurosci 15: 214-222.

382. Zirpel L, Rubel EW (1996) Eighth nerve activity regulates intracellular calcium concentration of avian cochlear nucleus neurons via a metabotropic glutamate receptor. J Neurophysiol 76: 4127-4139.

383. Zirpel L, Lippe WR, Rubel EW (1998) Activity-dependent regulation of [Ca2+]i in avian cochlear nucleus neurons: roles of protein kinases A and C and relation to cell death. J Neurophysiol 79: 2288-2302.

384. Zirpel L, Janowiak MA, Taylor DA, Parks TN (2000) Developmental changes in metabotropic glutamate receptor-mediated calcium homeostasis. J Comp Neurol 421: 95-106.

385. Zitt C, Zobel A, Obukhov AG, Harteneck C, Kalkbrenner F, Luckhoff A, Schultz G (1996) Cloning and functional expression of a human Ca2+-permeable cation channel activated by calcium store depletion. Neuron 16: 1189-1196.

386. Zitt C, Obukhov AG, Strubing C, Zobel A, Kalkbrenner F, Luckhoff A, Schultz G (1997) Expression of TRPC3 in Chinese hamster ovary cells results in calcium-activated cation currents not related to store depletion. J Cell Biol 138: 1333-1341.

387. Zitt C, Halaszovich CR, Luckhoff A (2002) The TRP family of cation channels: probing and advancing the concepts on receptor-activated calcium entry. Prog Neurobiol 66: 243-264.

388. Zweifach A, Lewis RS (1993) Mitogen-regulated Ca2+ current of T lymphocytes is activated by depletion of intracellular Ca2+ stores. Proc Natl Acad Sci U S A 90: 6295-6299.